The feasibility of a fully electric aircraft towing system

Master Thesis

E.V.M. van Baaren

Delft University of Technology

TU Delft

The feasibility of a fully electric aircraft towing system

Master Thesis

by

E.V.M. van Baaren

to obtain the degree of Master of Science
in Aerospace Engineering
at the Delft University of Technology,
to be defended publicly on Friday May 24, 2019 at 2:30 PM.

Student number:	1506641	
Date:	May 24, 2019	
Thesis committee:	Prof. dr. R. Curran,	TU Delft, chair
	Ir. P. C. Roling,	TU Delft, supervisor
	Dr. G.A. Bohlin,	TU Delft

An electronic version of this thesis is available at `http://repository.tudelft.nl/`.

TU Delft

Preface

Amusingly, I first heard of Air Transport Operations at the age of fourteen from one of my sport coaches, who at that time was a staff member at the department. Even back then, the combination of aviation and operations had my interest, and the subject never left my mind. I decided to study Aerospace Engineering at the TU Delft. I really enjoyed learning about all the different fields of aerospace engineering, but I always gravitated to the operational side of aviation. It did not take me long to decide I wanted to study Air Transport Operations.

I would like to thank my supervisor Paul Roling for all his time and effort he put into my thesis. He always had time to help and impressed me with his extensive knowledge in all areas. Not only has Paul been my supervisor during my thesis, but he was my supervisor during my second year project and design synthesis exercise. Therefore, I was excited to start the thesis under his supervision.

Furthermore, I would like to thank all the people on the third floor whom I got to know during my thesis and who helped me in times of need. A special thanks goes to the boys from room 3.15, and the upper house from the Control & Simulations. I definitely learned a lot from all the discussions we had, which I will miss.

Next, I would like to thank my parents and sister for their endless support throughout my studies. I could always count on them for advise. Also, I would like to thank my grandparents for their support, and especially my grandpa for proofreading my thesis. I am honoured to be a third generation engineer in my family graduating from the TU Delft. To all my friends, thank you for keeping me motivated and being understanding when I had less time for you.

E.V.M. van Baaren
Delft, May 2019

Abstract

Operational towing is a taxiing strategy to reduce the fuel consumption during the taxiing phase of a flight, which will decrease the cost and environmental impact of taxiing. Currently, no operational electric towing systems are available that are fully electric, do not require the auxiliary power unit (APU) to be on, and are compatible with both narrow- and wide-bodied passenger aircraft. To further reduce the fuel consumption, the novel concept for a fully electric towing system is envisioned, which is fully electric, takes over the functions of the APU, and is compatible with all common types of passenger aircraft.

The research objective is to determine if a fully electric towing system can be a technically and operationally feasible alternative to conventional taxiing operations. A proof of concept is used to demonstrate that a fully electric towing system concept exists that fulfils its technical and operational requirements. The method in this feasibility study consists of three parts: the conceptual design, the ground movements simulations, and a towing vehicle routing problem. During the conceptual design, three models of fully electric towing vehicles are established from the technical and operational requirements, and the kinematic performance is tested using a dynamic model of the towing scenario. Next, the fully electric towing vehicle designs are simulated towing a set of flights over a node and link system. The same set of flights are simulated taxiing conventionally, and compared to the fully electric towing simulations. The effectiveness of the fully electric towing system at reducing the fuel consumption of a set of flights is tested using a scheduling problem. The scheduling problem is solved with a towing vehicle routing problem. The solution is the subset of flights that should be towed to minimize the total fuel consumption, with the availability of a limited number of towing vehicles. The total fuel reduction and energy consumption by the fully electric towing system is determined from the solution. The number of fully electric towing vehicles deployed is varied to test the effectiveness of different fleet sizes of towing vehicles. Lastly, a sensitivity analysis is performed to test the effect the outside air temperature on the fuel reduction potential. Lighter and heavier versions of the towing vehicle concepts are tested as well to see the effect of the towing vehicle weight on the operational performance.

The method is applied to Rotterdam-the Hague Airport (a regional airport) and Amsterdam Airport Schiphol (an international hub airport). The results show that the difference in duration between a movement using a fully electric towing vehicle and a conventional movement is insignificant and that less fuel is consumed by the aircraft when towed. By implementing the fully electric towing system, the total fuel consumption per day by flights at Rotterdam-the Hague Airport and Amsterdam Airport Schiphol can be reduced by 65% and 82%, respectively. The system is the most effective at Amsterdam Airport Schiphol due to the large number of flights, but the implementation of the system at Rotterdam-the Hague Airport is simpler. The sensitivity analysis shows that the outside air temperature does not affect the fuel reduction potential of the towing vehicle models used, but does affect the energy consumption of the towing vehicles. Similarly, the alternative models tested have an indifferent fuel saving potential, but do consume a different amount of energy.

It is concluded that the concept of a fully electric towing system can be a technically and operationally feasible alternative to conventional taxiing, with a large fuel and emissions saving potential. The main disadvantages of this system is that it is expensive and there are many logistical challenges to overcome. More research into this subject is required to get more precise results.

Contents

List of Figures

List of Tables

1 Introduction

Global air traffic is growing due to increasing living standards, population and demographics, price and availability. Continued growth is expected for at least two decades, leading to more air traffic congestion and an increased impact on the environment. Air traffic congestion is problematic as it puts pressure on air traffic networks, causes extra delays and longer taxi times, which costs the airline sector a lot of money. The delays caused by congestion tend to cause undesirable chain reactions at airports, that can rapidly spread to other airports. Complete recovery from such chain reactions can take many hours, and the extended taxi times caused by congestion further increase emission production. Emissions have a large impact on the environment. The most common types of emissions produced by aircraft are: water, carbon dioxide, carbon monoxide, hydrocarbons, sulphur oxides, nitrogen oxides and particulate matter. The water produced through combustion is not necessarily undesirable, but the other emissions negatively affect health, wildlife, buildings, infrastructure, and global warming. Noise produced by the aircraft engines is another form of undesirable emission that has health and socio-economic implications. As a result, the airline industry has to deal with strict regulations to minimize fuel and noise emissions. Another incentive to reduce fuel consumption is the cost of fuel. Fuel costs are a large share of the direct operating costs. Airlines are further compelled to cut fuel consumption in the future as the fuel price is expected to rise in the coming decade [3].

According to the United States Environmental Protection Agency (EPA), the most effective method to decrease CO_2 emissions is to decrease fossil fuel consumption [1]. The taxi phase is a phase of flight where major reductions in fuel consumption and emissions can still be attained. Therefore, a lot of research is being done on the reduction of fuel consumption of the taxi phase, whilst juggling the increasing demand for aircraft movements at airports. One of the areas of research are alternative taxiing strategies.

The conventional method of aircraft taxiing is the utilization of all aircraft engines to produce thrust for propulsion. The advantage of this method is that it is readily available, a proven technology, and requires no or little intervention from external personnel. The main disadvantage of this method is that it is not the most fuel efficient method of taxiing. Three examples of alternative taxiing strategies that use less fuel are single-engine taxiing, operational towing, and landing gear mounted electrical taxiing systems. Each alternative taxiing strategy has its strengths and weaknesses.

According to a study by Ithnan et al. [12], single-engine operations are simple to implement but are limited by sharp turns and uphill slopes, have a limited fuel and emission reduction potential, and create a jet blast. Operational towing and landing gear mounted electrical taxiing show a larger fuel reduction potential.

Landing gear mounted electrical taxiing systems are still a young technology. Examples these systems are WheelTug and the Electric Green Taxiing System (EGTS). The main advantages of this strategy is that the aircraft does not use its main engines, is independent from external intervention, and the "pushback" time is reduced. With the engines shut off, a large amount of fuel can be saved and the risk of foreign object debris damages to the engines is decreased. Disadvantages are that they add weight to the aircraft and require modifications to the aircraft. Landing gear mounted electrical taxi systems, like WheelTug, travel much slower than conventional aircraft due to limited power of the auxiliary power unit (APU) and are not able to produce sufficient traction. Both the landing gear mounted taxi system and the electric towing strategy require the APU to provide power for heating and cooling of the cabin, on-board systems, and engine start up, whilst taxiing. The APU is also required to power the motors on the wheels in the case of the landing gear mounted system. This means that all current taxi strategies still rely on fuel and produce emissions, and that there are no electric taxi systems available that produce no fuel emissions during the taxi phase (other than the inevitable fuel emissions produced by the aircraft engines during engine warm up and cool down).

Operational towing is another taxiing strategy where the main engines of the aircraft can be shut off. Unlike the landing gear mounted electrical taxiing systems, operational towing can transport both narrow- and wide-bodied aircraft, and does not require modifications on or add weight to the aircraft. A disadvantage of operational towing is the additional traffic on the taxiways and the increased fatigue on the nose landing gear of aircraft. Ithnan states that if operational towing could be done electrically, further fuel and emissions reductions are possible. Currently, the only certified electric towing system in operation is TaxiBot, which is not fully electric but is hybrid powered.

A possible solution for a minimal emission taxiing system is a fully electric towing vehicle that is able to take over the functions of the main engines and APU during taxiing. This thesis will investigate the technical and operational feasibility of such a concept.

2

Background information

In this chapter, methods will be discussed that will be (partially) used in this thesis. A method to calculate the emission production is discussed in Section 2.1, a method to simulate ground movements is discussed in Section 2.2, and the Vehicle Routing Problem will be discussed in Section 2.3.

2.1. Emission calculations

The combustion of fossil fuels causes emissions. As mentioned in Chapter 1, the most common types of aircraft emissions are water, carbon dioxide, carbon monoxide, hydrocarbons, nitrogen oxides, suphur oxides, and particulate matter. A method to calculate the amount of emission produced is by using emission indices. An emission index is defined as the amount of emission produced per unit of fuel. Thus, the emissions can estimated from the amount of fuel consumed. Emission indices are dependent on the combustion process and differ per aircraft engine, atmospheric setting, and thrust setting. The International Civil Aviation Organization (ICAO) keeps a database of aircraft engine properties, which includes information on the fuel flow and emission indices for different phases of flight, i.e. take-off, climb out, approach, and idle [11]. The emission information in the ICAO database is limited to carbon monoxide, hydrocarbon, and nitrogen oxides. Kesgin [13] uses the following equation to estimate the amounts of emissions produced during multiple landing-take off (LTO) cycles;

$$E_{i,m} = \sum_{a} \sum_{e} n_a l_{a,e} F_{a,e,m} E_{e,m,i} t_{m,a} \tag{2.1}$$

where $E_{i,m}$ is the mass of emission i for mode m in kilograms, n_a is the number of engines on aircraft type a, $l_{a,e}$ is the number of LTO cycles for aircraft type a with engines type e, $F_{a,e,m}$ is the fuel consumption of aircraft type a with engine type e in mode m in kilograms per second, $E_{e,m,i}$ is the emission index for engine type e in mode m of pollutant i in grams per kilograms, and $t_{m,a}$ is the time in mode m for aircraft type a in seconds. This equation can be filled in for only the taxi mode of a single LTO cycle to calculate the emissions during taxiing.

2.2. Taxi planning model

Roling developed a traffic planning optimization tool for Amsterdam Airport Schiphol, which allows the routing of aircraft taxi movements to be simulated and optimized [16]. The planning tool is composed of the following components: airport model generator, route generator, MILP model builder, optimizer, output converter, and traffic simulator. The process used in the taxi planning model is depicted in Figure 2.1 and will be discussed in this section.

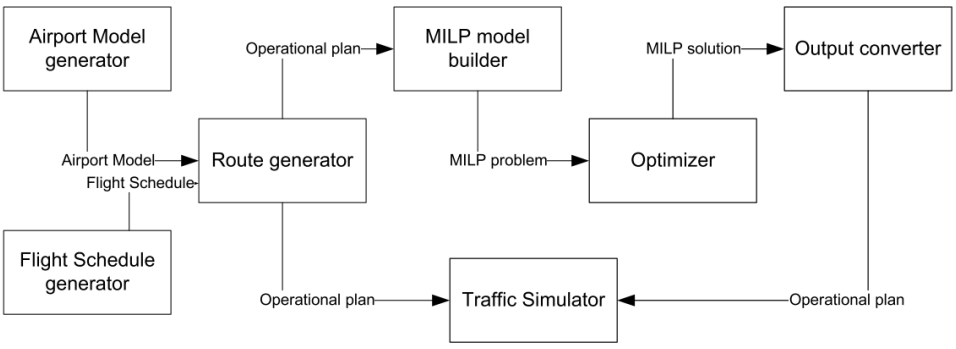

Figure 2.1: A schematic representation of the taxi planning tool.

Source: Roling [16]

Airport model generator
The airport model generator defines a model of the airport using a node a link system. Each node represents a location on the airport runways and taxiways, and the link represents a possible path between two nodes. Every node has properties associated with it, which include the location of the node, the connecting nodes, and the distance and speed limit between connecting nodes. Certain nodes can also represent start, end, or holding points. An aircraft can travel between connecting nodes across the link and will be constrained by the node properties. Links can allow travel in one direction or both direction depending on the properties assigned to the nodes. As examples, the airport models of Rotterdam-the Hague Airport and Amsterdam Airport Schiphol can be found in Appendix B. The number of nodes should be kept to an minimum, as well as two way travel options between nodes in order to keep the optimization time minimal. The computation time will increase exponentially with the number of decision variables.

Flight schedule generator
The flight schedule generator generates a flight schedule with information on the start node, end node, start time and end time. In the case of an arriving flight, the start node is the node on the runway near the exit ramp, the end node is the node of on the apron representing the gate, the start time is the time the aircraft leaves the runway, and the end time is the latest time the aircraft has to be at the gate. With a departing flight, the start node is the node of the gate, the end node is the node at the start of the runway, the start time is the earliest time the aircraft can leave the gate, and the end time is the scheduled take-off time. Realism can be improved by assigning maximum speeds to the flights, by introducing capacity constraints, and by introducing delays.

Route generator
The route generator generates all the possible routes the aircraft can take between start and end node on the airport model. The route generator uses brute force to search for all possible options. The algorithm starts at the begin node to look for the end node, by moving from connected node to connected node. The algorithm will stop searching if the end node is found to confirm a valid route, or if a node has been previously visited confirming an invalid route. The search is also discontinued when sufficient routes have been found, or when the limit of attempts is reached. A selection of routes will have to be made per flight. To avoid selecting similar routes a method is applied to judge the similarity between routes.

MILP model builder
The MILP model builder generates an input file for the optimizer that formulates the mixed integer linear programming (MILP) problem. A MILP consists of an objective function and constraints. The objective function in this tool is minimized based on the total taxi duration, the delay time, and the rerouting of each flight. The constraints are the rules the optimizer has to follow. The constraints include the occupancy of links, route constraints, delay constraints, and waiting time constraints.

Optimizer
The optimizer solves the MILP for the optimal solution. Commercial solvers like CPLEX [10] use the branch and bound method to solve the problem. The solution consists of integers assigned to the decision variables. A time limit can be set on the solver to stop searching for an optimal solution after the time limit has exceeded. The solution will be the best solution found until that moment. An absolute limit can be set as well, which stops the search when the best found solution falls within the limits set.

Output converter
The output converter translates the output file of the MILP into data that can easily be interpreted by the user. The traffic planning tool converts the output data to the route chosen and the delay time per segment for each flight. The converted data is saved to a database which can be used in the traffic simulator.

Traffic simulator
The traffic simulator visualizes the data from the output converter by plotting the aircraft position on a depiction of the airport model for every interval of time. An animation of the simulation is created by displaying the plots in sequence.

2.3. Vehicle Routing Problem

A Vehicle Routing Problem (VRP) is a form of MILP problem, that finds the optimal set of routes vehicles have to travel in order to deliver goods from a central location. Usually a VRP is optimized for the minimum total route cost, but can be optimized for other criteria, e.g. minimum time, delays, number of routes, or penalties for quality of service.

The VRP uses a node and link system to describe the network of customer locations. The nodes represent the customers with their demand, and the links are the cost of the route between customers. Each vehicle is given a delivery capacity which can not be exceeded on a delivery route. A schematic example of a VRP solution is displayed in Figure 2.2, where the numbers are the costs of every link.

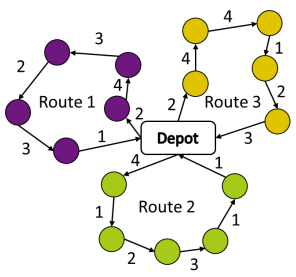

Figure 2.2: A schematic solution to a vehicle routing problem.

A VRP is composed of a cost function and constraints. The cost function is the summation of the costs of travelling between customers, and is the function that will be minimized or maximized. Equation 2.2 gives an typical example of the cost function for a VRP. The decision variables x_{ij} take the value 1 if the vehicles travel from node i to node j, and the value 0 if false. The cost coefficient c_{ij} represents the cost to travel from node i to node j.

$$min \sum_{i \in N} \sum_{j \in N} c_{ij} x_{ij} \tag{2.2}$$

As with the taxi planning model, the constraints are the set of rules that describe the problem, and will affect the decision variables in the cost function. Equation 2.3 states that every vehicle can visit a customer only once, and Equation 2.4 states that every vehicle can leave a customer only once. Equation 2.5 is the flow constraint, which says that if the vehicle visits customer p, the vehicle should also leave customer p. Equation 2.6 and 2.7 say that if F number of vehicles leave base, F number of vehicles should return to base. Equation 2.8 is the capacity constraint, stating that the total demand of the customers on route R should not exceed the capacity of the vehicle D.

$$\sum_{i \in N} x_{ij} = 1 \qquad \forall j \in N \backslash \{0\} \tag{2.3}$$

$$\sum_{j \in N} x_{ij} = 1 \qquad \forall i \in N \backslash \{0\} \tag{2.4}$$

$$\sum_{i \in N} x_{ip} = \sum_{j \in N} x_{pj} \qquad \forall p \in N \backslash \{0\} \tag{2.5}$$

$$\sum_{i \in N} x_{i0} = F \tag{2.6}$$

$$\sum_{j \in N} x_{0j} = F \tag{2.7}$$

$$\sum_{i \in R} \sum_{j \in R} d_j x_{ij} \leq D, \qquad \forall R \subseteq N \backslash \{0\} \tag{2.8}$$

$$x_{ij} \in \{0,1\} \qquad \forall i, j \in N \tag{2.9}$$

This is just an example of a basic vehicle routing problem, but many customized variants exist, e.g. Capacitated VRP, Time-dependent VRP, Multi-depot VRP. Macrina et. al [14] created a vehicle routing problem with a mixed vehicle fleet composed of electrical and conventional vehicles. Bay and Limbourg [4] defined a VRP on the classical Travelling Salesman Problem and the Pollution Routing Problem, and combined it with regenerative braking.

Vehicle Routing Problems are typically solved using computational solvers commercially available. The disadvantage of the Vehicle Routing Problem (VRP) is that this type of problem is NP-hard, which means that the computational time increases rapidly with the size of the problem. Most VRP tend to become large due to the use of binomial decision variables.

3

Research framework

The research framework is discussed in this chapter. First the research objective will be stated in Section 3.1, after which the sub questions will be listed in Section 3.2, followed by the research goals in Section 3.3. The scope is defined in Section 3.4 and the contribution of the thesis to research is written in Section 3.5.

3.1. Research objective

The following research objective is set:

"to reduce the cost and environmental impact of aircraft taxi operations, by designing a fully electric towing system."

This leads to the following research question:

"Can a fully electric towing system be a technically and operationally feasible alternative to conventional taxiing operations?"

3.2. Sub questions

Technical design feasibility

1. Is the system technically feasible?
2. What is the performance of the fully electric towing system?

Operational feasibility at regional and international hub airports

1. How will the system operate in a regional and an international hub airport environment?
2. Can the design omit the utilization of the auxiliary power unit during taxiing operations?
3. How effective is the system at reducing fuel consumption and emissions compared to full-engine-taxiing?
4. Is the fully electric towing system cost-effective?
5. Is the system operationally feasible?

3.3. Research goals

The following goals are set in order to answer the research questions:

1. Identify the technical and operational requirements of a fully electric towing system.
2. Develop a technical design for a fully electric towing system.
3. Develop a model to compare full-engine-taxiing and fully electric towing.
4. Develop a model to determine the effectiveness in fuel reductions for different fleet compositions of fully electric towing vehicles in an airport environment.

3.4. Scope

In order to complete the research within a limited amount of time and budget, the objective of the research is scoped. The scoping assumptions demarcate the context in which the research should be interpreted.

- This research focuses on the taxiing operations of commercial airlines at regional and international hubs. Cargo, general, and military aviation is not included in this research.

- Project scheduling and legal feasibility are not investigated. This research focuses on the technical and operational feasibility of a fully electric towing vehicle concept, where economic feasibility is investigated to a lesser extent.

- The research considers fully electric towing only. Operational towing strategies that use power sources other than electric will not be investigated. This includes towing with hybrid powered vehicles.

- No human-machine interactions will be considered. It is assumed the fully electric towing system can operate (semi-)autonomously, and that the vehicles are autonomously guided vehicles.

- The technical design will a high level design. Only the relevant and critical design features necessary to fulfil the research goals will be investigated.
- The effects of delays, runway traffic, or other taxiway obstructions are not considered.

- Aircraft taxiing noise is not included in the scope. Taxiing noise is considered less of a problem than aircraft noise during take-off, approach, and landing. Instead, it is assumed electrical operational towing is more silent than full-engine-taxiing.

3.5. Contribution

This feasibility study investigates if fully electric towing has the potential to be a realistic alternative to conventional taxiing of civil aircraft. The conclusions of this study should determine if further research into this area is of interest for future researchers. The novelty of this research is that it specifically investigates towing vehicles which are fully electric and take over the functions of the main aircraft engines and auxiliary power unit (APU) during ground movements. Additionally, this study investigates the electric towing of both narrow- and wide-bodied aircraft weighing up to 600,000 kg.

4

Method

This chapter describes the methodology that will be used to determine the technical and operational feasibility of a fully electric towing vehicle. The approach will be discussed in Section 4.1, after which every phase of the method will be discussed in detail in subsequent sections. First, the method to determine the conceptual design will be explained in Section 4.2. Next, the method to the simulate ground movements of aircraft and towing vehicles will be discussed in Section 4.3. Lastly, method to determine the effectiveness of the fully electric towing vehicle will be evaluated using the Vehicle Routing Problem is described in Section 4.4.

4.1. Research approach

The approach used to determine the feasibility of a fully electric towing system is a proof of concept (PoC). Demonstrating that a fully electric technical design exists that can reduce the fuel consumption during the taxi process will prove the feasibility of such a concept. Likewise, the concept is proven infeasible if the concept can not fulfil the requirements.

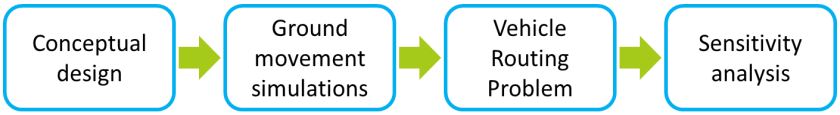

Figure 4.1: The phases of the proof of concept.

The proof of concept, consists of four phases as depicted in Figure 4.1. First the method to design a technical concept will be discussed. High level design requirements will be established from which a technical design of the fully electric towing vehicles will be conceptualized. In order to set up the towing vehicle routing problems for the fully electric towing vehicles in the third phase, the ground movements of aircraft and fully electric towing vehicles will be simulated in an airport environment. The simulations will determine the fuel and energy consumptions, the emissions production, and the taxi duration of conventional movements, fully electric tows, and ferry movements of the fully electric towing vehicles in between tows. With these outputs, a Vehicle Routing Problem can be formulated, necessary to solve a scheduling problem for a fleet of fully electric towing vehicles. This optimization will establish the optimal schedule for the deployment of fully electric towing vehicles to minimize fuel consumption of a set of flights. The effectiveness of the fully electric towing concept is measured in terms of the maximum fuel saving potential of a fleet of fully electric towing vehicles. Lastly, a sensitivity analysis will be performed to determine the effect of changes in the technical design and the environment. Figure 4.2 depicts the flow chart of the complete method.

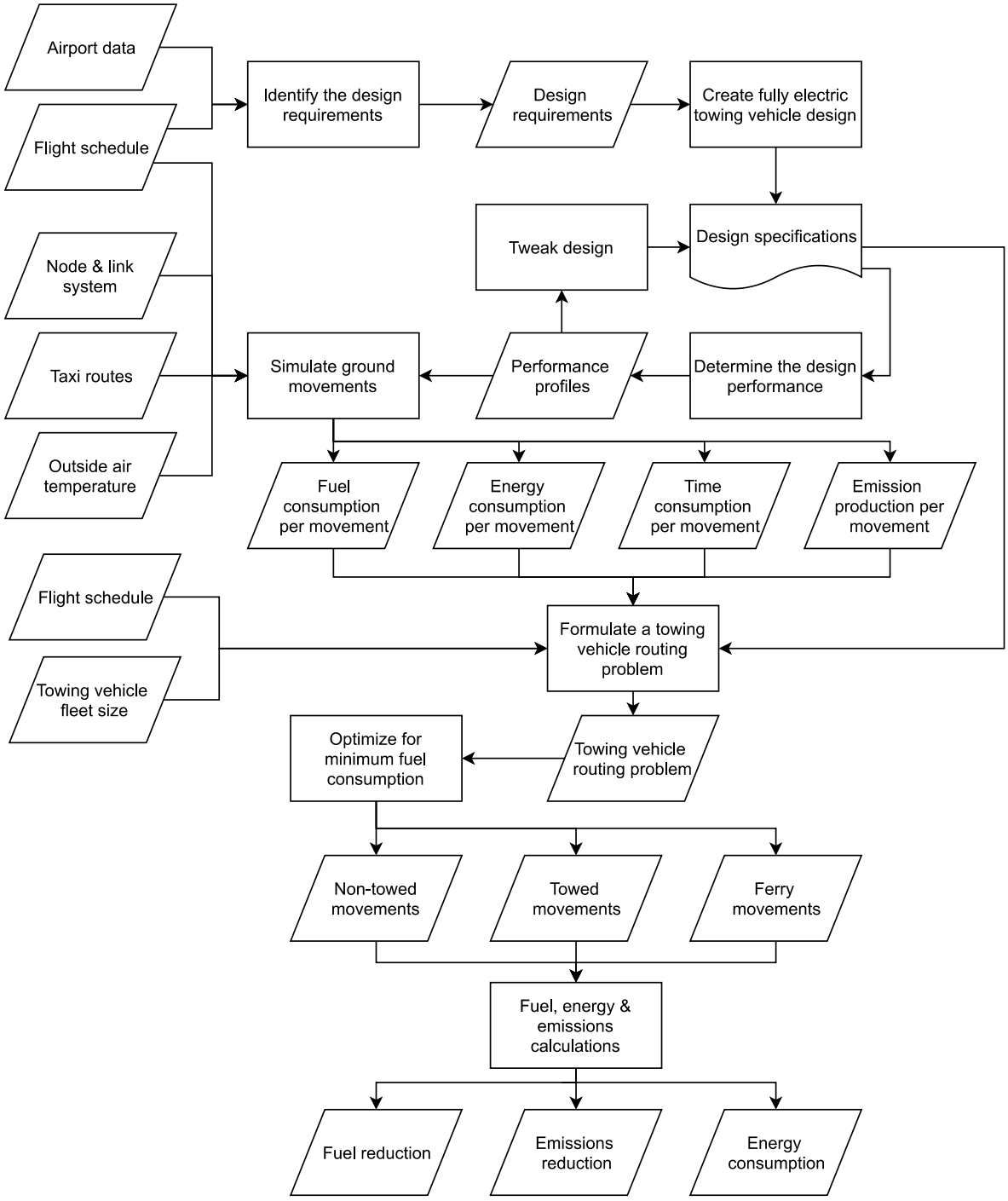

Figure 4.2: A flow chart of the method.

4.2. Conceptual design

The method to design a concept for the fully electric towing vehicle is composed of four parts. First the operational concept will be discussed, followed by the operational design requirements. Third, the methods used to determine the technical design will be discussed. Lastly, the method to determine the kinematic performance of the technical concept using a dynamic model will be explained.

4.2.1. Operational concept

Three models of fully electric towing vehicles will be designed. Each model will be compatible with a different category of aircraft as aircraft vastly differ in weight and dimensions. The category definitions are stated in Table 4.1. In general, the single-aisle aircraft fall in the medium category (excluding the Boeing 757), the double-aisle aircraft fall in the heavy category, and the double decker aircraft fall in the super heavy category.

Table 4.1: The definitions of the aircraft gross weight categories.

Category	Aircraft weight
Medium	weight ≤ A321
Heavy	A321 < weight < B747
Super heavy	weight ≥ B747

The concept of operational towing is based on the towing of aircraft between two locations with the engines shut off, with the purpose to save fuel. The fuel consumption is reduced as the towing vehicles are more fuel efficient at transporting the aircraft than the aircraft itself. The concept of fully electric towing is based on operational towing with electrically powered towing vehicles to save even more fuel. For addition fuel reduction, the fully electric towing concept includes the abstinence of auxiliary power unit (APU) use during taxiing.

Operational towing can be done by two types of tow trucks. The first type uses a tow bar that connects the tow truck to the noselanding gear of the aircraft. The second type is a towbarless option where the noselanding gear is mounted into the tow truck. In this research a towbarless design will be used. The main advantages of towbarless towing are better manoeuvrability and increased traction. The latter is due to part of the aircraft weight resting on the towing vehicle, which produces extra downforce. The fully electric towing vehicles will be all wheel drive in order to make maximum use of the downforce.

It is assumed that the fully electric towing vehicles are automated guided vehicles (AGV) and can drive around autonomously. The towing vehicles will have the option to be driven by humans if needed. In this research it is assumed that the towing vehicles will not remain with the aircraft during the turn-around time, but continue on to the next assignment. In this way, costs are reduced as less towing vehicles are needed.

Rechargeable batteries will be used to power the vehicles instead of hydrogen fuel cells or a conductor rail. The reason for not using hydrogen fuel cells is because they are expensive, complicated and dangerous to operate, and the high energy density is not essential in this electric towing concept. The conductor rail option is neglected because it restricts the towing vehicles to the conductor rail, and the rail has to be resistant to the weight of an aircraft. A battery powered concept is relatively safe, gives the towing vehicles freedom, and electricity is widely available. The high weight of batteries is advantageous as it helps produce traction. The downside of a battery concept is that it requires battery charging. The fully electric towing vehicles will have to charge at a depot in between tows or whilst waiting for an aircraft (if the aircraft stand has charging facilities). It is expected that all towing vehicles return to the depot if the vehicle is inactive for longer periods of time.

In order for the APU and main engines to be shut off during the taxi process, the fully electric towing vehicle needs the ability to take over their functions. These functions are providing the aircraft with cooling or heating, power for the on-board systems, and power or air for the engine start up. Ground service equipment exist that have exactly these functions. A preconditioned air unit (PCA) is a type of ground service equipment (GSE) that provides the aircraft with heated or cooled air. A ground power unit (GPU) is a type of GSE that provides the aircraft with power, and the air start unit (ASU) is a type of GSE that provides electricity or compressed air to start the engine. Commonly these types of equipment are bulky machines located on the aircraft stand. The concept design for the fully electric towing vehicle will integrate these systems into the vehicle. The electric power can be directly provided from the batteries. The ASU and PCA can be combined as both systems compress air. For an engine start highly compressed air will be used. The system will switch to low pressure air for heating and cooling. Heating elements and direct expansion will be used to heat or cool the air, respectively.

Intervention from ground personnel will be required to connect and disconnect the power cable and air ducts leading to the aircraft. One of the challenges with a fully electric towing system concept is providing a smooth transition between power sources, i.e. the ground power unit and the fully electric towing vehicle. The switch in power source will have to go almost instantaneously to prevent systems from shutting off. This can be achieved is by using a y-shaped power cable, where one of the short ends is connected to the towing vehicle, the other short end is connected to the GPU, and the long end is connected to the aircraft. A switch can be used to switch between the short ends, thus changing the power source instantaneously. This will also solve the problem in the case the GPU runs on AC current, whilst the towing vehicle will always provide DC current.

As the towing vehicles are shared between the aircraft and do not remain with a specific aircraft during the turnaround time, the power cables have to remain with the aircraft to ensure a continuous supply of power. Therefore, upon arrival of an aircraft, the power cables should be provided to the aircraft at the runway exit ramp, and deposited at the runway in the case of a departure. Another option is that the towing vehicle is supplied with a power cable before heading to the pick up location of an arriving flight, and the power cable is returned to the depot after dropping off a departing flight. Both options will require the management of power cables.

As the procedure differs between a taxi-in and a taxi-out tow, the steps in each process will be described. With a departing tow, the towing vehicle will arrive at the aircraft at a couple of minutes before departure. The towing vehicle will have come from the towing vehicle depot or from a previous tow. The noselanding gear will be mounted into the towing vehicle, the electricity cable will be connected from the aircraft to the towing vehicle, and the air ducts will be connected from the towing vehicle to the aircraft. The towing vehicle will supply preconditioned air and electricity as soon as the connections are made. Once the aircraft is released, the towing vehicle will perform a pushback, followed by a tow towards the runway. In order for the towing vehicle to be fast yet energy efficient, the vehicle will accelerate as fast as possible to the maximum allowed velocity. When approaching a turn, the vehicle will coast to slow down instead of braking to avoid wasting unnecessary energy. Braking is performed only when the taxiway straight is insufficiently long to coast to the required velocity to take the turn. Some of the kinetic energy will be recovered to partially recharge the towing vehicle batteries if the brakes are applied. As the aircraft engines need to be warmed-up before flight, the engines have to be started during the tow. The first engine will be started using the ASU or electric starter on-board the towing vehicle, after which bleed air from the first engine is used to start the other engine(s). The engine start requires high power, therefore it may be necessary for the towing vehicle to perform the first engine start during deceleration or standstill, and the supply of PCA may have to be paused. The engine start should take 30-60 seconds. Once the first engine has started, the towing vehicle is no longer required to provide preconditioned air and electricity as the first engine will have taken over these tasks. The towing vehicle will continue towing the aircraft towards the runway. Having arrived at the runway, all cables and ducts will be disconnected by ground personnel, and the aircraft will be dismounted from the towing vehicle. This moment marks the end of the tow, and the towing vehicle will either return to the towing vehicle depot or head to another aircraft.

The taxi-in procedure is comparable to the taxi-out but in the reverse order. Also, the engine is shut off instead of started. The fully electric towing vehicle will wait at a designated spot near the exit ramp, shortly before the arriving aircraft lands. The aircraft is mounted onto the towing vehicle once it has arrived at the exit ramp, and all cables and ducts will be connected by ground personnel. Preconditioned air and electricity will not yet be supplied. As with the taxi-out, towing will be done with maximum acceleration and minimum braking. The fully electric towing vehicle will start supplying air and electricity when the aircraft engines have cooled down enough to be shut off. Upon arrival at the aircraft stand, the towing vehicle will be dismounted and disconnected form the aircraft and the GSE will take over. This moment marks the end of the taxi-in and the towing vehicle will continue to the next aircraft or return to the depot to charge.

This is the operational concept in summary, which is the context in which this research will be performed. Next, the operational design requirements will be discussed.

4.2.2. Operational design requirements

The technical design of the fully electric towing vehicle models is dependent on technical and operational requirements. The added value of a design increases the better it fulfils its tasks. As airports differ, the operational design requirements should be studied per airport so that they can be considered in the design process.

The layout of an airport is an aspect that is different for most airports. The layout affects the towing distances, but also the distances travelled by the towing vehicles when ferrying between aircraft. The distances in turn affect the towing vehicle energy consumption and travel duration. Longer distances require more energy and time than short distances. Therefore, the airport layout should be studied so that the design takes into account the distance requirements. Next to the layout, the runway usage should be investigated. The runway usage tends to differ between runways due to conditions or airport preferences. The towing system should be designed to have the greatest fuel reduction potential, which may require the design to focus on the most active runways only. For example, there is little added value for a design that has a good endurance performance and a bad sprint performance, if most tows are short distances. The runway usage should be separated in arrivals and departures, as the distance from the exit ramp to the gate is different from the distance from the gate to the runway start location. The frequency of aircraft movements should also be taken into account when designing the models. A high frequency will require a high number of tows within a period of time. This will either require a large fleet of towing vehicles or the towing durations should be shortened by making the towing vehicles faster. The types of aircraft that require towing will influence the vehicle designs. Even though the aircraft are categorized in three groups, the aircraft type composition should still be taken into account. For example, if 90% of the flights are with a certain aircraft type, and the remaining 10% of the flights are with another aircraft type in the same category, the towing vehicle design should focus on the first type to maximize the fuel reduction effectiveness. Therefore, the aircraft type composition at the airport should be studied. The wheel loading of the towing vehicle on the taxiways may be a design limitation. As the taxiways are not designed for operational towing, the taxiways may get damaged due to the heavy weight of the towing vehicle. The impact on the taxiway is extra large due to the high velocities of operational towing compared to a pushback on the apron. The towing vehicle design may have to weigh less to reduce the wheel loading. Another operational requirement is the climate. Warm weather requires extra energy to cool the aircraft, and cold weather requires extra energy to heat the aircraft. Therefore, the number of hot and cold days per year affect the energy consumption of the towing vehicle, which should be taken into account in the design.

These were some of the operational design requirements that should be considered in the design process of the technical concept. Next, the method to determine the technical design will be discussed.

4.2.3. Technical design requirements

To test the feasibility of a fully electric towing concept a technical design is needed. The technical design in this research will remain a high level and abstract design, as the general concept is tested and not a specific detailed design. Only, when the general concept is promising, should time be invested in a highly detailed design. The two main design aspects in this research are the towing vehicle weight and the batteries, from which the performance can be derived. The methods used to determine the towing vehicle weight and battery requirements will be discussed in the coming parts.

The design weight
The towing vehicle weight plays an important role in the design for the following reasons. The weight of the vehicle contributes to the amount of traction the vehicle can be produced. Traction is important to prevent the powered wheels from spinning. Towing an aircraft requires a lot of power that has to be transferred to the wheels without wheel spin. If the traction is too low, the towing vehicle will not be able to tow an aircraft forward. Also, the more traction the towing vehicle has, the faster the vehicle can accelerate. Weight is also important for dynamic stability. As the aircraft momentum is great at high towing velocities, the reaction forces between the aircraft and the towing vehicles will be large. By increasing the mass of the towing vehicle, the inertia of the towing vehicle is increased making it more resistant to the reaction forces. The design weight of the towing vehicle will also determine the amount of batteries the towing vehicle can hold, which in turn will determine the maximum power that can be supplied, and the total battery capacity. The number of batteries that can be added to the vehicle increases with the design weight.

The previous reasons all advocate for a high design weight, but increasing the weight will increase the power required to accelerate the vehicle. As a result the energy consumption will increase and the endurance of the towing vehicle will decrease. A balance has to be found between performance and energy cost.

The towing vehicle weight will be sized using reference literature. TaxiBot is currently the most successful (hybrid-)electric towing system. Unfortunately, the only a few technical specifications of the TaxiBot are made public, which does not include the TaxiBot weights. An economic feasibility study on the TaxiBot by Hospodka [9] states that the wide-body TaxiBot has approximately 1119 kW of power and can tow an Airbus A380 up to 10.3 m/s. Hospodka also states that the narrow-body TaxiBot has the high speed record of towing an Airbus A320 up to 11.8 m/s. However, nothing is stated about the aircraft weight, so the TaxiBot masses can not be derived from this information. A study by Guillaume [8] estimates the weight of the narrow body TaxiBot to weigh 10,000 kg and the wide body TaxiBot to weigh 50,000 kilograms.

Information on pushback trucks is more widely available. The Goldhofer AST-1X towbarless pushback truck is able to tow aircraft weighing up to 600,000 kg using a 500 kW engine. The pushback truck weighs 30,000 kg and is able to produce a maximum tractive force of 212 kN. The Goldhofer AST-2X 490 towbarless pushback truck is capable of high speed towing and compatible with aircraft weighing up to 352,000 kg, i.e. Boeing 737-300 to Airbus A340-200. The Goldhofer AST-2X 490 weighs 15,900 kilograms. Its maximum towing speed is 8.9 m/s, the maintenance towing speed with 60% of the maximum aircraft weight is 8.3 m/s, and a pushback speed with maximum aircraft weight of 3.3 m/s. With a 360 kW engine it can produce a maximum tractive force of 125 kN. From these examples, it can be concluded that the fully electric towing vehicles should be more powerful and heavier in order to reach 14 m/s with a fully loaded aircraft.

The design weights of the fully electric towing vehicles will be determined through an iterative process. First an estimated guess of the weights will be made for each model based on the the previous information. After the performance of the design is tested using a dynamic model of the system, the design weight will be adapted until the model shows the desired performance.

Next to the design weight, the power source of the vehicle is important to the design. Batteries are used in the case of the fully electric towing vehicle. The amount of batteries will determine the endurance of the towing vehicle, but also the power supply ability. First the method to determine the power demand by the towing vehicle will be explained, after which the method to determine the energy demand will be given. Once the power and energy demand is established, a type of battery can be selected for the conceptual design, and the amount of batteries needed. The power demand consists of four parts: the power required for transportation, the power required for the on-board systems, the power required for engine start up, and the power for providing air conditioning or heating.

The power demand
The power demand for transportation can be estimated by the power required to propel the towing vehicle and aircraft forward up to the maximum required velocity. The thrust force (tractive force) as a result of the motor power should exceed the drag force composed of the wheel ground drag, aerodynamic drag, and the weight component due to inclination. However, aerodynamic drag is negligible compared to ground drag at low velocities, which can be shown numerically using Equation 4.1:

$$\frac{D_{aero}}{D_g} = \frac{C_{D,ac}\frac{1}{2}\rho V^2 S + C_{D,t}\frac{1}{2}\rho V^2 A}{\mu_g(N_{ac}+N_t)} < 5\% \qquad \forall V \leq 15 m/s \tag{4.1}$$

where μ_g is the ground drag coefficient, ρ is the air density, A is the front cross sectional area of the towing vehicle in m^2, $C_{D,ac}$ is the coefficient of aerodynamic drag of the aircraft, $C_{D,t}$ is the coefficient of aerodynamic drag of the towing vehicle, D_{aero} and D_g are the aerodynamic drag and wheel ground drag respectively, N_{ac} is the normal force of the aircraft, N_t is the normal force of the towing vehicle, S is the wing surface area of the aircraft in m^2, and V is the velocity in m/s.

The power available on the wheels of the towing vehicle should exceed the power required to tow the aircraft-towing vehicle system at maximum velocity, as shown in Equation 4.2. It must be noted that this equation assumes that the taxiway has zero percent inclination. The specific power can be calculated using Equation 4.3. The power provided by the electric motor(s) of the fully electric towing vehicle will have to take into account power lost due to inefficiencies.

$$P_a \geq (P_r)_{max} = D_g \cdot V_{max} = \mu_g mg \cdot V_{max} \tag{4.2}$$

$$P_s = \frac{P_a}{m} \geq \mu_g g \cdot V_{max} \tag{4.3}$$

where P_a is the power available at the wheels in W, P_r is the power required at the wheels in W, P_s is the specific power at the wheels in W, g is the acceleration of gravity, and m is the total mass of the towing vehicle and aircraft in kilograms. The minimum power demand will be estimated as the product of the specific power and the mass of the towing vehicle with the heaviest aircraft type in its category. Next method to determine the on-board power will be discussed.

The on-board systems requiring power include: lighting, the flight instruments, the entertainment systems, the galley systems, and the anti-icing system. As on-ground anti-icing is a seldom occurrence, the towing vehicle will not be required to provide power for the on-board anti-icing systems. The electricity demands vary depending on which systems are on. A study by Rensen [15] estimates the average power demands per ICAO aircraft category. These demands are given in Table 4.2, and will used in this thesis as well.

Table 4.2: The estimated electrical load per ICAO aircraft approach category.

ICAO aircraft category	Electrical load [kW]
C	3.7
D	14.1
E	21.8
F	33.9

The engine start-up of the first engine is conventionally done using the APU or the air start unit (ASU). An ASU works by blowing pressurized air into an engine duct, propelling a turbine connected (by a clutch) to the compressor of the engine. When the compressor rotates fast enough, fuel is ignited in the combustion chamber to complete the engine start-up. This process should take approximately 30-60 seconds. Air starter units are rated in pounds per minute (PPM), referring to the mass flow of air and the pressure they can produce. Larger engines require ASUs with higher PPM ratings than smaller engines. It is possible for small engines to use ASUs with high PPM ratings, but these ASUs require more power, are bulkier, and are heavier. The General Electric GE90 engines, commonly used on the Boeing 777, are the largest and most powerful jet engines used by airlines. As the Boeing 777 is classified as a heavy category aircraft, the heavy category towing vehicles require the most powerful category of ASU. From reference ASU models it is estimated that ASUs with the properties displayed in Table 4.3 should be powerful enough for all aircraft in that category.

Table 4.3: The required ASU properties per aircraft category.

Aircraft category	PPM [lbs/min]	Pressure [kPa]	Power [kW]
Medium	270	290	384
Heavy	400	290	783
Super Heavy	400	290	783

Next, the method to determine the power demand for preconditioned air is explained. The power demand for the preconditioned air highly depends on the outside air temperature. The method is largely based on the thermodynamic method used by Rensen [15], which calculates the amount of work required by the PCA to condition the air to the desired temperature. The following assumptions are made:

1. the air flow in the aircraft is a steady flow process;
2. the mass flow of the air and electrical loading is constant per ICAO aircraft approach category;
3. the type of PCA unit used is a Direct Expansion (DX) unit;
4. the Coefficient of Performance of the DX-unit is 3 [-];
5. the solar loading is constant regardless of the number of closed windows;
6. the passenger load factor is assumed to be 1.0;
7. the conduction constant per ICAO aircraft approach category is constant;

Figure 4.3 shows a graph of the temperatures at different locations in the process, where T_1 is the ambient temperature outside the aircraft, T_2 is the air temperature directly behind the heating/cooling unit, T_3 is the temperature of the air entering the cabin, and T_4 is the desired air temperature in the cabin. The blue line represents the temperatures in a cooling process, and the red line represents the temperatures in a heating process. All temperatures are in degrees Celsius.

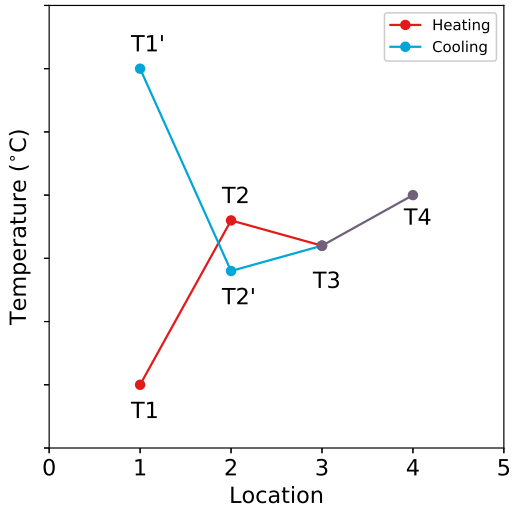

Figure 4.3: Temperature stages of the PCA heating/cooling process.

Temperatures T_1 and T_4 are known and by working backwards, from the cabin to the PCA, T_2 and T_3 can be determined. The first law of thermodynamics (see Equation 4.4) can be used to calculate the required temperature of the air entering the cabin (T_3). Q is the thermal energy of the system, W is the work done by the system, E is the total energy of the system, U is the internal energy of the system, KE is the kinetic energy of the system, and PE is the potential energy of the system.

$$Q - W = \Delta E = \Delta U + \Delta KE + \Delta PE \tag{4.4}$$

With no changes in kinetic and potential energy, thermal energy equals to the change in enthalpy. In this equation p is the pressure in pascals, V is the volume in cubic meters, and H is the enthalpy in joules.

$$Q = \Delta U + W = \Delta U + p\Delta V = \Delta H \tag{4.5}$$

With a constant mass flow, Equation 4.5 can be converted to Equation 4.6 to include time into the equation. In this equation $\dot{Q}$ is the flow of thermal energy in Watt, $\dot{m}$ is the mass flow of air in kilograms per second, and h is the specific enthalpy in joules per kilogram.

$$\dot{Q} = \dot{m}\Delta h \tag{4.6}$$

The heating of the air between location 3 and 4 is an isobaric process, therefore Equation 4.7 may be substituted in Equation 4.6 to get Equation 4.8, where c_p is the specific heat capacity at constant pressure in joules per kilogram Celsius, and T is the air temperature.

$$\Delta h = c_p \Delta T \tag{4.7}$$

$$\dot{Q}_{34} = \dot{m} c_p (T_4 - T_3) \tag{4.8}$$

The temperature rise in the cabin is caused by the thermal conduction of the aircraft hull as a result of the temperature difference between the interior and exterior of the aircraft, the solar radiation entering the aircraft through the windows, and the heat produced by the on-board instrumentation and occupants. The thermal loading in the cabin $(\dot{Q}_{34})$ equals to the sum of the loads given in Equations 4.9-4.10 and Table 4.2. $\dot{Q}_{occupancy}$ is the heat produced by on-board instruments and occupants, $\dot{Q}_{solar}$ is the solar radiation, $\dot{Q}_{conduction}$ is the heat flow through thermal conduction, N_{pax} is the number of passengers, $N_{windows}$ is the number of windows, k is the thermal conductivity coefficient in Watt per meter Kelvin, A is the surface area of the fuselage, and L is the fuselage thickness (including insulation panels) in meters. The electrical load $(\dot{Q}_{elec})$, estimated by Rensen [15], can be determined from Table 4.2.

$$\dot{Q}_{occupancy} = N_{pax} \cdot 65 \tag{4.9}$$

$$\dot{Q}_{solar} = N_{windows} \cdot 45 \tag{4.10}$$

$$\dot{Q}_{conduction} = k \cdot \frac{A}{L} \cdot (T_1 - T_4) \tag{4.11}$$

After the thermal loads are summed to get $\dot{Q}_{34}$, Equation 4.8 can be rearranged to determine T_3. The air temperature is assumed to increase by 10% in the ducts between the PCA unit and the cabin in the case of cooling. Therefore, temperature, T_2, can be determined by Equation 4.12. In the case of heating, the temperature in the duct is assumed to decrease by 10%. In that case, the temperature at location 2 can be determined using Equation 4.13.

$$T_2 = \frac{T_3}{1.1} \tag{4.12}$$

$$T_2 = \frac{T_3}{0.9} \tag{4.13}$$

The power demand of the PCA-unit itself is composed out of the power required for the fan, controls, and for the heating/cooling of the air. The first two power requirements can be determined from Table 4.4.

Table 4.4: The assumed PCA-unit characteristics per ICAO aircraft approach category.

Characteristic	C	D	E	F
Mass flow [kg/s]	2.0	5.2	5.5	6.5
PCA-unit control power [kW]	10.0	10.0	10.0	10.0
PCA-unit fan power [kW]	10.0	20.0	26.0	30.0

The power demand for the heating/cooling can be calculated using Equation 4.14. The enthalpies at point 1 and 2 can be determined using a psychometric chart as the relative humidity and temperatures are known at both points, the mass flow can be determined from Table 4.4 and the coefficienct of performance (COP) of the direct expansion unit is assumed to be 3.

$$P_{heating/cooling} = COP \cdot \dot{Q}_{12} = COP \cdot \dot{m}(h_2 - h_1) \tag{4.14}$$

The total power required by the PCA can be calculated by Equation 4.15

$$P_{PCA} = P_{heating/cooling} + P_{control} + P_{fan} \tag{4.15}$$

The energy demand

The total energy required for a tow consists of two parts: the towing vehicle ferrying to a tow and the tow itself. The energy demand for the ferry is solely the energy required for the towing vehicle to relocate. The energy demand during the tow depends on the duration of the processes involved. A taxi-in tow requires power for transportation, pre-cooled air and the on-board systems. A taxi-out requires the same processes plus the engine start up, and the power supplication pre-release.

The energy demand for transport depends on the kinematics of the tow. The other process are assumed to require a constant power, therefore the energy demand is dependent on the duration of each process. The durations of power for the on-board systems and PCA differ between taxi-in and taxi-out because of the amount of time the main engines are on. It is assumed that the engine warm-up time takes longer than the engine cool-down time. Also, additional energy is supplied during the taxi-out as the towing vehicle starts supplying power moments before the aircraft release, when the ground power gets disconnected.

Assuming it takes three minutes between the disconnection of ground power and the aircraft release, the engine warm-up time takes five minutes, the engine cool down-time takes 2.5 minutes, and the engine start-up time takes 45 seconds the total duration each process requires power can be calculated. An overview of the durations for taxi-out is given in Table 4.5, and an overview of the durations for taxi-in is given in Table 4.6.

Table 4.5: The duration of each (non-transport) taxi-out process.

Process	Pre-release [min]	Taxi-out (engines off) [min]	Engine start-up [min]	Taxi-out (engines on) [min]	Total duration [min]
On-board systems	3	transportation time - 5	0.75		transporation time - 1.25
Pre-conditioned air	3	transportation time - 5			transporation time - 2
Air starter unit			0.75		0.75

Table 4.6: The duration of each (non-transport) taxi-in proccess.

Process	Taxi-in (engines on) [min]	Taxi-in (engines off) [min]	Total duration [min]
On-board systems		transportation - 2.5	transportation - 2.5
Pre-conditioned air		transportation - 2.5	transportation - 2.5

The energy demand of each process can be calculated by multiplying the durations and power demand of each process. The energy demand for transportation needs to be determined through simulations of each tow. The energy required for the tow (excluding ferrying) can be determined using Equation 4.16. For the initial towing vehicle design, before the simulations, the energy demand will be predicted by estimating the durations.

$$E_{tow} = P_{on-board} \cdot t_{on-board} + P_{PCA} \cdot t_{PCA} + P_{ASU} \cdot t_{ASU} + \int P_{transport} \cdot dt_{transport} \tag{4.16}$$

Battery requirement

The minimum amount of batteries required can be estimated once the power and energy demand are estimated. First a battery type should be chosen that will be used in the vehicle. The battery will either be a type of lithium-ion, nickel-cadmium, or lead acid battery because they have to be safe and rechargeable. Using the specific power, specific energy, and energy density of the battery type, the minimum amount of batteries will be calculated to fulfil the power and energy demand. One of the three battery properties will be the limiting factor. The minimum battery requirement will be taken into account in the design process. An iterative design approach will be used to come to a final design to ensure the design fulfils all requirements. Once a technical design is established, its kinematic performance will be tested using a dynamic model. The method to test the kinematic performance will be explained in the next section.

4.2.4. Kinematic performance

A dynamic model of the technical design towing an aircraft will describe the motion of the system. The model consists of equations describing the forces on the system, which can be solved for the resultant motion of the system. A free body diagram of the towing vehicle-aircraft system is shown in Fig. 4.4.

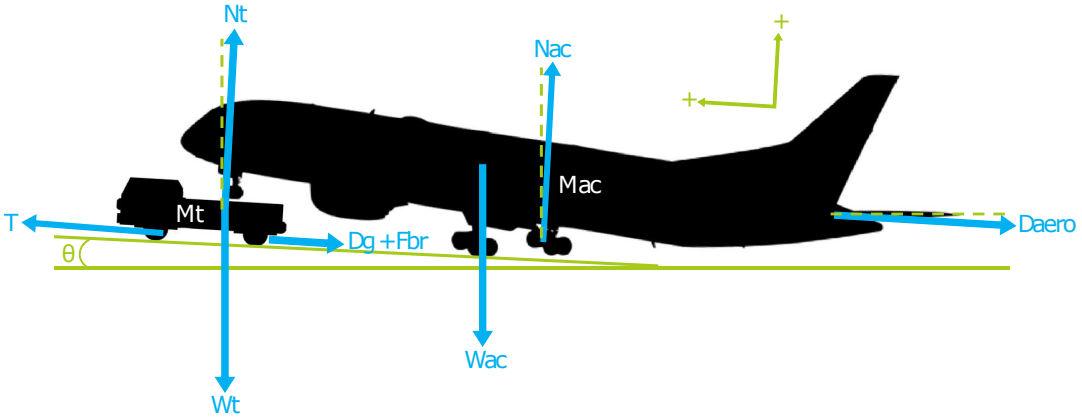

Figure 4.4: A free body diagram of dynamic system

where θ is the slope angle of the ground in radians, D_{aero} is the aerodynamic drag, D_g is the wheel ground drag, F_{br} is the braking force, N_t is the normal force acting on the towing vehicle, N_{ac} is the normal force acting on the main landing gear, T is the thrust force generated by the towing vehicle, W_{ac} is the weight of the aircraft on the main landing gear in Newtons, W_t is the weight of the aircraft on the nose landing gear plus the weight of the towing vehicle in Newtons, m_{ac} is the mass of the aircraft, and m_t is the mass of the fully electric towing vehicle. The equations describing the system will be derived from Newton's laws of motion in the next part. It must be noted that the acceleration perpendicular to the direction of motion is zero as the aircraft produces insufficient lift during taxiing to become airborne. Therefore, only equations of motion in the longitudinal direction are required. Applying Newton's second law of motion to the free body diagram yields Equation 4.17:

$$T - D_g - D_{aero} - F_{br} - (W_t + W_{ac})\, sin\theta = (m_t + m_{ac})\, a \tag{4.17}$$

Normal forces, N_{ac} and Nt

A part of the aircraft rests on the nose landing gear and the remaining weight rests on the main landing gear. The model assumes a towbarless situation, where the weight of the aircraft is used for downforce on the towing vehicle. Hence, the normal force at the tug wheels is given by Equation 4.18, and the normal force at the main landing gear is given by Equation 4.19.

$$N_t = \left(c_{NLG} m_{ac} + m_t\right) g cos\theta \tag{4.18}$$

$$N_{ac} = c_{MLG} m_{ac} g cos\theta \tag{4.19}$$

c_{NLG} and c_{MLG} are coefficients representing the weight distributions of the aircraft weight on the nose- and main landing gears respectively. The sum of the weight coefficients equal to one, as shown in Equation 4.20.

$$c_{NLG} + c_{MLG} = 1 \tag{4.20}$$

Thrust force, T

It is assumed that all the thrust is generated by the tug, and no thrust is produced by the aircraft engines when idle. All thrust is caused by the tractive force between ground and towing vehicle wheels. The thrust force can therefore never exceed the traction limit. The amount of thrust is determined by the input power of the tug drive train, and can be controlled.

Rolling resistance, D_g

The rolling resistance is the drag caused by the deformation of the aircraft and tug tires, and by any parts of the wheel resisting the motion of a turning wheel. The kinetic energy of the wheels is partially converted into heat. The rolling resistance is proportional to the normal force perpendicular to the rolling wheel and is approximated by the rolling resistance coefficient, μ_g. This coefficient depends on the tire and road surface, but is assumed to be the same for the tug and aircraft wheels for simplification. Therefore, Equation 4.21 can be used for the rolling drag of the entire system.

$$D_g = \mu_g N = \mu_g \left(m_t + m_{ac}\right) g cos\theta \tag{4.21}$$

Aerodynamic drag, D_{aero}

Both the tug and the aircraft will experience some aerodynamic drag. However, the aerodynamic drag can be neglected as mentioned earlier. For completeness, the aerodynamic drag caused by the aircraft and towing vehicle can be given by Equation 4.22.

$$D_{aero} = D_{ac} + D_t = C_{D,ac} \frac{1}{2} \rho V^2 S + C_{D,t} \frac{1}{2} \rho V^2 A \tag{4.22}$$

In this equation, $C_{D,ac}$ is the coefficient of drag of the aircraft, $C_{D,t}$ is the coefficient of drag of the towing vehicle, ρ is the air density, V is the true airspeed, and S is the wing surface area, and A is the characteristic frontal area of the towing vehicle.

Braking force, F_{br}
The braking force is a friction force between tires and surface. In the dynamic model it is assumed that the towing vehicle does the braking. However, the dynamic model can be altered, so that the aircraft does the braking, or that both the aircraft and the tug brake. The braking force is approximated by Equation 4.23.

$$F_{br} = c_{br}\mu_{br}N_{br} \tag{4.23}$$

In this equation, c_{br} is a coefficient representing the intensity of the braking. mu_{br} is the braking coefficient, and N_{br} is the normal force acting on the braking wheels.

Slope, F_{slope}
The ground inclination or slope causes of forward or backward component of the weight. The magnitude of this component can be calculated using Equation 4.24.

$$F_{slope} = Wsin\theta = (W_{ac} + W_t)sin\theta = (m_{ac} + m_t)gsin\theta \tag{4.24}$$

The inclination angle, θ, is positive for uphill slopes, and negative for downhill slopes. Assuming the slope is zero over the taxiways, Equation 4.17 can be simplified to:

$$T - D_g - F_{br} = (m_{ac} + m_t)a \tag{4.25}$$

The dynamic model will be applied to three kinematic phases: acceleration, constant velocity, and deceleration.

Acceleration phase
During acceleration the thrust needs to be larger than the drag. The larger the thrust, the faster the acceleration. Torque to the wheels is produced by motor, which is converted to thrust as the resultant tractive force between ground and wheels. Therefore, the thrust can never exceed the maximum friction between tire and ground (F_{fr}). Wheel spin will occur if too much torque is supplied. This implies that not all of the power available by the engine can be applied to accelerate when the traction is limiting. Thus, the maximum thrust (T_{max}) and maximum applicable power ($P_{max,applicable}$) when traction is limiting is given by Equations 4.26 and 4.27 respectively.

$$T_{max} = F_{fr} = \mu_{fr}N_t = \mu_{fr}(c_{NLG}m_{ac} + m_t)g \tag{4.26}$$

$$P_{max,applicable} = T_{max}V = F_{fr}V \tag{4.27}$$

The maximum power available by the motor is finite. At a certain point, the maximum power available will be limiting instead of the traction. As a result, the thrust will decrease with velocity, until the thrust equals the drag at the maximum velocity, and the acceleration is zero. In this phase, the maximum thrust and maximum applicable power is given by Equations 4.28 and 4.29 respectively.

$$T_{max} = \frac{P_{max,available}}{V} \tag{4.28}$$

$$P_{max,applicable} = P_{max,available} \tag{4.29}$$

During acceleration it is assumed the brakes are not applied and thus the braking force is zero.

$$F_{br} = 0 \tag{4.30}$$

Figure 4.5, demonstrates the relationships between the maximum thrust and maximum applicable power as a function of velocity. The left side of the diagram is the phase where traction is limiting, and the right side of the diagram is the phase where the available power is limiting.

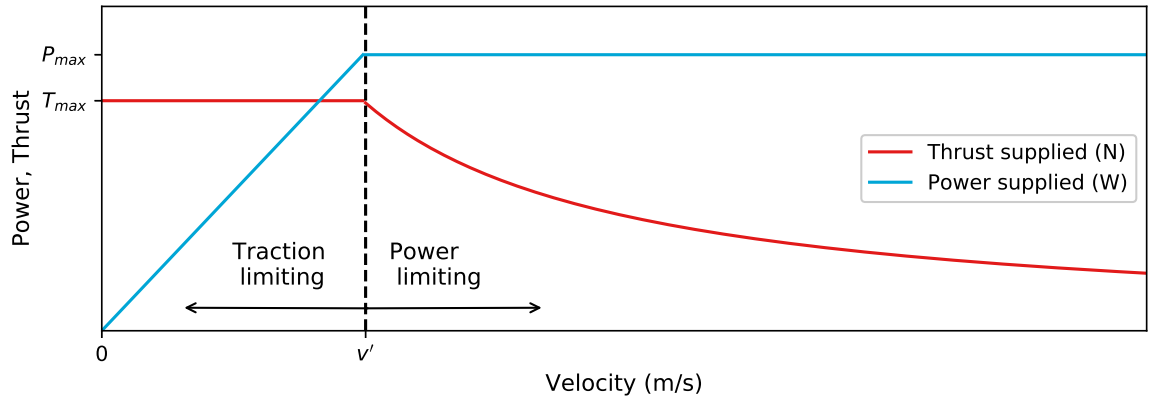

Figure 4.5: The behavior of the maximum thrust and the maximum applicable power as a function of velocity.

Constant velocity phase
The thrust equals the drag at constant velocity. Additionally, it is assumed that the brakes are not applied when traveling at a constant velocity. The equations for thrust, power supplied, and braking force in this mode are the following:

$$T = D = D_g = \mu_g(N_{ac} + N_t) \tag{4.31}$$

$$P_{supplied} = TV = \mu_g(N_{ac} + N_t)V \tag{4.32}$$

$$F_{br} = 0 \tag{4.33}$$

Deceleration phase
It is assumed that no thrust is applied during deceleration. Hence, no power is supplied by the engine. The braking intensity, c_{br}, controls the braking force. With a braking intensity of zero, the system will coast. The equations for the power supplied, thrust and braking applied are the following:

$$T = 0 \tag{4.34}$$

$$P_{supplied} = 0 \tag{4.35}$$

$$F_{br} = c_{br}\mu_{br}(N_{ac} + N_t) \tag{4.36}$$

By solving the ordinary differential equation (Equation 4.25), the distance travelled, velocity, acceleration, thrust, and result force can be determined for every moment in time.

Performance profiles
The dynamic model will be used to determine the performance of each fully electric towing vehicle and aircraft type combination. The performance profiles should be generated for acceleration and deceleration, which can be used to evaluate if the technical design performs realistically and meets the requirements. Any violations of the requirements means that the technical design has to be adapted. The following performance profiles will be generated, where the distance, velocity, and power profiles will be required in Section 4.3. Note that the performance is different for taxi in and taxi out because of the gross weight of the aircraft.

1. distance-time
2. velocity-time
3. acceleration-time
4. power-time
5. thrust-time
6. resultant force-time

This concludes the method to determine the conceptual design. Next, the method to simulate ground movements will be discussed.

4.3. Ground movement simulations

An agent-based model will be used to simulate the aircraft and fully electric towing vehicle in a node and link model of the airport. The aim of each simulation is to determine the fuel and energy consumption, and the duration of the taxi movement. Three situations need to be simulated for the Vehicle Routing Problems in Section 4.4:

1. the aircraft taxiing individually between two locations
2. the fully electric towing system towing an aircraft between two locations
3. the fully electric towing system ferrying (without an aircraft) between two locations

An agent-based simulation consists of two components: the agent and the airport model. The agent is either the aircraft, the fully electric towing vehicle towing an aircraft, or the fully electric towing vehicle without an aircraft. The airport model is a node and link model describing the network of runways and taxiways of the airport. The nodes represent the location of every taxiway intersection and the links represent the taxiways between the intersections. The length and maximum speed limit of each link is known, as well as in which direction(s) the taxiway may be used.

In this method, the agent will follow the shortest route between its origin and destination. Dijkstra's algorithm can be used to determine the shortest route between two nodes, and can be programmed to not violate one way directions. In this method it is assumed that there is no interference of other traffic. Furthermore, a ferrying towing vehicle may use a different network of roads around the airport than an aircraft, and would require an adapted node and link network.

A route consists of a series of connected links, each with corresponding maximum speed limit and distance. In the simulation, the aircraft/towing vehicle will attempt to travel at the speed limit across the link in order to be as quick as possible. As the speed limits can differ between consecutive links, the vehicle may have to accelerate or decelerate. In this method it is chosen to split every link into an acceleration/deceleration phase and a constant velocity phase, as shown in Figure 4.6. In the first part of the link, the vehicle accelerates or decelerates from the final velocity of the previous link to the speed limit of the present link. In the second part of the link, the vehicle travels at a constant velocity for the remaining distance of the link. The goal is to determine the travel duration, energy and fuel consumption across the link.

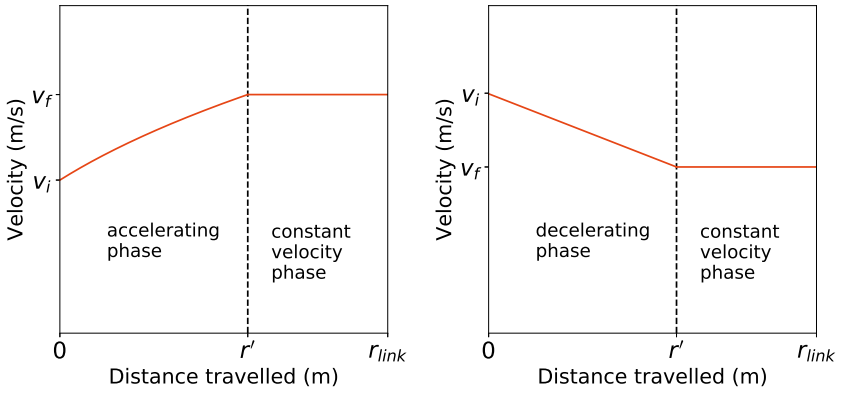

(a) acceleration

(b) deceleration

Figure 4.6: The phases across a link, showing an acceleration scenario in (a), and a deceleration scenario in (b)

In order to simulate the fully electric towing vehicle during the acceleration/deceleration phase of the link, Equations 4.37-4.41 can be used in combination with the performance profiles generated in Section 4.2. Figures 4.7a-4.7c are examples of performance profiles of the aircraft-tug system accelerating, from which the variables for Equations 4.37-4.41 can be determined. Similarly, the profiles for deceleration need to be used in the case of deceleration.

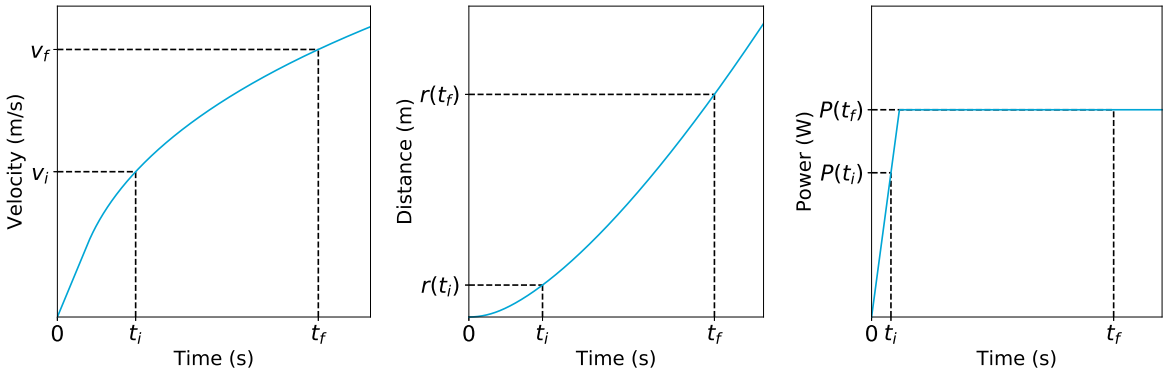

(a) velocity-time

(b) distance-time

(c) power-time

Figure 4.7: The performance profiles of an accelerating aircraft-towing vehicle system.

The initial time is represented by t_i, t_f is the final time, t_{acc} is the acceleration duration, r_{acc} is the distance travelled during acceleration, E_{acc} is the energy consumed during acceleration, P is the power.

$$t_i = t(v_i) \tag{4.37}$$

$$t_f = t(v_f) \tag{4.38}$$

$$t_{acc} = t_f - t_i \tag{4.39}$$

$$r_{acc} = r(t_f) - r(t_i) \tag{4.40}$$

$$E_{acc} = \int_{t_i}^{t_f} P(t)dt \tag{4.41}$$

Similarly, Equations 4.42-4.44 can be used for the constant velocity phase, where r_{const} is the distance travelled at a constant velocity, r_{link} is the length of the taxiway link, t_{const} is the travel duration at constant velocity, v_{max} is the maximum allowed velocity on the link, and E_{const} is the energy consumed travelling at constant velocity.

$$r_{const} = r_{link} - r_{acc} \tag{4.42}$$

$$t_{const} = \frac{r_{const}}{v_{max}} \tag{4.43}$$

$$E_{const} = P(v_f) \cdot t_{const} \tag{4.44}$$

In order to simulate the conventional taxiing aircraft, the same method is applied, but instead of using the performance profiles, it is assumed that aircraft accelerates and decelerates at 0.7 m/s^2 [6]. Newton's laws of motion are used to calculate the acceleration duration and distance. The thrust setting by the aircraft engines is required to determine the fuel consumption and emission production. The thrust setting during acceleration can be approximated using Equation 4.45, and the thrust setting at constant velocity or deceleration is assumed to be the thrust setting at idle. The fuel consumption during each phase can be estimated by Equation 4.46.

$$T_{\%} = \frac{M_{ac}a + \mu_g M_{ac} g}{n \cdot F_{rated}} \tag{4.45}$$

$$f = \frac{T_{\%}}{T_{\%,idle}} \cdot FF \cdot t \cdot n \tag{4.46}$$

where $T_{\%}$ is the thrust setting of the aircraft engines in percent, $T_{\%,idle}$ is the thrust setting of the aircraft engines at idle in percent, n is the number of aircraft engines, F_{rated} is the thrust rating of the aircraft engine in Newtons, FF is the fuel flow in kilograms per second, a is the average acceleration, f is the fuel consumed in kilograms, and t is the duration of the phase in seconds.

The mass of each emission produced by the aircraft can be determined using Equation 4.47, with the majority of the emissions consisting of carbon monoxide, carbon dioxide, hydrocarbons, sulphur oxides and nitrogen oxides. M_x is the emission mass, EI_x is the emission index of the aircraft engine at idle from the ICAO Aircraft Engine Emissions Databank [11], f_{acc} and f_{const} are the fuel consumptions of the two phases.

$$M_x = EI_x \cdot (f_{acc} + f_{const}) \tag{4.47}$$

In certain cases, the taxiway is not long enough for the aircraft or towing vehicle to reach the maximum velocity. In those cases, the final velocity of the link is the maximum attained velocity, which will be used as the initial velocity on the following link. Also, the taxiway can be too short for the towing vehicle to slow down without braking. In those cases, the brakes are applied to decelerate at 1 m/s. Kinetic energy is recovered whilst braking to partially recharge the batteries. The amount of energy recovered can be calculated using Equation 4.48, where η_{gen} is the efficiency of kinetic energy recovery, E_{gen} is the recovered kinetic energy in joules, M_{ac} is the aircraft gross weight in kilograms, M_t is the towing vehicle weight in kilograms, a is the acceleration, and r_{link} is the total distance of the link.

$$E_{gen} = \eta_{gen}(M_t + M_{ac})a \cdot r_{link} \tag{4.48}$$

The total travel duration, energy and fuel consumption, and emission production across the link is the summation of the acceleration phase and constant velocity phase. The result over the entire route is the sum of all the individual links that are part of the route.

As vehicles need to slow down for sharp turns, additional penalties are given for every sharp turn encountered on route. Deciding which turns are sharp is subjective as no data is available on the speeds aircraft or fully electric towing vehicle would take the turn. Furthermore, the radius of curvature changes throughout a turn, and the start and end of the turn are unclear. Therefore, the decision is made by visually assessing an aerial image of the airport. The rule of thumb used in this method is the following: a turn is considered to be sharp if the turn is over 45° and the average radius of curvature is less than 100m.

A fixed time penalty will be assigned for every sharp turn, which will be added on top of the total travel duration of the route. Likewise, an emission penalty is assigned for every sharp turn a conventional taxiing aircraft makes, and an energy penalty is assigned for every sharp turn the fully electric towing vehicle makes. The time penalty for conventional aircraft is 15 seconds per turn and 25 seconds for the electric towing vehicle (as the towing vehicle attempts to avoid braking). The emission penalty is calculated using Equations 4.45-4.47, where the duration is the time it takes to accelerate from 5 to 10 m/s at 0.7 m/s^2 (7.1 seconds). The energy penalty is the maximum available power multiplied with half the time penalty.

The total energy demand for the fully electric towing vehicle (including the energy for on-board systems PCA and ASU) can then be calculated using the power and energy demand methods described in Subsection 4.2.3. The total transportation duration calculated in this section can be substituted in Tables 4.5-4.6.

Fully electric towing still produces emissions during the moments the aircraft engines are on for cool-down and warm-up. Again, it is assumed that the thrust setting of the main engines are idle during these moments, and Equations 4.45-4.47 can be used to calculate the fuel consumption and emission production. The assumed durations of engine warm-up and engine cool-down are 5 and 2.5 minutes respectively.

During conventional pushback the main aircraft engines are assumed to be off and the APU on. The fuel consumption and emission production can be calculated as in previous cases. However, the APU emission indices should be used instead of the main engine emission indices. The duration of pushback is assumed to be three minutes.

The output data of this section will be the travel duration, fuel and energy consumption, and emission production between any two nodes.

4.4. Vehicle routing problem

In this section, the method to determine the effectiveness of a fully electric towing vehicle will be explained. The effectiveness will be measured in terms of the reduction in total aircraft fuel consumption. The effectiveness in emission reduction is approximately linear proportionate the the fuel reduction. The effect the fully electric towing vehicle has on the total fuel and emission reduction can be established by varying the fleet size of electric towing vehicles. At the same time the relationship between the fleet size and total energy consumption can be established. Additionally, the maximum allowable costs of a fully electric towing vehicle unit can be estimated based on the fuel saved.

The maximum fuel reduction can be determined by a scheduling problem, which optimizes the deployment schedule of a fleet of fully electric towing vehicles, that maximizes the fuel reduction. The output of the scheduling problem determines which flights will be towed and which flights will taxi conventionally. However, the number of fully electric towing vehicles in the fleet are limited, and are constrained by time and their battery capacity. Therefore, a Vehicle Routing Problem (VRP) is required to determine the availability of a towing vehicle for a tow. In other words, a VRP is used to solve the scheduling problem. The VRP will determine the optimal set of routes travelled by every towing vehicle to minimize the total fuel consumption at the airport. Using the towing simulations data, the total fuel and energy consumption, and emission production can be calculated. Figure 4.8 gives an overview of the process.

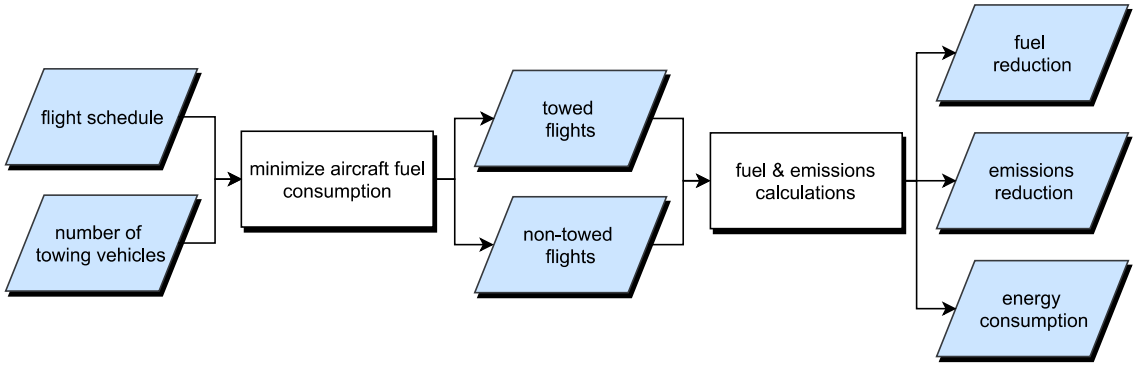

Figure 4.8: A flow chart of the scheduling problem.

A separate vehicle routing problem will be formulated for each aircraft category in order to minimize the computation time. This should not affect the results, as it is assumed that the fully electric towing vehicles can only tow vehicles in their design category. Separate category-based input flight schedules will be used for each problem.

In the following sections, the mathematical formulation of the vehicle routing problem will be explained. First the model assumptions will be stated in Subsection 4.4.1, after which the variables and parameters will be named in Subsection 4.4.2. Next, the objective function is explained in Subsection 4.4.3, followed by an explanation of each constraint in Subsection 4.4.4. Finally, Subsection 4.4.5 will state the outputs of the vehicle routing problem, how to convert them into fuel and emission reduction, and how to calculate the maximum cost of a fully electric towing vehicle.

4.4.1. Assumptions

The following assumptions will be made:

1. the system is ideal;
2. all events occur as scheduled;
3. all towing vehicles are identical and equal;
4. towing vehicles can only tow aircraft in their respective category;
5. the towing vehicle can be fully charged in the minimum charging time;

4.4.2. Variables and parameters

All the variables and parameters required for this optimization problem are listed in this subsection. First, the decision variables are listed, followed by the cost variables, the constants, and the time and energy parameters.

Decision variables
$x_{i,j}^{k,r}$: binary variable; equals one if fully electric towing vehicle k tows flight i and j consecutively in route r.
y_j: a binary variable; equals one if flight j is not towed.

Cost variables
f_j: fuel consumption of flight j when towed by a fully electric towing vehicle.
F_j: fuel consumption of flight j when taxiing using all its aircraft engines.

Constants
N_v: number of fully electric towing vehicles in the uniform fleet.
N_c: maximum number of routs r a towing vehicle k is allowed to make.
N_f: number of flights in the flight schedule.
M: a very large positive integer.

Time and energy parameters
E_j: energy consumption by fully electric towing vehicle towing flight j.
$e_{i,j}$: energy consumption by fully electric towing vehicle transferring between tows of flight i and flight j.
Q: energy capacity of the towing vehicle.
C: minimum towing vehicle charging time.
WC_i: engine warm-up or cool-down time of flight i (dependent on direction).
t_j^a: latest arrival time of a fully electric towing vehicle at the aircraft of flight j.
t_i^f: finish time of the tow of flight i by a fully electric towing vehicle.
$t_{i,j}$: transfer time of a fully electric towing vehicle between tows of flight i and flight j.
$t_{cool-down}$: time required for the engines to cool-down after landing before shutting off.
$t_{warm-up}$: time required for the engines to warm-up before taking off.

4.4.3. Objective function

The objective is to minimize the total fuel consumption. The optimization will select which towing vehicle will tow which flights in order to minimize fuel consumption. The objective function, shown in Equation 4.49, consists of two parts; the left part is the total fuel consumption of towed flights, and the right part is the total fuel consumption of non-towed flights. Every flight will fall into one of two categories.

$$\min z = \sum_{k=1}^{N_v} \sum_{r=1}^{N_c} \sum_{i=0}^{N_f-1} \sum_{j=1}^{N_f} f_j x_{i,j}^{k,r} + \sum_{j=1}^{N_f} F_j y_j \tag{4.49}$$

4.4.4. Constraints

Binary decision variables

The decision variables are binary, thus can only take the values of 0 or 1. An event is selected to be true when the decision variable has value 1, otherwise the event has the value 0 and is false. Equations 4.50 and 4.51 ensure that all decision variables are binary.

$$x_{i,j}^{k,r} \leq 1 \qquad \forall i \in \left\{0,1,...,N_f\right\}, \forall j \in \left\{1,2,...,N_f+1\right\}, \forall k \in \{1,2,...,N_v\}, \forall r \in \{1,2,...,N_c\} \tag{4.50}$$

$$y_j \leq 1 \qquad \forall j \in \left\{1,2,...,N_f\right\} \tag{4.51}$$

Visiting and leaving a flight

All flights should either be towed by or not towed. Additionally, a flight should be visited a maximum of one time by a vehicle. Equation 4.52 combines this into a single equation. Similarly, a flight should be left a maximum of one time by a vehicle, which is translated into Equation 4.53.

$$\sum_{k=1}^{N_v} \sum_{r=1}^{N_c} \sum_{i=0}^{j-1} x_{i,j}^{k,r} + y_j = 1 \qquad \forall j \in \left\{1,2,...,N_f\right\} \tag{4.52}$$

$$\sum_{k=1}^{N_v} \sum_{r=1}^{N_c} \sum_{j=2}^{N_f+1} x_{i,j}^{k,r} + y_i = 1 \qquad \forall i \in \left\{1,2,...,N_f\right\} \tag{4.53}$$

Flow constraint

A number of flights will be towed every route a towing vehicle make. The flow constraint strings those flights into a chronological sequence. The flow constraint is described by Equation 4.54.

$$\sum_{i=0}^{p-1} x_{i,p}^{k,r} - \sum_{j=p+1}^{N_f+1} x_{p,j}^{k,r} = 0 \qquad \forall p \in \left\{1,2,...,N_f\right\}, \forall k \in \{1,2,...,N_v\}, \forall r \in \{1,2,...,N_c\} \tag{4.54}$$

Completing a route

A vehicle should complete a route, if it starts a route. This constraint, shown in Equation 4.55, prevents the vehicle from stopping in the middle of a route, and not returning to the towing vehicle depot.

$$\sum_{j=1}^{N_f} x_{0,j}^{k,r} - \sum_{i=1}^{N_f} x_{i,0}^{k,r} = 0 \qquad \forall k \in \{1,2,...,N_v\}, \forall r \in \{1,2,...,N_c\} \tag{4.55}$$

Route indexation

Every route is indexed in order to distinguish between routes. Equation 4.56 forces the indexes to be consecutive numbers. In combination with other constraints, this will cause the indexes to correctly represent the vehicle route numbers.

$$\sum_{j=1}^{N_f} x_{o,j}^{k,r+1} - x_{o,j}^{k,r} \leq 0 \qquad \forall k \in \{1,2,...,N_v\}, \forall r \in \{1,2,...,N_c-1\} \tag{4.56}$$

Route discrimination
Equations 4.57 and 4.58, prevent routes by the same vehicle to be assigned the same index. Equation 4.57 states that a vehicle k can only leave the towing vehicle depot once every route. Similarly, Equation 4.58 states that a vehicle k can only enter the towing vehicle depot once every route.

$$\sum_{j=1}^{N_f} x_{0,j}^{k,r} \leq 1 \qquad \forall k \in \{1,2,...,N_v\}, \forall r \in \{1,2,...,N_c\} \tag{4.57}$$

$$\sum_{i=1}^{N_f} x_{i,0}^{k,r} \leq 1 \qquad \forall k \in \{1,2,...,N_v\}, \forall r \in \{1,2,...,N_c\} \tag{4.58}$$

Deploying all towing vehicles
Equation 4.59 forces all vehicles to be utilized. This is done by stating that every towing vehicle has to leave the towing vehicle depot on its first round.

$$\sum_{j=1}^{N_f} x_{0,j}^{k,0} = 1 \qquad \forall k \in \{1,2,...,N_v\} \tag{4.59}$$

Rolling horizon
A rolling horizon is implemented to reduce the optimization durations, by decreasing the number of decision variables. With a rolling horizon, two flights can only be stringed together in sequence if they fall within a certain time interval. Additionaly, a rolling horizon prevents the vehicle from waiting on the apron for large amounts of time in between jobs, whilst it could return to the depot in the mean time. Equation 4.60 precludes all combinations of flights from being towed, where the end time of the previous tow t_i^f and the scheduled arrival time at the next tow t_j^a exceed a certain time period, T.

$$\sum_{k=1}^{N_v} \sum_{r=1}^{N_c} (t_j^a - t_i^f) x_{i,j}^{k,r} < T \qquad \forall i \in \{1,2,...,N_f-1\}, \forall j \in \{2,3,...,N_f\} \tag{4.60}$$

Overlap constraint
The overlap constraint prevents the optimizer from selecting connecting tows that overlap in time, or where there is insufficient time for a towing vehicle to ferry in between tows. Equation 4.61 states that the time between the end of the previous tow and the scheduled arrival time of the next tow, should be greater or equal to the time required to ferry between those tows.

$$\sum_{k=1}^{N_v} \sum_{r=1}^{N_c} (t_j^a - t_i^f - t_{i,j}) x_{i,j}^{k,r} \geq 0 \qquad \forall i \in \{1,2,...,N_f-1\}, \forall j \in \{2,3,...,N_f\} \tag{4.61}$$

Energy capacity
The energy required for all tows and ferries between tows on a route should not exceed the energy capacity of the towing vehicle. Equation 4.62 translates this into an equation. It is assumed that the towing vehicle is fully charged when leaving the depot.

$$\sum_{j=1}^{N_f+1} \sum_{i=0}^{N_f} \left(E_j + e_{i,j}\right) x_{i,j}^{k,r} \leq Q \qquad \forall k \in \{1,2,...,N_v\}, \forall r \in \{1,2,...,N_c\} \tag{4.62}$$

Minimum charging time between routes
A route is ended every time a towing vehicle returns to the towing vehicle depot, and a new route is started every time the towing vehicle leaves the depot. There should be sufficient time between the last tow of a route and the first tow of a new route for the vehicle to ferry to and from the depot, and charge in between. Equation 4.63 states that the time at the depot should be larger than the minimum charging time. As

$$\sum_{j=1}^{N_f} \left(t_j^a - t_{0,j}\right) x_{0,j}^{k,r+1} - \sum_{i=1}^{N_f} \left(t_i^f + t_{i,0}\right) x_{i,0}^{k,r} + M - M \sum_{j=1}^{N_f} x_{0,j}^{k,r+1} \geq C \qquad \forall k \in \{1,2,...,N_v\}, \forall r \in \{1,2,...,N_c-1\} \tag{4.63}$$

Short tows
Aircraft engines have to be warmed up before take-off and cooled down before shut down. Equation 4.64 prevents all flights whose engines would be on the entire towing duration from being selected for towing.

$$\sum_{k=1}^{N_v} \sum_{r=1}^{N_c} \sum_{j=1}^{N_f+1} (t_i^f - t_i^s - WC_i) x_{i,j}^{k,r} \geq 0 \qquad \forall i \in \{1,2,...,N_f\} \tag{4.64}$$

4.4.5. Outputs

The problem will be solved using CPLEX. The outputs of the vehicle routing problem are the binary decision variables $x_{i,j}^{k,r}$ and y_j, that state which flights are towed and which flights are not towed. Another output of the optimization is the total fuel consumption which is the resultant value of the minimized objective function. The total emission production can be calculated knowing which aircraft will and will not be towed, together with the taxi simulations results in Section 6.2. The total emission production is the sum of the emissions of all non-towed aircraft plus the sum of the emissions of the towed aircraft. The total energy consumption can be calculated as the sum of the energy required to tow the towed flights plus the energy required to ferry between those tows.

5

Case studies

The feasibility of a fully electric towing vehicle will be investigated for a regional airport and an international hub airport. The regional airport type will be represented by Rotterdam-the Hague Airport and the international hub airport type will be represented by Amsterdam Airport Schiphol. The case on Rotterdam-the Hague Airport will be given in Section 5.1, and the case on Amsterdam Airport Schiphol will be discussed in Section 5.2.

5.1. Rotterdam-the Hague Airport

Rotterdam-The Hague Airport (IATA: RTM, ICAO: EHRD) is a regional airport for general and civil aviation, located in the Netherlands. The airport is the third busiest airport in the Netherlands, handling approximately 17,000 scheduled flights annually [2]. The airport has a bidirectional runway (06/24), where both directions can be used for take-off and landings. The terminal apron is located approximately 400 meters from the southwest end of runway and approximately 2,300 meters from the northeast end of the runway. The apron has four transporter platforms (A-D) close to the terminal building. A complete aerodrome chart of Rotterdam-the Hague Airport is available in Appendix A. The runway direction is mainly dependent on the direction of the wind. As a result, runway 24 is used more often than runway 06 [2][19][21][20]. Runway 24 is used for approximately 60% of the movements.

The flight schedule used for Rotterdam-the Hague Airport is the flight schedule for Tuesday 25^{th} July 2017. The data is derived from the airport's official website [17], and the missing information is complemented using the FlightStats website [7]. The resultant flight schedule can be found in Appendix A.

The flight schedule consists of 39 movements in total; of which 19 arrivals and 20 departures. All aircraft are considered medium category aircraft according to Table 4.1. The composition of aircraft types is represented in Figure 5.1, where 82% of the movements are with aircraft of the Boeing 737 family because Rotterdam-the Hague Airport is one of the home bases for Transavia. The remaining types of aircraft handled by the airport that day are the Embraer E190/195 and Bombardier CRJ 700 aircraft types. The number of movements for this day were slightly below the yearly average, but the aircraft type composition is typical [2]. The average temperature that day was 17°C.

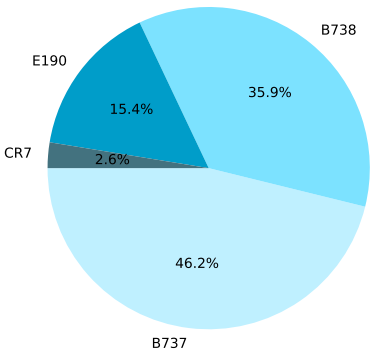

Figure 5.1: The composition of the aircraft types at Rotterdam-the Hague Airport on 25^{th} July, 2017.

5.2. Amsterdam Airport Schiphol

Amsterdam Airport Schiphol (IATA: AMS, ICAO: EHAM) is a large international hub airport located in the Netherlands. Aside from civil aviation, the airport handles cargo and general aviation. It ranks among the busiest airports by passenger traffic and aircraft movements in the world. The airport is located proximate to a heavily urbanized area and is heavily restricted on the production of fuel and noise emissions.

The airport terminal configuration for civil aviation consists of a transporter platform (A), and seven finger piers (B-H), with a new A-pier being built. The terminal buildings are landlocked in between six runways (04/22, 06/24, 09/27, 18L/36R, 18C/36C, 18R/36L). Conventionally, Schiphol utilizes eight runway directions for arrivals and seven runway directions for departures. The "Polderbaan" (runway 18R/36L) is remotest runway, with a distance of approximately 11 kilometers from the furthest pier. The apron is largely surrounded by a dual lane taxiway, with a single way taxiway to complete the ring. A detailed aerodrome chart can be found in Appendix A.

The flight schedule data for Friday 13^{th} October 2017 is collected using the "Flight API" from Schiphol's application developer website [18]. This date is selected due to the limited availability of data for other dates. The flight API is the best source available due to high detail; as it is an official Schiphol publication. The 13^{th} October 2017, could be described as an average day at Schiphol, with an average air temperature of 14°C . The flight schedule is slightly altered to account for missing data and errors.

According to the flight schedule, 1430 aircraft movements took place that day; 714 movements were departures and 716 movements were arrivals. The aircraft type composition is composed of forty aircraft types, reduced down to twenty-one aircraft families (e.g. E190, A320, B737, A330, B747, A380). By aircraft category, as defined in Table 4.1, there were 1230 movements with medium category aircraft, 173 movements with heavy category aircraft, and 27 movements with super heavy category aircraft. Figure 5.2 shows the relative share of aircraft movements per category. Figure 5.3 shows the relative share of aircraft movements per aircraft type.

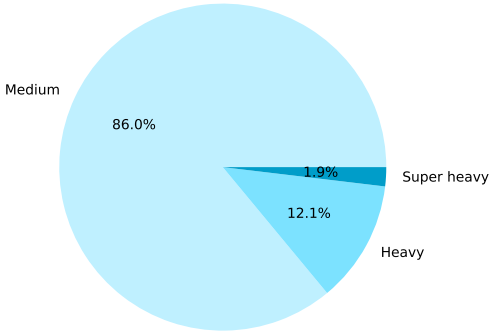

Figure 5.2: The composition of the aircraft categories at AAS on 3rd October, 2017.

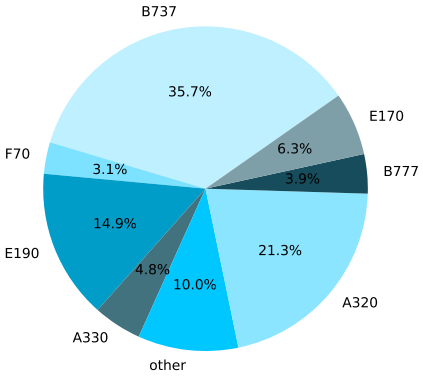

Figure 5.3: The composition of the aircraft types at AAS on 3rd October, 2017.

The runway utilization between 2^{nd}-8^{th} October, 2017 is shown in Figure 5.4. The data is displayed separately per direction of movement. The data shows that the most active runway is the "Polderbaan" (runway 36L/18R), which handles approximately 30% of all the movements. In this set of data, runway 36L/18R was used equally as much for arrivals as for departures. The "Kaagbaan" (runway 06/24) handled the most departures during the period measured, and the "Buitenveldertbaan" (runway 09/27) handled the most arrivals. The "Oostbaan" (runway 04-22) utilization is kept to a minimum because the standard terminal arrival route of this runway forms a nuisance to a large group of people. The "Buitenveldertbaan" was hardly used for departures in the period of data collection.

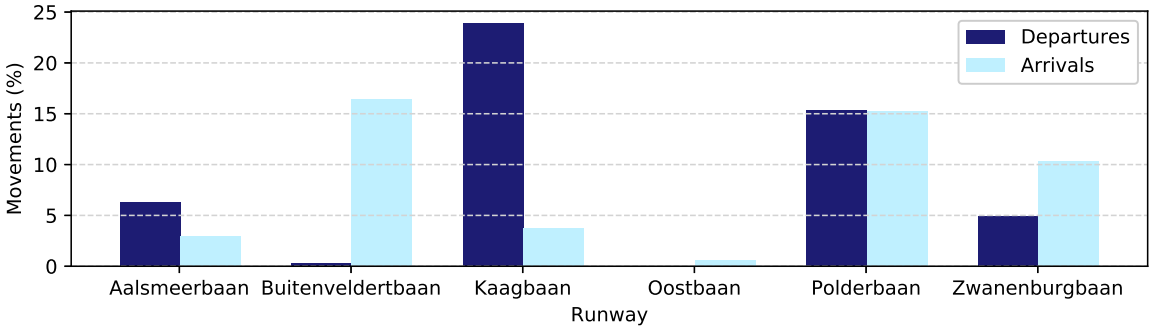

Figure 5.4: The runway utilization of Amsterdam Airport Schiphol between 2-8^{th} October, 2017.

6

Results

In this chapter the results of Rotterdam-the Hague Airport and Amsterdam Airport Schiphol will be discussed. In Section 6.1 the conceptual designs will be given of the three towing vehicle models. The ground movement simulation results of conventional movements and towed movements are compared in Section 6.2. The input parameters and results of the Vehicle Routing Problems are stated in Section 6.3, and the conclusions of the results are discussed in Section 6.4.

6.1. Conceptual design

The towing vehicle designs are the same for both Rotterdam-the Hague Airport and Amsterdam Airport Schiphol, in order to fairly test the same concept in different airport environments. The commonality of the towing vehicles at different airports will reduce production and service costs of each fully electric towing vehicle unit as well. However, the optimal design of a fully electric towing vehicle will differ between airport types as each airport type has different requirements. In this thesis, only the medium category towing vehicles are common to both airports.

6.1.1. Power demand

The minimum power demands for the on-board systems and engine start up were determined in Section 4.2. The power required for the on-board systems of aircraft of ICAO aircraft category C, D, E and F, are 3.7, 14.1, 21.8 and 33.9 kW, respectively. The minimum power required for the medium aircraft ASU is 384 kW, and 783 kW of power is required for the heavy and super heavy aircraft ASUs. The minimum specific power required for transportation is calculated assuming a ground drag coefficient of 0.02 for both the towing vehicle and aircraft wheels. The results are given in Table 6.1.

Table 6.1: The specific required power for transportation per maximum velocity.

Maximum velocity (m/s)	Specific power (W/kg)
10	1.96
11	2.16
12	2.35
13	2.55
14	2.75
15	2.94
16	3.14

The results show that the specific power required for transportation should be at least 2 W/kg. In order to reach 14 m/s, typically the maximum speed of conventional traffic at Amsterdam Airport Schiphol, at least 2.75 W/kg is required. Heavier aircraft require more power to be transported at a certain velocity than a lighter aircraft, therefore the minimum power requirement for transportation is calculated for the heaviest aircraft in the category. The heaviest aircraft in the medium category is the Boeing 737-800. The medium category towing vehicle needs to be able to supply at least 218 kW in order to transport a fully loaded Boeing 737-800 at 14 m/s. The heaviest aircraft in the heavy category is the Airbus A340-500. At least 1027 kW of power is required to transport a fully loaded A340-500 to 14 m/s. The heaviest aircraft in the super heavy category is the Airbus A380-800. At least 1582 kW of power is required to transport the A380-800 to 14 m/s.

The power demand for preconditioned air is dependent on the outside air temperature. Figure 6.1 gives the power demand estimates per aircraft type for a range of temperatures, where the colour and marker indicate the aircraft category. The desired cabin temperature is taken to be 20°C, the thermal conductivity coefficient as 0.05 $\frac{W}{m \cdot K}$ [5], the specific heat constant of air under constant pressure at 1.006 $\frac{kJ}{kg \cdot K}$, the coefficient of performance as 3 [15], and the fuselage thickness with panels as 3 cm. The surface area of the fuselage was

approximated by product of the fuselage circumference and length for each aircraft type. Figure 6.1 shows the preconditioned air power demand for different aircraft types exposed to a range of outside air temperatures.

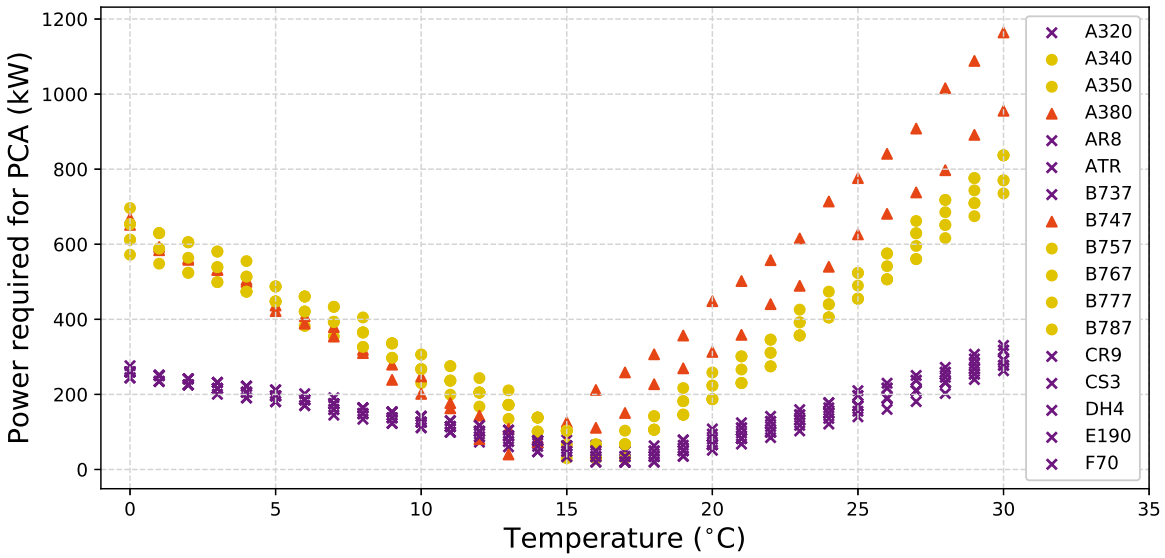

Figure 6.1: The power demand of the PCA for different air temperatures.

The least amount of power for PCA is required around 15-17°C, and the power requirement increases with the air temperature deviation from this point. The graph shows that the power requirement for cooling is proportionate with the aircraft size. The results also show that similar amounts of power are required for heating heavy and super heavy aircraft at temperatures above 0°C. Less power is required for the heating of medium aircraft than for the aircraft of the other two categories.

6.1.2. Technical design

Three high level technical designs of fully electric towing vehicles were generated using the method in Section 4.2. An overview of the main components of the technical designs is given in Table 6.2.

Table 6.2: The towing vehicle designs for each aircraft category.

	Medium	Heavy	Super Heavy
Total mass $[kg]$	25,000	45,000	60,000
Battery type $[-]$	LiFe	LiFe	LiFe
Battery mass $[kg]$	7,000	14,000	21,000
Battery volume $[m^3]$	3.82	7.64	11.45
Battery capacity $[kWh]$	840	1,680	2,520
Max. power $[kW]$	1,400	2,800	4,200
Max. ASU/PCA power $[kW]$	436	783	783
Drive train $[-]$	4x4	6x6	6x6

The type of batteries used in the design are lithium iron phosphate batteries (LiFe). The reasons for selecting lithium iron phosphate batteries are because they are rechargeable, have a high specific power, a long life span, good thermal stability, are considered very safe, and are tolerant to full charge conditions. The battery has a relatively low specific energy compared to other lithium-ion batteries, which is not problematic as the towing vehicle will require additional ballast for traction. The secondary function of the batteries will be to provide ballast. Nickel-cadmium or lead acid batteries were not selected because lithium iron phosphate can produce a higher voltage, has a higher energy density, is more resistant to changes in temperature, and does not have the memory effect (thus can be recharged when not entirely empty). The main disadvantage of lithium-iron phosphate batteries is that they are expensive to manufacture.

The towing vehicle models are designed in an iterative process, due to the interdependency of subsystems. The starting point of the design process was an initial estimate of the total mass of the towing vehicle based on reference vehicles, like pushback trucks and TaxiBot. The mass of the batteries is estimated to be the remainder of the total mass after the estimated masses of the subsystems have been subtracted. The resultant battery mass is between 28-35% of the total vehicle mass. Using the specific power it is checked that the batteries are capable of delivering the minimum power demand. The battery capacity is calculated using the specific energy and checked if it exceeds the minimum energy demand of the longest tow. The battery volume is calculated using the energy density, and estimated

if the volume could realistically fit on a towing vehicle. The high power availability is the result of the large amounts of batteries, which helps the towing vehicle reach high velocities.

The heavy and super heavy towing vehicle designs have six wheels instead of four because as the vehicles will be longer and heavier than the medium towing vehicle. Extra wheels do not have an effect on traction, but do reduce the wheel loading, which reduces the wear of the taxiway and apron surfaces. All three models are all-wheel-drive in order maximise the use of the weight as downforce.

6.1.3. Performance profiles

The maximum acceleration performance profiles generated with the technical design are given in Figures 6.2-6.7. Not all aircraft types are represented in the figures. Only the lightest and heaviest aircraft in each category are selected, as the aircraft mass largely determines the performance. The aircraft weights used are the taxi-out weights.

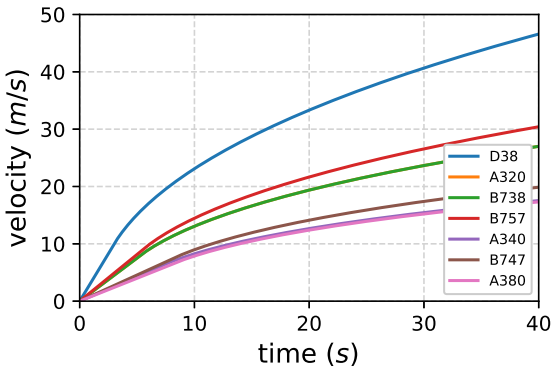

Figure 6.2: velocity-time (accelerating)

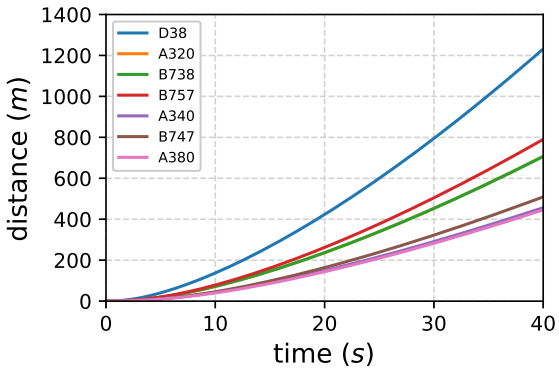

Figure 6.3: distance-time (accelerating)

Figure 6.2 shows a velocity-time plot of the aircraft selection during acceleration. All the aircraft represented are capable of reaching higher velocities than required due to the large amount of power available. Most importantly, all the aircraft can accelerate to 14 m/s within a short amount of time. It can be observed that the lighter aircraft accelerates faster than the heavier aircraft in each category. The Dornier 328 is very fast because the medium category towing vehicle is overpowered for an aircraft type of that mass. Figure 6.3 shows the distance-time profiles for the same aircraft. It takes less than 200 meters for all aircraft to accelerate to 14 m/s.

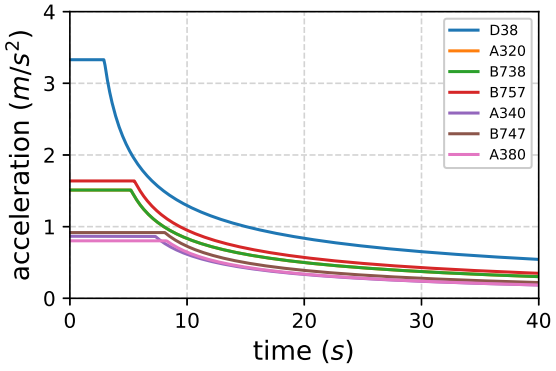

Figure 6.4: acceleration-time (accelerating)

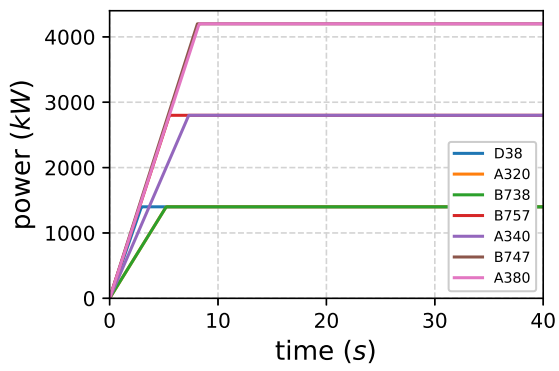

Figure 6.5: power-time (accelerating)

The acceleration profiles are shown in Figure 6.4. As explained in Section 4.2, horizontal part of the curve is the part where the acceleration is limited by traction. More traction will narrow the horizontal part and shift it upwards, resulting in a higher maximum acceleration. An increase in power will shift the whole curve upwards, but the maximum acceleration remains constant if the traction remains the same. From the curves it can be seen that the super heavy aircraft and the A340 have a maximum acceleration at around 0.9 m/s^2, which is desirable for passenger comfort. The A320, B738, and B757 have a maximum acceleration of around 1.6 m/s^2, and the D38 has a maximum acceleration of 3.3 m/s^2. An acceleration of 3.3 m/s^2 is relatively high, but it does occur during conventional taxiing for short during burst accelerations. It must be noted that it is possible to accelerate slower as these curves show the maximum acceleration.

Figure 6.5 shows the power required over time. The sloped part of the curve is determined by the amount of traction and the height of the curve is determined by the power available at the wheels of the towing vehicle. The figure shows that the maximum power required is equal for all aircraft in the same category, as the power available is dependent on the towing vehicle.

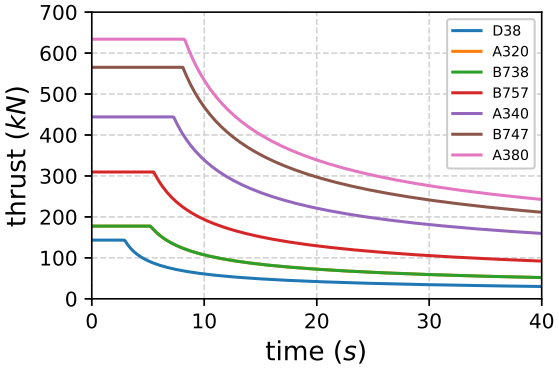

Figure 6.6: thrust-time (accelerating)

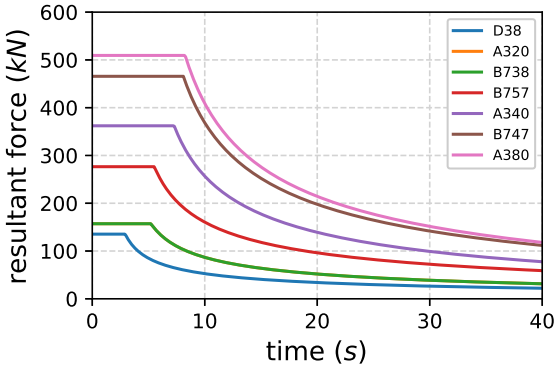

Figure 6.7: resultant force-time (accelerating)

The tractive force, or thrust, is plotted against time in Figure 6.6. These curves have a similar shape as the curves in the acceleration-time plot for the same reason. The horizontal part of the curve is due to limited traction, after which the thrust decreases due to limited power. This graph shows that the tractive force is proportional to the normal force on the wheels. Furthermore, the tractive forces are much higher than that of pushback trucks, and may damage the noselanding gear. As a result, the maximum tractive force may have to be limited, which will lower the maximum acceleration. Figure 6.7 shows the results force on the aircraft-towing vehicle system. The curves are similar to the curves in Figure 6.6, but translated down. The reason for this is that the resultant force in the dynamic model is calculated as the thrust force minus the ground drag, which is a constant value.

The deceleration performance profiles when decelerating from 16 to 0 meters per second are given in Figures 6.8-6.13. The same aircraft types are represented as in the acceleration profiles. The deceleration is done by coasting, so no thrust in provided as can be seen in Figure 6.12. Instead, the deceleration is entirely due to the ground drag which is a constant. As the ground drag is directly proportionate to the mass of the system, the deceleration is equal for all aircraft, as can be seen in Figures 6.8-6.11. The resultant force, which equals to the ground drag, is plotted in Figure 6.13, and shows that the ground drag is proportionate to the mass of the system. These plots verify the dynamic model as everything is as expected. The roll-out distance and time between two velocities can be determined form Figures 6.8 and 6.9

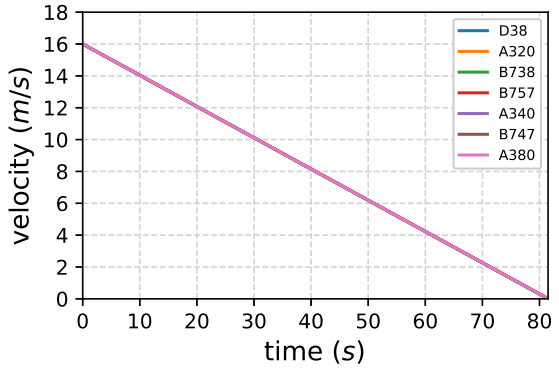

Figure 6.8: velocity-time (decelerating)

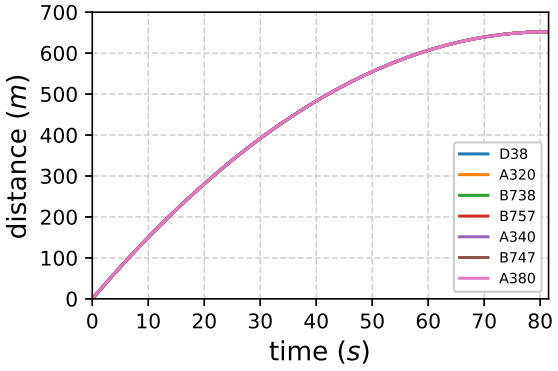

Figure 6.9: distance-time (decelerating)

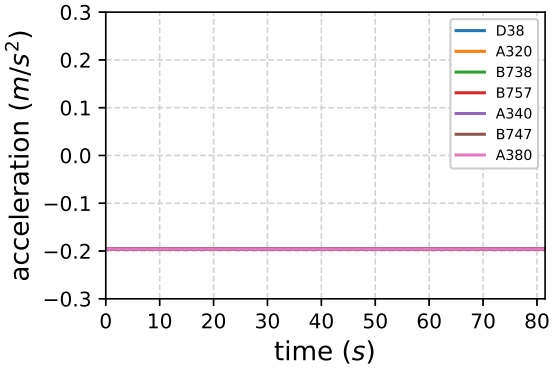

Figure 6.10: acceleration-time (decelerating)

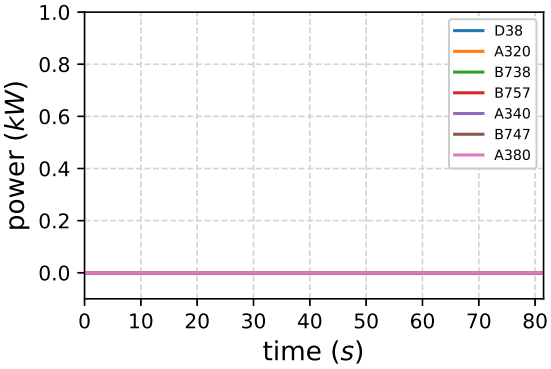

Figure 6.11: power-time (decelerating)

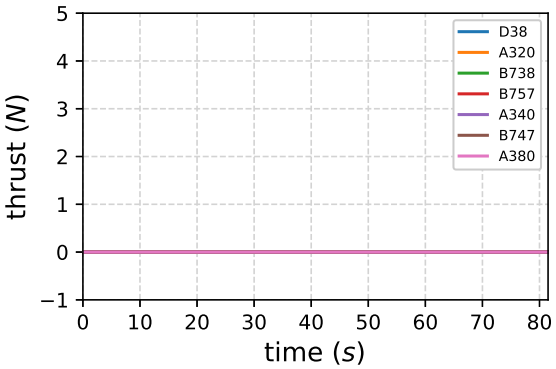

Figure 6.12: thrust-time (decelerating)

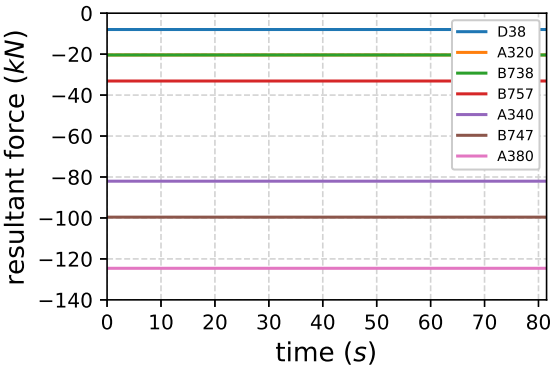

Figure 6.13: resultant force-time (decelerating)

6.2. Ground movement simulations

Conventional taxi movements and fully electric tows are simulated for each movement on the flight schedule. Furthermore, the ferry movements of the fully electric towing vehicles are simulated for all possible gate-runway, runway-runway, and gate-gate combinations, as this data is necessary for the towing vehicle routing problem.

The simulations are performed using the flight schedules of both Rotterdam-the Hague Airport and Amsterdam Airport Schiphol. The node and link data used for Rotterdam-the Hague Airport can be found in Appendix B.1, and the node and link data used for Amsterdam Airport Schiphol can be found in Appendix B.3. The outside temperature used for both airports is 14°C.

6.2.1. Rotterdam-the Hague Airport

The comparison between conventional taxiing and fully electric towing is done per gate-runway-direction-aircraft type combination. The difference in travel duration is plotted in Figure 6.14, the difference in fuel consumption is plotted in Figure 6.15, and the difference in battery energy for transport consumed is plotted in Figure 6.16. The frequency of occurrence is plotted on the x-axes.

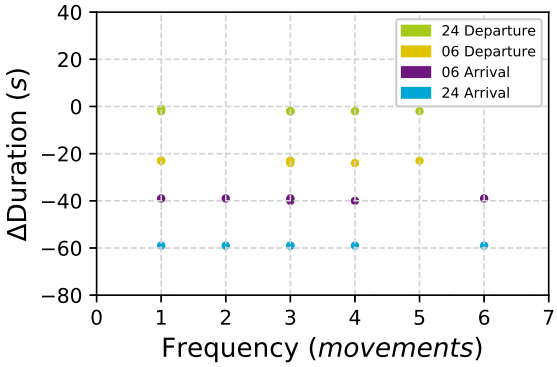

Figure 6.14: The difference in travel time between conventional taxiing and electric towing per gate-runway-direction-aircraft type combination at Rotterdam-the Hague Airport, plotted against the frequency of occurence.

Figure 6.14 shows that conventional taxiing is faster than fully electric towing in all cases (as all values are negative). However, if the pure travel time is considered (the duration without time penalties or additional processes), the fully electric towing system is faster than the aircraft. This is because the fully electric towing vehicle can accelerate faster than the aircraft that is limited at 0.7 m/s^2. With the larger time penalty per turn for the electric towing vehicle, and with the additional time required for attaching the aircraft to the vehicle upon landing, conventional taxiing at Rotterdam-the Hague Airport is faster.

The travel time of the conventional taxiing simulations are independent of aircraft type, as it is assumed that all aircraft accelerate and decelerate at 0.7 m/s^2. It turns out that the aircraft type affects the travel time for the electric towing simulations by a maximum of one second. Therefore, the difference in duration between conventional and electric towing will be similar for multiple gate-runway-direction-aircraft type combinations. For those combinations, the data point will vary horizontally in Figure 6.14, depending on the number of occurrences in the flight schedule.

A possible explanation to why the durations of electric towing are close in time for different aircraft types on the same route is that the routes are relatively short and straight, so only a few accelerations and decelerations are required that can affect the duration. Furthermore, the difference in duration between conventional and electric taxiing is approximately constant for combinations with the same direction and runway, even though the tow durations differ up to a minute for different routes. A possible explanation is that the aircraft stands at Rotterdam-the Hague Airport have a grid structure, thus every movement makes the same number of turns per route, resulting in a constant amount of penalty time for turns. The extra distance covered for longer routes takes approximately equally as long for conventional and electrical taxiing, thus do not significantly affect the difference in travel duration between the two.

The electric taxiing system is around two seconds slower than conventional aircraft with departures to runway 24 and around 59 seconds slower with arrivals from runway 24. The towing system is approximately 24 seconds slower than aircraft taxiing on their own engines for departures to runway 06, and around 40 seconds slower with arrivals from runway 06. The additional process where the aircraft has to be connected to the towing system is the reason why the system is significantly slower with arrivals. The reason why no extra time is reserved for disconnecting the aircraft from the towing vehicle for departing flights, is because this time is included in the 180 seconds pushback time. Conventional taxiing aircraft have to disconnect from the pushback truck as well, just at a different moment.

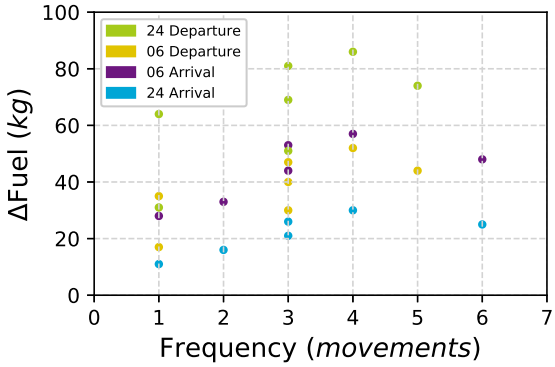

Figure 6.15: The difference in fuel consumption between conventional taxiing and electric towing per gate-runway-direction-aircraft type combination at Rotterdam-the Hague Airport, plotted against the frequency of occurence.

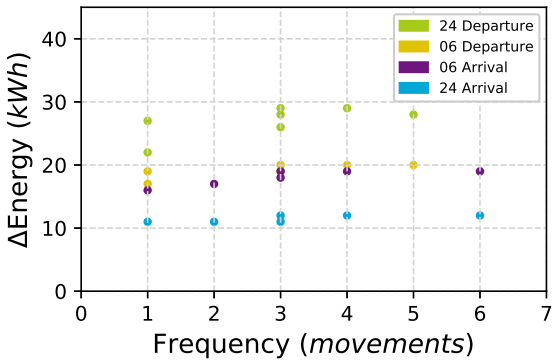

Figure 6.16: The difference in battery energy consumed (for transport only) between electric towing and conventional taxiing per gate-runway-direction-aircraft type combination at Rotterdam-the Hague Airport, plotted against the frequency of occurence.

As expected, Figure 6.15 shows that the fully electric taxiing system saves fuel on all tows. The most fuel can be saved when the aircraft travels to or from the far end of the runway, i.e. arrivals on runway 06 and departures on runway 24. With runway 06 active, tows save between 7-57 kg of fuel per tow, averaging 36 kg per tow. If runway 24 is active, 11-76 kg of fuel can be saved per tow, with an average of 40 kg per tow.

All tows of arrivals from runway 24 take less than 144 seconds, which means that the aircraft main engines are on the entire travel time as it was assumed that the engine cool down takes 150 seconds. Still less fuel is used by the electric towing system even though the travel time is similar to that of conventional taxiing. This is because the thrust setting is increased when accelerating conventionally as opposed to the engines being idle when towed.

Figure 6.16 shows the difference in battery energy consumed for transportation. As conventional taxiing does not use battery power, the difference in energy is purely the battery energy consumed by the fully electric towing system. For this reason, the sign of the y-axis is changed. As a form of verification, all values are positive meaning that more battery energy is consumed towing than conventionally taxiing. As with fuel consumption, the longer routes require more energy than the short routes. With runway 06 active, 16-20 kWh of energy is used per tow, with an average of 19 kWh per tow. When runway 24 is active, a tow requires 11-29 kWh of energy per tow, with an average of 20 kWh per tow.

6.2.2. Amsterdam Airport Schiphol

The same plots are made for Amsterdam Airport Schiphol, but the data is displayed per aircraft category instead of displaying the data per runway.

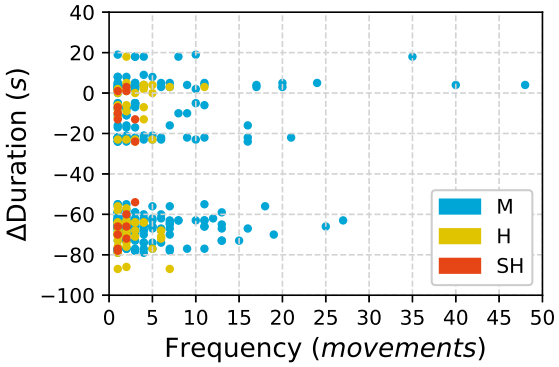

Figure 6.17: The difference in travel time between conventional taxiing and electric towing per gate-runway-direction-aircraft type combination at Amsterdam Airport Schiphol, plotted against the frequency of occurence.

Two clusters of data points are visible in Figure 6.17. The top cluster is composed solely out of departures, and the bottom cluster is composed solely out of arrivals. The fully electric towing system is slower than conventional taxiing for all arrivals. With departures, the fully electric towing system is slower in the majority of the cases, but in many cases the system is equally as fast or faster. No clear differences are observed between towing vehicle categories.

The arrival and departure clusters are approximately sixty seconds apart, which can be explained by the extra sixty seconds required to attach the aircraft to the towing system upon arrival. Conventional taxiing does not require this extra process, so the difference in travel duration increases by sixty seconds.

Similarly to the simulations of Rotterdam-the Hague Airport, the pure transport duration of the fully electric towing system is shorter than that of conventional taxiing in all cases. However, conventional taxiing is quicker in the majority of the cases after time penalties and the attachment procedure. The towing system will not hinder other traffic while taxiing because of the towing velocities, apart from possible hinder near the runway exit ramp due to the extra attachment procedure. However, this can be solved by other traffic taking a different exit ramp.

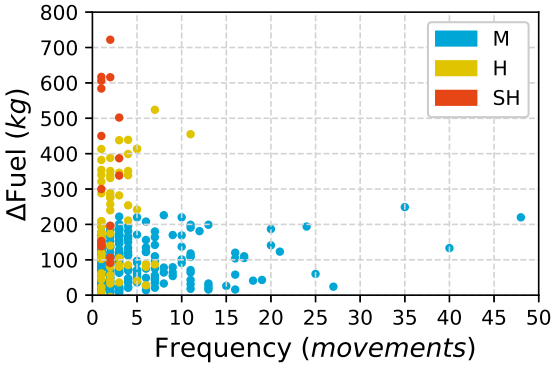

Figure 6.18: The difference in fuel consumption between conventional taxiing and electric towing per gate-runway-direction-aircraft type combination at Amsterdam Airport Schiphol, plotted against the frequency of occurence.

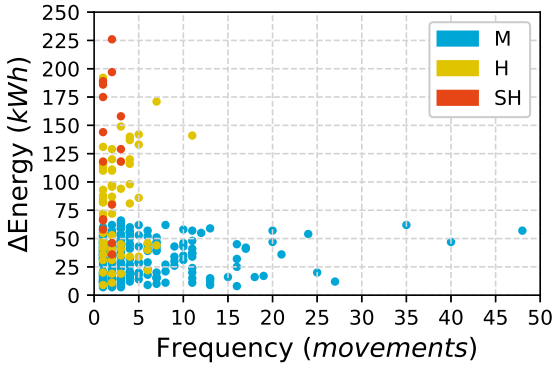

Figure 6.19: The difference in battery energy consumed (for transport only) between conventional taxiing and electric towing per gate-runway-direction-aircraft type combination at Amsterdam Airport Schiphol, plotted against the frequency of occurence.

Figure 6.18 shows that in general, more fuel can be saved the heavier the aircraft category. This can be explained by the fact that more energy is required to transport a heavier mass over a certain distance, than with a lighter mass. It was observed that the difference in fuel consumed is larger for departures than for arrivals on average. This is because the aircraft are heavier during taxi-out than taxi-in due to unburned fuel. The medium category towing vehicles can save 29-249 kg of fuel per tow, with an average of 106 kg per tow. Compared to Rotterdam-the Hague Airport, much more fuel can be saved by this category towing vehicle due to the longer taxi routes. The heavy category towing vehicles can save between 17-524 kg of fuel per tow according to the simulations, with an average of 225 kg of fuel. The super heavy category towing vehicle can reduce fuel consumption by 113-722 kg per tow, with an average reduction of 383 kg.

Figure 6.19 is similar to that of the difference in fuel consumption. This can be explained by the fact that both fuel and electricity are sources of energy, and that more energy is required to move heavier objects or the same mass object over a longer distance. Therefore, a movement requiring a large amount of fuel, will require a large amount of electricity for transport. A medium category towing vehicle consumes 7-66 kWh of energy per tow, with an average of 33 kWh per tow. The longer routes at Amsterdam Airport Schiphol causes the maximum energy consumption per tow to be much higher than the maximum energy consumption per tow at Rotterdam-the Hague Airport. The heavy category towing vehicles consume 9-192 kWh per tow, with an average of 79 kWh. The super heavy category utilizes 36-226 kWh per tow, averaging 125 kWh per tow. As with the difference in fuel consumption, departures consume more energy than arrivals on average, because the aircraft are heavier during tow-out than tow-in.

The simulation models can be further improved as the durations assumed for pushback, attaching and detaching the aircraft are constant and have a large influence the outcome. A more accurate simulation model will give betting insight into the towing durations, which in turn will give a better estimate of the fuel and energy consumptions. The main conclusions that can be drawn from these results are that the fully electric taxiing system travels faster, but takes longer in the majority of the cases due to additional attaching process and the additional time it takes in the corners. The other conclusion that can be drawn is that the fully electric taxiing system is only a bit slower than conventional taxiing between origin and destination, but not on the taxiways. Therefore, the system should not cause hinder to other traffic. It must be noted that if aircraft were to accelerate and decelerate faster than 0.7 m/s^2, as often done in real life, hinder may occur.

6.3. Vehicle routing problem

The results of the Vehicle Routing Problem will be discussed in this section. The results of Rotterdam-Hague Airport will be discussed in Subsection 6.3.1, and the results of Amsterdam Airport Schiphol will be discussed in Subsection 6.3.2. The results of the ground movement simulations are used to formulate the Vehicle Routing Problem.

6.3.1. Rotterdam-The Hague Airport

The depot for the fully electric towing vehicle fleet is located on the south side of the apron at node 37 of the airport model. This location is chosen because of its proximity to the aircraft stands, yet clear from major activity. In this way, less energy and time is wasted ferrying between the depot and aircraft stands. The input parameters for the vehicle routing problem are given in Table 6.3.

Table 6.3: The input parameters for the vehicle routing problem at Rotterdam-the Hague Airport.

Parameter		Symbol	Value
Number of flights	[flights]	N_f	39
Fleet size	[vehicles]	N_v	0-10
Maximum number of routes	[routes/vehicle]	N_c	12
Minimum charging time	[min]	C	6
Rolling horizon	[min]	T	40
Big-M	[-]	M	10^{10}

All the results are for the medium category towing vehicles as all flights at Rotterdam-the Hague Airport are with medium category aircraft. Furthermore, the vehicle routing problem is solved for a scenario where all flights use runway 06, and a scenario where all flights use runway 24. The same flight schedule is used in both scenarios.

The total fuel consumption of all flights at Rotterdam-the Hague airport (for both scenarios) are plotted against the fleet size of fully electric towing vehicles deployed in Figure 6.20. In both cases, the total fuel consumption decreases with increasing fleet size until a lower limit where all aircraft are towed. The lower limit is non-zero as fuel is consumed by the aircraft during engine warm-up and cool down. The curves are different for the two runways as the scenarios are different. For example, a departing flight to runway 06 travels a shorter distance than the same departing flight to runway 24. Therefore, more fuel can be saved from the departure to runway 24. The scenarios are different as well when zero towing vehicles are deployed.

In the scenario with runway 06 active, 2,379 kilograms of fuel is consumed by all the aircraft together if no fully electric towing vehicles are deployed. The total fuel consumption can be reduced by 1,548 kilograms (65%) by deploying five towing vehicles. Deploying more than five towing vehicles will have no effect on the total fuel consumption as all flights are towed. Figure 6.21 shows the marginal fuel reduction every time an additional fully electric towing vehicle is deployed. The effectiveness of the first towing vehicle is the greatest, lowering the total fuel consumption by 1,021 kilograms (43%). The effectiveness of every new vehicle decreases due to the law of diminishing marginal utility. The energy consumed by the fleet of fully electric towing vehicles is shown in Figure 6.22. The energy consumption of the fleet of fully electric towing vehicles increases the more vehicles are deployed, until all flights are towed. After this point, no tasks exist that will require the fleet to consume extra energy. It must be noted that the total energy consumption is not constant for a fleet size larger than four towing vehicles because the vehicle routing problem optimizes for minimum fuel and does not take into account energy minimization. Multiple solutions can exist, of which some are more energy efficient than others. The discrepancy in total energy consumption is due to the set of ferry movements of towing vehicles. The total amount of energy required to tow all aircraft electrically is approximately 1110 kWh.

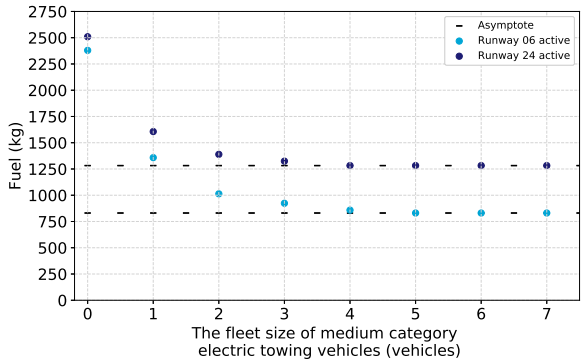

Figure 6.20: The aggregate fuel consumption by aircraft at Rotterdam-the Hague Airport with a varying number of medium category towing vehicles deployed.

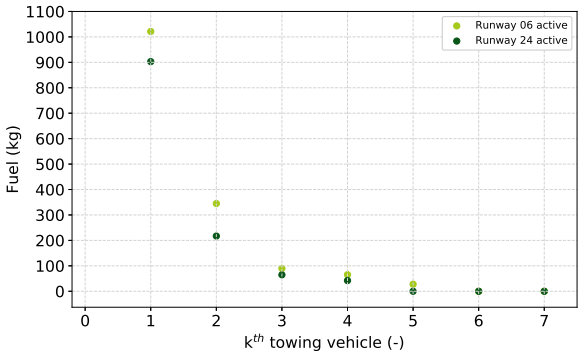

Figure 6.21: The marginal fuel reduction per medium category towing vehicle at Rotterdam-the Hague Airport.

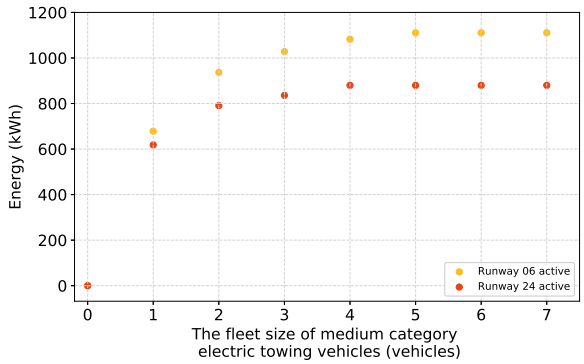

Figure 6.22: The aggregate energy consumption at Rotterdam-the Hague Airport with a varying number of medium category towing vehicles deployed.

In the scenario with runway 24 active, the total fuel consumption by the aircraft is 2509 kilograms if no fully electric towing vehicles are deployed. The deployment of fully electric towing vehicles has the potential to reduce the total fuel consumption by 1227 kilograms (49%). In this case a fleet of four towing vehicles is sufficient to maximize the fuel reduction. The marginal fuel reduction potential is greatest for the first towing vehicle, which is able to reduce the fuel consumption by 36%. The utility per vehicle rapidly decreases for every new towing vehicle addition, i.e. the third and fourth vehicle each save less than 100 kilograms of fuel per day. As shown in Figure 6.22, the energy consumption increases the more flights are towed. The total energy required to tow all aircraft electrically is approximately 882 kWh.

6.3.2. Amsterdam Airport Schiphol

The flight schedule of Amsterdam Airport Schiphol is split up by aircraft category. This results in a flight schedule of 1230 medium category flights, a flights schedule with 173 heavy category flights, and a flight schedule with 27 super heavy category flights.

The total number of decision variables is kept to a minimum in order to keep the computational time as low as possible. Thus, it is not possible to set the value for the maximum number of routes to an arbitrary high value, which will not limit the vehicle to less routes than possible. This challenge is overcome by solving the problem for increments of the value for the maximum number of routes, starting from one. The problem is considered minimized once the objective value is constant for five consecutive increments.

Even with a rolling horizon of forty minutes, the computation time for the heavy and super heavy categories is extensive and impractical. A further reduction in the rolling horizon will severely limit the selection of flights. Instead, it is chosen to split the flight schedules into parts with the same number of flights. The flight schedule for the heavy aircraft is split into two parts, and the flight schedule for the super heavy aircraft is split into twenty-five parts. Each part is treated as an independent problem. Thus, all vehicles start and end at the depot in every part. The limitation of this method is that the results are less optimal as there is no information transferred between parts. Also, it assumes that the vehicles are fully charged at the start of each part, whereas the vehicle would be empty in the previous part.

The depot for the fully electric towing vehicle fleet is located on the parking/holding stand in between crossing A12 and A13, north east of the E-pier. On the airport model the depot is located at node 70. This location is chosen as it central to most piers and a number of runways. The input parameters for the vehicle routing problem are given in Table 6.4.

Table 6.4: The input parameters for the vehicle routing problem at Amsterdam Airport Schiphol.

Parameter		Symbol	Value		
			Medium	Heavy	Super heavy
Number of flights	[flights]	N_f	1230	173	27
Fleet size	[vehicles]	N_v	0-42	0-20	0-10
Maximum number of routes	[routes/vehicle]	N_c	127	14	13
Minimum charging time	[min]	C	6	6	6
Rolling horizon	[min]	T	40	40	40
Big-M	[-]	M	10^{10}	10^{10}	10^{10}

Medium category

The total fuel consumption by medium category aircraft at Amsterdam Airport Schiphol is plotted against the fleet size of medium category fully electric towing vehicles in Figure 6.23. The total fuel consumption by medium category aircraft is 170,105 kilograms with no towing vehicles deployed. The maximum reduction potential in fuel is 141,043 kilograms (83%) of fuel, which would require 42 fully electric towing vehicles. A fleet of eleven towing vehicles is sufficient to reduce the total fuel consumption by 50%, and a fleet of 24 towing vehicles is sufficient to reduce the total fuel consumption by 75%.

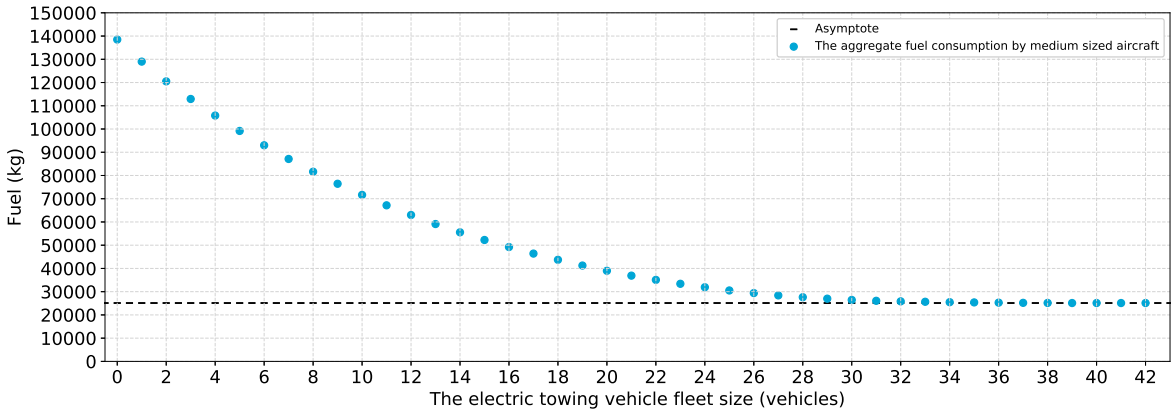

Figure 6.23: The total fuel consumption by medium category aircraft with a varying number of medium category towing vehicles deployed at Amsterdam Airport Schiphol.

Figure 6.24 shows the marginal fuel reduction per medium category towing vehicle. The utility of an extra towing vehicle decreases the larger the fleet size. The effectiveness of the first fully electric towing vehicle is the greatest, potentially decreasing the fuel consumption by 11,335 kilograms of fuel, which is 8% of the fuel reduction possible.

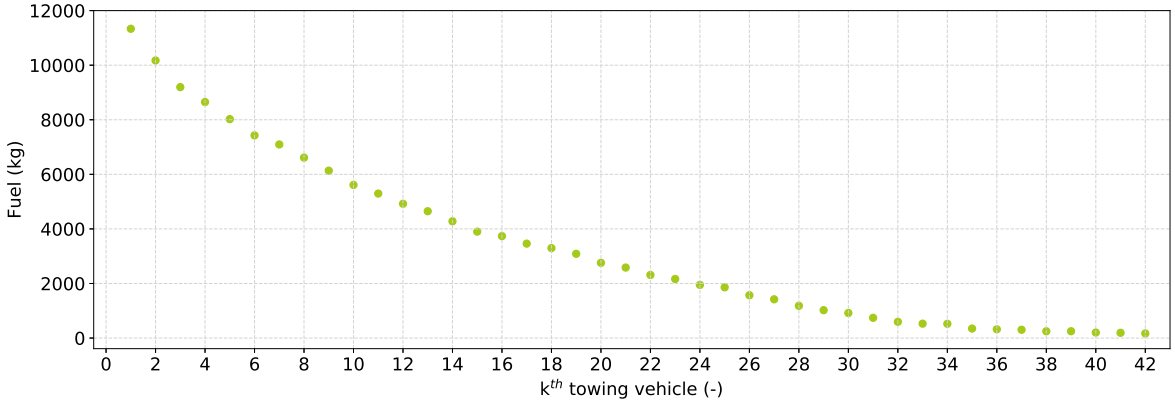

Figure 6.24: The marginal fuel reduction per medium aircraft towing vehicle at Amsterdam Airport Schiphol.

The energy consumption by the fleet of medium category fully electric towing vehicles is shown in Figure 6.25. As in the cases at Rotterdam-the Hague Airport, the energy consumption increases with the number of towing vehicles deployed until all flights are towed. The total energy consumed in order to tow all medium category flights is approximately 66,967 kWh.

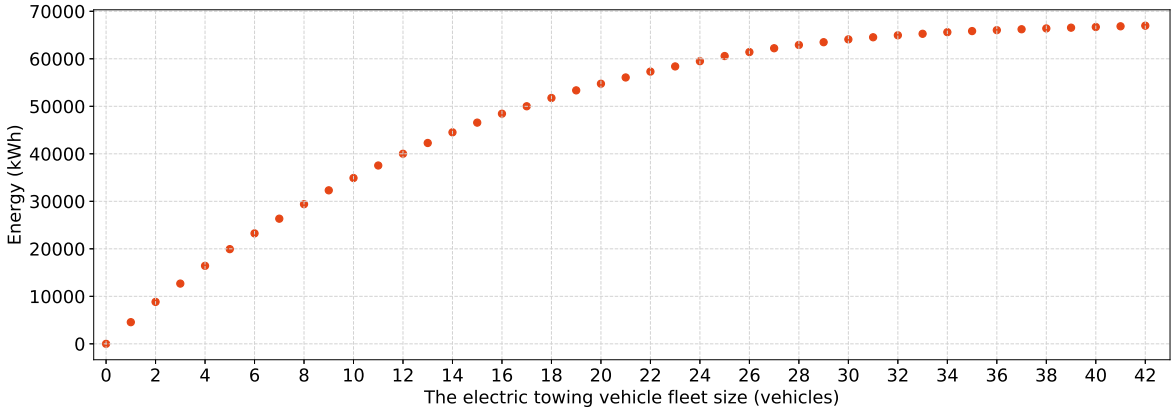

Figure 6.25: The aggregate energy consumption at Amsterdam Airport Schiphol with a varying number of medium category towing vehicles deployed.

Heavy category

The same plots are made for the heavy category fully electric towing vehicles. The total fuel consumption of all heavy category flights is plotted against the fleet size of heavy category towing vehicles in Figure 6.26. The marginal fuel reduction per heavy category towing vehicle per marginal heavy category towing vehicle is plotted in Figure 6.27. The total energy consumption by heavy category fleet is plotted against the fleet size of heavy category fully electric towing vehicles in Figure 6.28.

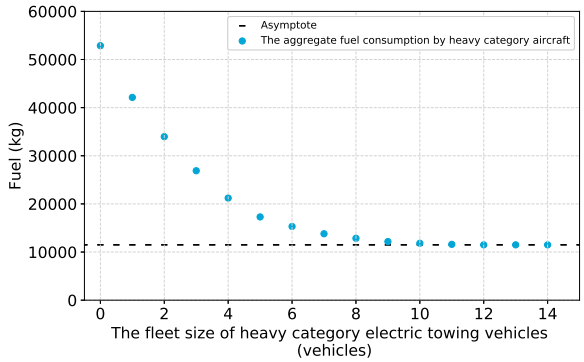

Figure 6.26: The total fuel consumption by heavy category aircraft with a varying number of heavy category towing vehicles deployed at Amsterdam Airport Schiphol.

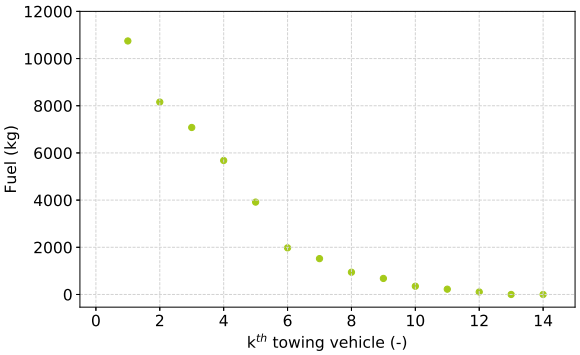

Figure 6.27: The marginal fuel reduction per heavy aircraft towing vehicle at Amsterdam Airport Schiphol.

The total fuel consumed by heavy category flights without operational towing is 52,872 kilograms of fuel. The maximum reduction in total fuel consumption is 41,377 kilograms (78%), with a fleet of twelve heavy category fully electric towing vehicles. Electrically towing all flights will cost approximately 19,460 kWh of energy. Approximately 50% fuel can be saved by deploying three towing vehicles, which will require around 11,879 kWh of energy. Approximately 75% fuel can be saved by deploying eight towing vehicles, which will cost around 18,818 kWh of energy. As with the medium category towing vehicles, the law of diminishing marginal utility applies. The marginal utility of the first heavy towing vehicle is 10,746 kilograms of fuel reduction.

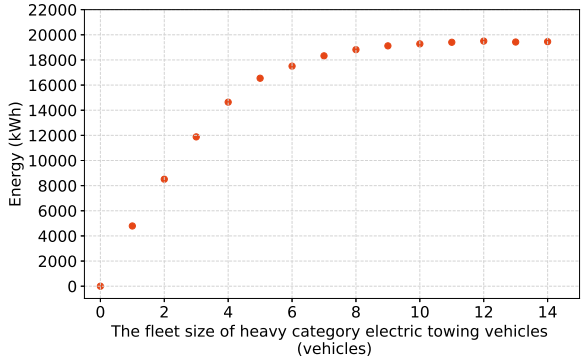

Figure 6.28: The aggregate energy consumption at Amsterdam Airport Schiphol with a varying number of heavy category electric towing vehicles deployed.

Super heavy category

The same plots are made for the super heavy category fully electric towing vehicles. The total fuel consumption of all super heavy category flights is plotted against the fleet size of super heavy category towing vehicles in Figure 6.29. All 27 super heavy category flights together consume 11,767 kilograms of fuel without electric towing. The maximum possible fuel reduction is 10,196 kilograms (86%), requiring four super heavy category towing vehicles. Again, the effectiveness of every additional towing vehicle decreases due to the law of diminishing marginal utility, as can be seen in Figure 6.30.

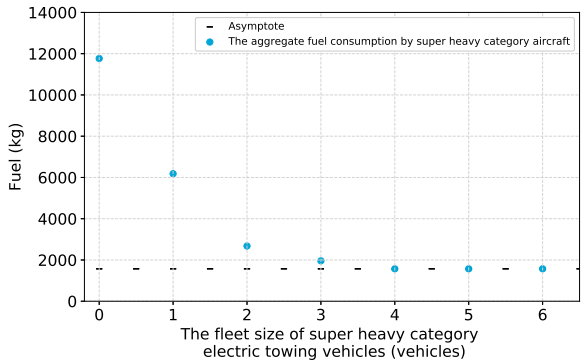

Figure 6.29: The total fuel consumption by super heavy category aircraft with a varying number of super heavy category towing vehicles deployed at Amsterdam Airport Schiphol.

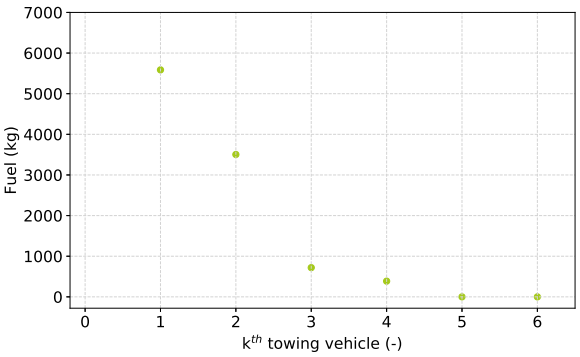

Figure 6.30: The marginal fuel reduction per super heavy aircraft towing vehicle at Amsterdam Airport Schiphol.

The total energy consumption by the super heavy category fleet is plotted against the fleet size of super heavy category fully electric towing vehicles in Figure 6.31. The maximum amount of energy required to tow all super heavy flights is approximately 4,260 kWh.

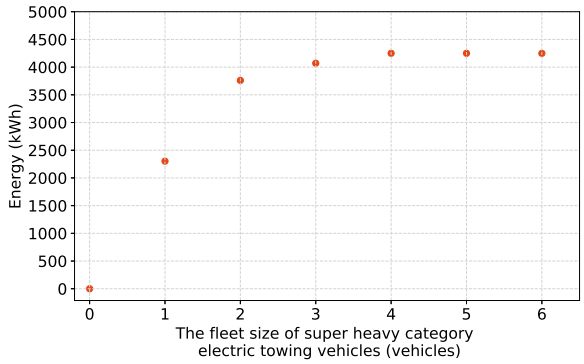

Figure 6.31: The aggregate energy consumption at Amsterdam Airport Schiphol with a varying number of super heavy category electric towing vehicles deployed.

The reduction in carbon monoxide, carbon dioxide, hydrocarbons, and nitrogen oxides are approximately linear proportionate to the reduction in fuel consumption. Plots with the reduction of these emissions at both Rotterdam-the Hague Airport and Amsterdam Airport Schiphol can be found in Appendix C.

6.4. Conclusions of results

The effectiveness of the fully electric towing vehicles is higher at Amsterdam Airport Schiphol than at Rotterdam-the Hague Airport. This is due to the on average longer taxi routes at Schiphol in combination with more flights, resulting in more time the towing vehicles are operational. When looking at Schiphol alone, the largest fuel reduction potential is with the medium category vehicles, followed by the heavy category vehicles, as there is more fuel to be saved. The marginal utility of fully electric towing vehicles diminishes exponentially with increasing fleet size.

For the fully electric towing system to be economically feasible, the fuel savings per vehicle minus the energy costs per vehicle over its lifetime must be greater than the fully electric towing vehicle unit costs. Therefore, the following equation must hold:

$$\frac{T}{N_f}\left(p_f \cdot F(N_f) - p_e \cdot E(N_f)\right) \geq C \tag{6.1}$$

where T is the operational life span in days, N_f is the fleet size of homogeneous towing vehicles, p_f is the fuel price per kilogram, p_e is the electricity price per kilowatt hour, F is the total fuel savings for a specific fleet size in kilograms per day, E is the total energy consumption for a specific fleet size in kilowatt hours per day, and C is the maximum allowable cost per towing vehicle over its lifetime.

Equation 6.1 shows that the economic feasibility is dependent on a number of factors:

- Higher fuel prices increase the economic feasibility for the fully electric towing system, whilst higher electricity prices will decrease the feasibility. Fuel prices are expected to increase in the future [3].
- The operational life span for th medium category towing vehicles will probably be longer at Rotterdam-the Hague Airport than at Schiphol, due to the lower operational time per day.

- The ratio of fuel saved per kilowatt hour of electricity invested decreases as the fleet size increases. This means that for a fixed fuel and electricity price, the budget per towing vehicle decreases with increasing fleet size.

The maximum allowable towing vehicle cost is calculated for different towing vehicle fleet sizes, assuming the results for Rotterdam-the Hague Airport and Amsterdam Airport Schiphol are representative for every day of the year, and that the fully electric towing vehicle unit has a lifespan of five years. The current price of Jet A1 fuel price at the pump in the Netherlands is €1.10/kg for international flights under air operator's certificate (AOC) [May 2^{nd}, 2019]. The electricity price is dependent on the energy source, cost of transportation, the consumption amount, and the time of consumption. It is assumed that batteries are charged during off peak hours when possible. Off peak hours in the Netherlands are between 11 p.m. and 7 a.m.. The current electricity price is estimated to be €0.0589/kWh (excluding VAT) for large electricity consumers in the Netherlands [May 2^{nd}, 2019].

At Amsterdam Airport Schiphol the maximum allowable unit costs exceeds €5 million for all three categories of towing vehicle models. This implies that the fully electric towing system is economically feasible at this airport under the consumptions, and has the potential to significantly reduce the total fuel costs. Looking at the towing vehicle categories separately, the maximum allowable super heavy towing vehicle cost ranges between €5-11 million per unit depending on the fleet size. The maximum allowable unit cost of a heavy towing vehicle is €6-21 million, and the maximum allowable unit cost of a medium category towing vehicle is €6-22 million.

The maximum allowable medium towing vehicle cost at Rotterdam-the Hague Airport is lower than at Schiphol, ranging between €0.6-1.7 million. This is due to lower utility for the towing vehicles resulting from a lower number of flights movements at the airport. However, the towing vehicle lifetimes will increase as a result of lower utility which increases the maximum allowable towing vehicle cost. A towing vehicle lifespan of ten years will allow the towing vehicles to cost between €1.2-3.4 million. Fully electric towing vehicles will be expensive due to the costs of lithium iron phosphate batteries, the ground service equipment it carries, the automated guided system, and the maintenance required, therefore unit costs may exceed €0.6 million. However, at least the first unit can be considered to be economically feasible, therefore the fully electric towing system can be considered economically feasible at Rotterdam-the Hague Airport. Depending on the vehicle cost, motives for implementation of the fully electric towing system might shift from financial to purely environmental benefits at this airport.

A limitation of the fully electric towing system are the high power demands. Amsterdam Airport Schiphol and Rotterdam-the Hague Airport respectively require approximately 91 MWh and 1 MWh of electricity per day for the cases investigated. High electrical loads are demanded from the power source in order to fulfil the energy needs, for which the current electricity infrastructure to both airports is not designed. The implementation of the fully electric towing system may require an on site power station or an adaptation to the power grid. Also, the charging of towing vehicles may become dependent on the availability of power, and affect the scheduling of tows. The electricity management for the fully electric towing system requires further research, which is out of the scope for this thesis.

7

Sensitivity analysis

A sensitivity analysis is performed to evaluate the effect of the input variables on the outputs. The conceptual designs are discussed in Section 7.1, and the Vehicle Routing Problem results are discussed in Section 7.2. An overview of the new input settings are given in Table 7.1. Settings 1 and 2 are chosen to investigate the effect of the outside temperature on operations with the standard electric towing vehicle designs. 0°C and 30°C are chosen for the outside temperature because they are near both ends of the Dutch climate spectrum, and they are approximately equidistant from 14°C. Settings 3 and 4 are done to investigate the effect of the towing vehicle mass on operations under normal conditions. It is reasoned that the change in mass will partially be realized by a change in the amount Lithium Iron Phosphate batteries on-board. Therefore, Settings 3 and 4 will indirectly test the effect of battery capacity on operations under normal conditions as well.

Table 7.1: The four different settings for the sensitivity analysis.

Setting	Version type	Outside temperature
Original	*Normal designs*	$14°C$
1	Normal designs	$0°C$
2	Normal designs	$30°C$
3	Light designs	$14°C$
4	Heavy designs	$14°C$

7.1. Conceptual designs

The specifications of the light designs are given in Table 7.2. The light versions are 10,000 kilograms lighter than the normal designs. The battery mass is determined by scaling down the components of the normal design, after which the remaining mass is dedicated to batteries. It must be noted that the PCA unit is not scaled down from the normal design as it should be equally powerful. The battery capacity and maximum power are much lower due to the reduction in batteries.

Table 7.2: The light versions of the towing vehicle designs for each aircraft category.

	Medium	Heavy	Super Heavy
Total mass $[kg]$	15,000	35,000	50,000
Battery mass $[kg]$	3,250	10,500	16,000
Battery volume $[m^3]$	1.77	5.73	8.73
Battery capacity $[kWh]$	390	1,260	1,920
Max. power $[kW]$	650	2,100	3,200
Drive train $[-]$	4x4	6x6	6x6

The specifications of the heavy designs are given in Table 7.3. The heavy verions are 10,000 kilograms heavier than the normal designs. The sizing process is the same as with the design of the lighter versions, but then scaled up instead of down. The battery capacity and the maximum available power have significantly increased due to the up-sizing of batteries.

Table 7.3: The heavy versions of the towing vehicle designs for each aircraft category.

	Medium	Heavy	Super Heavy
Total mass $[kg]$	35,000	55,000	70,000
Battery mass $[kg]$	12,500	18,000	26,000
Battery volume $[m^3]$	6.82	9.82	14.18
Battery capacity $[kWh]$	1,500	2,160	3,120
Max. power $[kW]$	2,500	3,600	5,200
Drive train $[-]$	4x4	6x6	6x6

Figures 7.1-7.4 show the acceleration and deceleration performance profiles of the light, normal, and heavy versions of the fully electric towing vehicles. The aircraft represented in the graphs are the heaviest in their category.

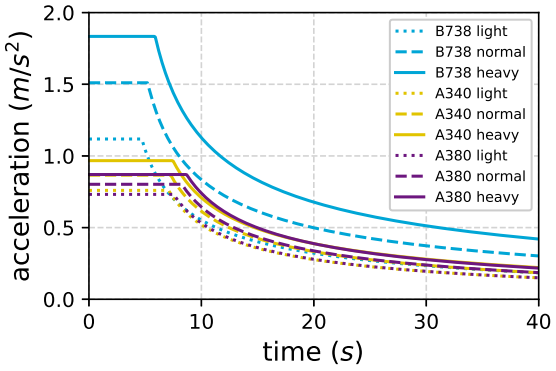

Figure 7.1: acceleration-time (accelerating)

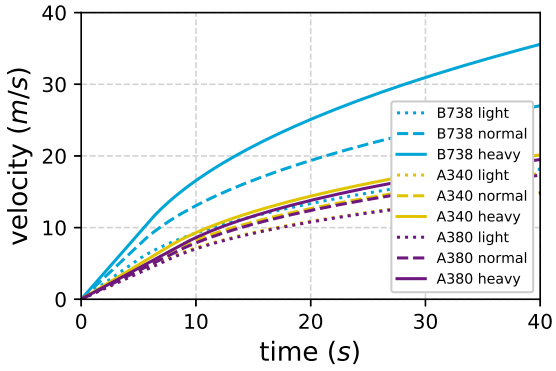

Figure 7.2: velocity-time (accelerating)

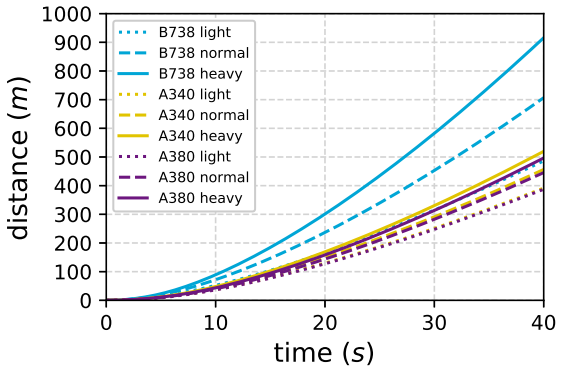

Figure 7.3: distance-time (accelerating)

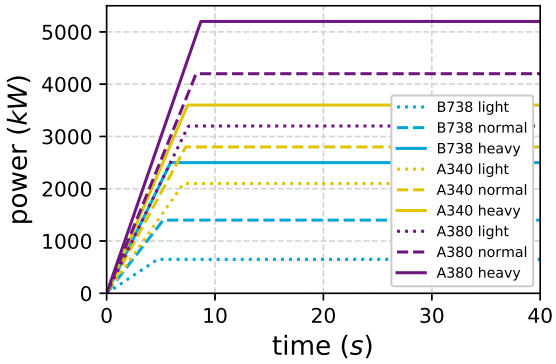

Figure 7.4: power-time (accelerating)

Figure 7.1 shows a plot of the maximum acceleration versus time. It shows that the maximum acceleration of the normal versions are higher than that of the light versions, but lower than that of the heavy versions. This is due to the the extra down force. The difference in weight and power has the most effect on the medium category towing system as the relative change in weight is much larger than for the other categories. The same effect can be observed in Figures 7.2 and 7.3. The maximum acceleration of the represented aircraft are within the desired limits for all versions. The distance-time plot shows that difference in duration to travel a certain distance is insignificant at low velocities for the different versions. The difference is at most five seconds when accelerating from standstill, yet the towing vehicles will mostly be operating between 4-10 m/s. The cost of accelerating faster will cost 1-2 MW of extra power, which can been seen in Figure 7.4, where the power required is plotted against time. On the other hand, the battery capacity will be larger when the towing vehicle is heavier.

Figures 7.5-7.8 show the performance during deceleration from 16 m/s to stand still. Figure 7.5 shows that all the aircraft decelerate at 0.2 m/s^2 as the wheel drag is proportionate to the weight of the system. Thus, increasing or decreasing the mass of the system will not affect the acceleration. It must be noted that this is only the case because the wheel drag coefficient is assumed to be 0.02 for both the towing vehicle and aircraft tyres. As a result the velocity-time and distance-time profiles are exactly the same for all aircraft, as shown in

Figures 7.6 and 7.7. The change in wheel drag of 1.96 kN between versions can be observed in Figure 7.8, which is due to the 10,000 kg change in mass.

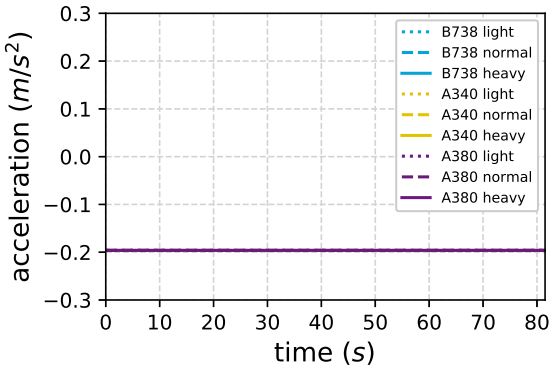

Figure 7.5: acceleration-time (decelerating)

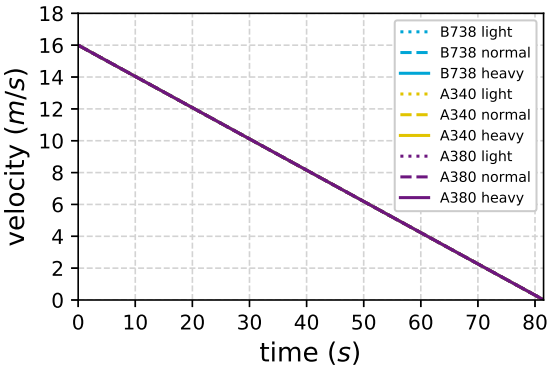

Figure 7.6: velocity-time (decelerating)

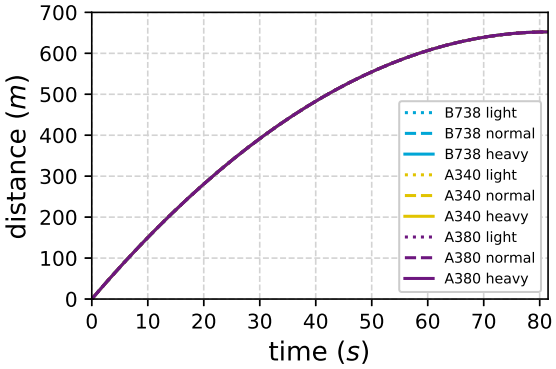

Figure 7.7: distance-time (decelerating)

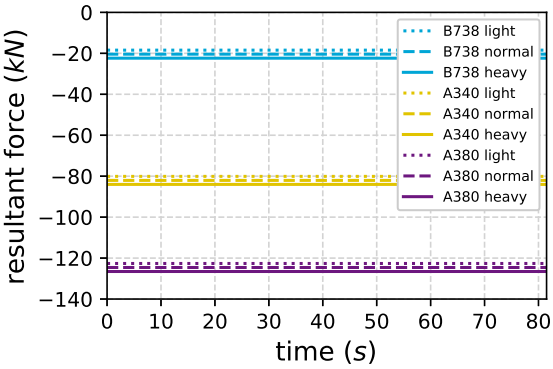

Figure 7.8: resultant force-time (decelerating)

From the results it can be concluded that the light versions of the fully electric towing vehicles are slower than the normal versions, and that the heavy versions are the fastest. However, a lot more power is required the heavier the version of towing vehicle, whilst the time advantage is insignificant for operational towing. Furthermore, all versions are fast enough to be integrated into traffic with conventional taxiing.

7.2. Vehicle routing problems

The ground movements of the fully electric towing vehicle at Rotterdam-the Hague Airport and Amsterdam Airport Schiphol are simulated for the four different settings from Table 7.1. The outputs are used to set up new vehicle routing problems. The results of the vehicle routing problem can be found in Figures 7.9-7.18.

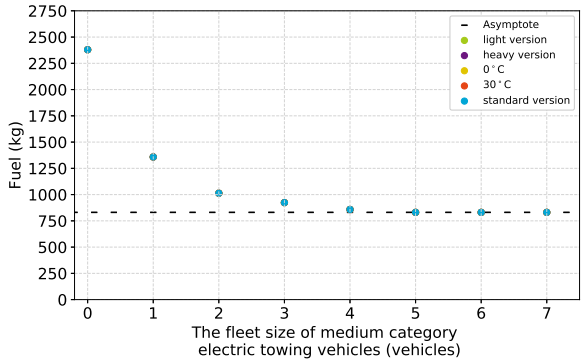

Figure 7.9: The aggregate aircraft fuel reduction with a varying number of medium towing vehicles deployed with runway 06 active, for five different settings.

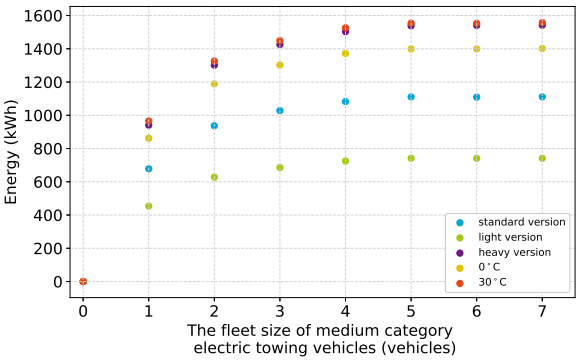

Figure 7.10: The aggregate energy consumption with a varying number of medium towing vehicles deployed with runway 06 active, for five different settings.

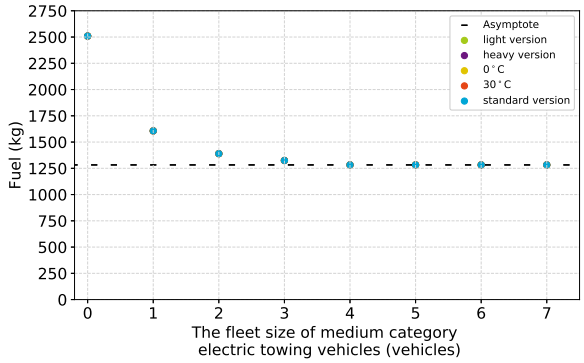

Figure 7.11: The aggregate aircraft fuel reduction with a varying number of medium towing vehicles deployed with runway 24 active, for five different settings.

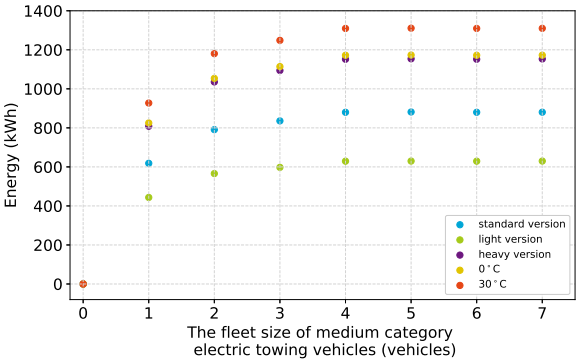

Figure 7.12: The aggregate energy consumption with a varying number of medium towing vehicles deployed with runway 24 active, for five different settings.

A maximum fleet size of twenty towing vehicles was used in the sensitivity analysis for Amsterdam Airport Schiphol, due to the extensive run times required to solve the NP-hard Vehicle Routing Problems.

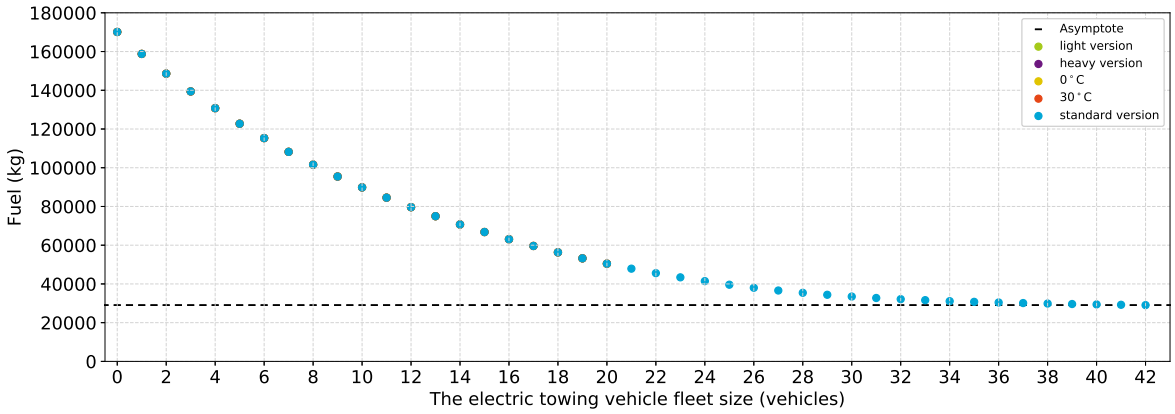

Figure 7.13: The aggregate aircraft fuel reduction with a varying number of medium towing vehicles deployed at Amsterdam Airport Schiphol, for five different settings.

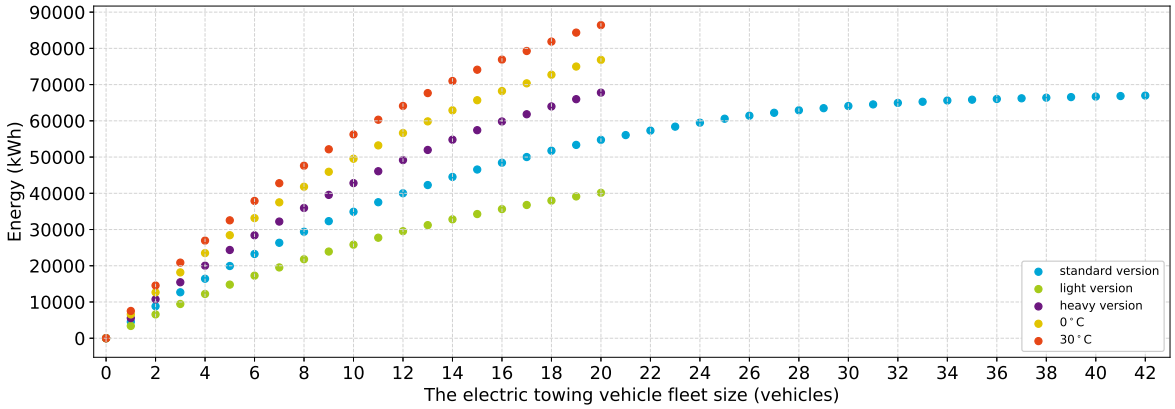

Figure 7.14: The aggregate energy consumption with a varying number of medium towing vehicles deployed at Amsterdam Airport Schiphol, for five different settings.

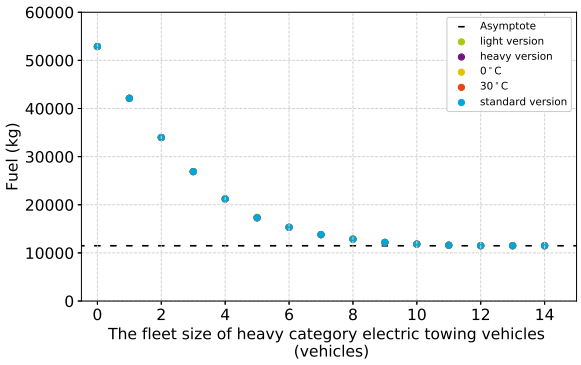

Figure 7.15: The aggregate aircraft fuel reduction with a varying number of heavy towing vehicles deployed at Amsterdam Airport Schiphol, for five different settings.

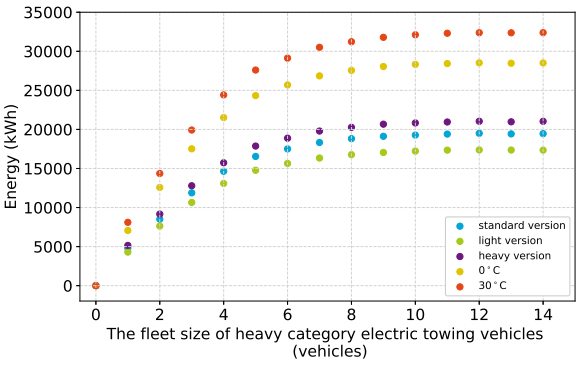

Figure 7.16: The aggregate energy consumption with a varying number of heavy towing vehicles deployed at Amsterdam Airport Schiphol, for five different settings.

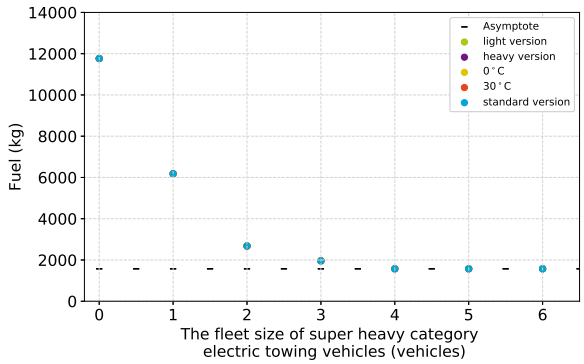

Figure 7.17: The aggregate aircraft fuel reduction with a varying number of super heavy towing vehicles deployed at Amsterdam Airport Schiphol, for five different settings.

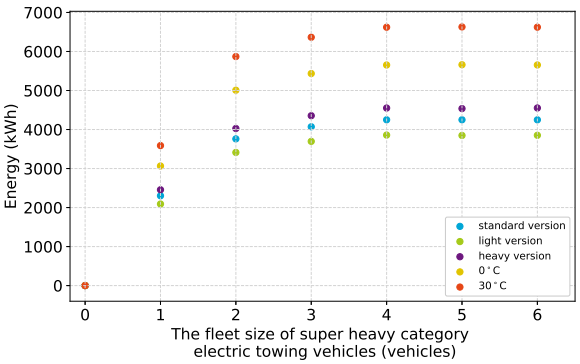

Figure 7.18: The aggregate energy consumption with a varying number of super heavy towing vehicles deployed at Amsterdam Airport Schiphol, for five different settings.

All the results of the vehicle routing problems show that the different settings of the sensitivity analysis do not affect the total fuel consumption at both airports. Neither the outside air temperature nor the different versions of fully electric towing vehicle affect the total fuel consumption. The results of the total energy consumption show that the energy consumption differs for the different settings. The normal version towing vehicle consumes more energy than the light version, and less energy than the heavy version. This is logical as more energy is required to bring a heavier object into motion. The figures also show that more energy is required in very warm and very cold conditions, when the PCA power demand is high. Cooling the aircraft requires more energy than heating the aircraft. The results show that the total fuel reduction potential is independent of the total energy consumption for the situations tested.

A possible explanation to why the fuel consumption is equal in all cases, is that the flight schedules are the constraining factor and not the battery capacity of the towing vehicles. Another possible explanation is that the vehicle routing problem is based on invalid assumptions. One of the assumptions made is that the towing vehicle is always fully charged when leaving the depot. This is not the case in real life, if the towing vehicle has insufficient time at the depot to fully charge. Another assumption made is that a minimum charging time at the depot. This assumption was made in order to force every towing vehicle to charge before leaving the depot. However it also prevents the towing vehicle from leaving, even if the towing vehicle is almost fully charged. For this reason the minimum charging time is decreased to five minutes. The combination of both assumptions implies that any towing vehicle can leave the depot fully charged after charging for five minutes, no matter how empty the battery when it arrived. The scheduling results are analysed in order to check if this flaw occurs.

At Rotterdam-the Hague Airport, the energy required to tow all the aircraft is less than the battery capacity of a single towing vehicle. Therefore, the towing vehicles at this airport do not require a recharge during the day. Next, the times at the depots are checked for the super heavy towing vehicles at Schiphol. The minimum time at a depot is 12 minutes. The recharging time in almost all cases are over 90 minutes. In the few cases where the recharging time is less, the energy consumed by the towing vehicle the entire day is less than the battery capacity. In these cases the flaws in the vehicle routing problems are not the reason why the total fuel consumption is constant for the different settings, suggesting the flight schedules are the limiting factor. The battery capacity will become the limiting factor if reduced sufficiently.

It can be concluded that the battery capacity of the fully electric towing vehicles are over-dimensioned. The same fuel reduction potential can be achieved with less battery capacity. As lithium ion batteries are expensive, it would be better to reduce the number of batteries, thereby reducing the cost of a towing vehicle. The same applies for the towing vehicle mass, which increases the energy consumption, but not the fuel saving potential.

8

Conclusions, limitations, and recommendations

In this chapter the conclusions of the feasibility study will be stated in Section 8.1. The limitations of the research are stated in Section 8.2, and the recommendations for the future are stated in Section 8.3.

8.1. Conclusions

A feasibility study is performed to show that operational towing can be done fully electrically, without the utilization of the aircraft main engines or auxiliary power unit. The feasibility study consists of a conceptual design, of which the operational performance is simulated at a regional and an international hub airport, after which the fuel reduction potential at those airports is calculated for a single day using real flight schedules.

The concepts for three models of fully electric towing vehicles are generated to enable the fully electric towing of all common passenger aircraft at speeds in excess of 14 m/s. The concepts have the ability to move around autonomously, do not require modifications to the aircraft, and do not require the utilization of the main engines or the APU during a tow. Based on the dynamic model used, the kinematic performance of the fully electric towing vehicles are quick enough for the concept to be integrated into conventional traffic. It can be concluded that the fully electric towing vehicle concept is technically feasible, under the presumption that such a system can be built.

The fully electric towing vehicle designs are simulated for all the taxi movements of a single day at Rotterdam-the Hague Airport and Amsterdam Airport Schiphol. Similarly, the taxiing performance of full-engine taxiing aircraft is simulated for the same flights and compared to fully electric towing performance. The comparison criteria are: the travel duration, the fuel consumption, and energy consumption. The results show that the towed aircraft move at higher speeds than the conventional taxiing aircraft, but the attaching and detaching processes of the fully electric towing require additional time. As a result, the fully electric towing vehicles tend to be equally fast or up to 1.5 minutes slower. Furthermore, the fully electric towing vehicle has the potential to reduce the fuel consumption for all taxi movements. In general, more fuel can be saved per tow the heavier the aircraft type, but also costs extra energy. The same applies between departing and arriving aircraft, where the departing aircraft are heavier than arriving aircraft. As the fully electric towing vehicle fulfils the operational requirements and is able to operate in an airport environment to reduce the aircraft fuel consumption of all flights, it can be concluded that the fully electric towing vehicle is operationally feasible.

A scheduling problem was formulated for the deployment of a fleet of fully electric towing vehicles at Rotterdam-the Hague Airport and Amsterdam Airport Schiphol in order to calculate the fuel saving potential with the corresponding energy costs. The scheduling problem is solved by solving a Vehicle Routing Problem of a fleet of towing vehicles and a set of flights representing a single day of flights at both airports. The fleet size of fully electric towing vehicles is varied to test the effectiveness of different fleet sizes on the fuel saving potential. The results show that the total fuel consumption per day by all flights at Rotterdam-the Hague Airport can be reduced by at least 65% (1,548 kg). This requires the deployment of five medium category towing vehicles and costs approximately 1,1 MWh of power without losses due to charging. For every kilowatthour of electricity invested, 1.4 kilograms of airplane fuel can be saved. At Amsterdam Airport Schiphol, the total fuel consumption per day can be reduced by at least 82% (192,600 kg). This will require forty-two medium, twelve heavy and four super heavy category towing vehicles, and costs approximately 90.4 MWh of power without losses due to charging. For every kilowatt-hour of electricity invested, 2.1 kilograms of airplane fuel can be saved. The medium category towing vehicle has the largest fuel reduction potential at Schiphol due to the large number of medium category flights. By towing all the medium category flights, 60% less fuel will be consumed. Furthermore, the marginal utility of a fully electric towing vehicle decreases exponentially the larger the fleet size of deployed towing vehicles due to the law of diminishing marginal utility.

With the current fuel price of €1.10/kg and electricity price of €0.0589/kWh, it is shown that the maximum allowable unit cost of a fully electric towing vehicle of any category is above €5 million at Amsterdam Airport Schiphol. From this it can be concluded that the fully electric towing system can be economically feasible at an international hub airport. The economic feasibility of the fully electric towing system at Rotterdam-the Hague Airport is less clear as the maximum allowable unit cost is lower. Assuming a vehicle lifespan of five years, the maximum allowable unit cost ranges between €0.6-1.7 million depending on the fleet size. With a lifespan of ten years, the maximum allowable unit cost ranges between €1.2-2.4 million, which is more plausible. The maximum allowable cost of the first towing

vehicle unit is in excess of €1.7 million, making the fully electric towing system economically feasible at Rotterdam-the Hague Airport.

A sensitivity analysis is performed to test the effect of the outside temperature on the system's performance and to test the effect of lighter and heavier designs of the fully electric towing vehicle on the operational performance. The results show that the total fuel consumption at both airports is not affected by the outside air temperature or the differences in towing vehicle models. The total energy consumption is affected by the outside air temperature. Warm and cold weather increase the total energy consumption due to cooling and heating. The normal versions of the fully electric towing vehicles consume more energy than the light versions, and less energy than the heavy versions. The most probable explanation why the different models are equally effective in reducing fuel, is that the flight schedule is the limiting factor and not the battery capacity for these models. It can be concluded that the standard towing vehicle models are overpowered and can be downsized to reduce financial and energy costs.

The fully electric towing concept will be difficult to integrate at an international hub airport. The high frequency of movements will require a large number of towing vehicles, manned waiting zones for the towing vehicles near the exits ramps of runways and the airside traffic will increase on both the apron and taxiways. Towing vehicle depots will have to be placed airside, the scheduling of towing vehicles will have to be managed, and maintenance will have to be performed on the towing vehicles. The noselanding gear of aircraft are not designed for operational towing and will get fatigued due to towing, requiring additional maintenance and costs. Furthermore, the system will require a large financial investment. The management and integration of the fully electric towing system at a regional airport will be less complicated as only a few towing vehicles are required that only need to recharge a single time overnight. As the frequency of movements is low at regional airports, the additional traffic will not be problematic.

It can be concluded that the fully electric towing system can be a technically and operationally feasible alternative to conventional taxiing operations at regional and international hub airports, with large fuel and emission reduction potentials. The system can be used to the reduce cost and environmental impact of aircraft taxi operations. The system should be integrable with conventional traffic. The contribution of this research to the body of knowledge is that the concept of a fully electric towing system discussed is not proven to be infeasible and shows potential to have a positive impact. This study encourages additional and a more detailed research on this topic, which is required before the realization of a fully electric towing system.

8.2. Limitations

The research has its limitations due to the scope, methods used, and the assumptions made. The limitations of this research will be discussed in this section, and should be considered when interpreting the conclusions.

The conclusions of the feasibility of a fully electric towing system does not rule the concept to be definitely feasible. Instead, the feasibility of the concept is only considered valid under the assumptions made. Further research may prove the concept to be infeasible. In the scope of this research, only part of the technical and operational feasibility of the implementation of a fully electric towing system is investigated, and the economic feasibility was touched upon. Also, only a single fully electric towing concept is investigated in this thesis, where alternative fully electric towing concepts may be more promising. The results of this thesis show that the technical design of the towing vehicle models can be improved.

No fully electric towing system is commercially available that provides power for PCA, the on-board systems, and the engine start-up, making this concept a novel idea. The research was performed at a high level to get an initial indication of the operational feasibility of this concept. Relatively simple models were used in the methodology as little research is available that could be built upon. An investigation at a lower level will give more precise and accurate results. Furthermore, many assumptions had to be made due to the lack of reference literature.

The computation time of the Vehicle Routing Problems used to solve the scheduling problem is extensive due to large number of decision variables involved. The number of decision variables have to be kept to a minimum for the method to be practical. Sets with a large number of flights need to be split up to reduce the computation time. The method described in this thesis does not consider the interaction between split parts. The method can be improved by using the outputs of a part as inputs in the subsequent part.

The following are limitations due to the simplifications in the models:

- Traffic was not considered for the ground movement simulations and Vehicle Routing Problem, which could affect the total fuel and energy consumption, the travel duration and delays. Delays were also not included in the research, which would influence the scheduling problem and affect the fuel reduction potential.

- Even though the effect of the outside air temperature was considered in this research, the effects of weather were not. The weather can affect the ground friction and the battery performance. A slippery ground surface due to rain or snow will reduce the traction, ground drag, and will require towing at lower speeds. Furthermore, the outside temperature can affect the chemical reactions in batteries. It may be possible that the fully electric towing system can not operate in cold and slippery weather conditions. Furthermore, the outside temperature used in the investigation was assumed to be constant the entire day, which should vary during the day for more accurate results.

- The cost function of the Vehicle Routing Problem only minimized for the total fuel consumption, but not also for the total energy consumption. As a result, the total energy required may have turned out higher than necessary. A multi-objective cost function can solve this issue, by considering both the minimization of total fuel and energy consumption.

- The cases investigated are only for a set of flights for a single day. The conclusions drawn are based on these cases, but may not be valid for other cases. Multiple days and special cases, i.e. the most and least busy days, will have to be investigated to further validate the conclusions drawn.

8.3. Recommendations

This section lists recommendations for future research. The following list of recommendations will help improve the research performed in this thesis:

- Investigate critical cases to test the robustness of the fully electric towing system. The following are critical cases that can be investigated:
  - the most and least busy day of the year
  - the warmest and the coldest day of the year
  - a low and high ground friction coefficient
- Investigate the feasibility of less powerful and lighter designs. In this thesis it is concluded that the fully electric towing vehicle designs were unnecessarily powerful and heavy. Reducing the mass and power of the design will lower the unit and operation costs.
- Find the limit where the battery capacity is the limiting factor for the towing vehicle routes, instead of the schedule. The results will help size the battery capacity of a better towing vehicle design, where energy is not wasted transporting excess battery mass.
- Apply the method to a wider range of airports to test the feasibility and effectiveness of a fully electric towing system at those airports. Airports differ and only two airports were investigated in this thesis. The concept is possibly suitable for military or cargo aircraft as well.
- Investigate a scheduling strategy where the vehicles stay with the aircraft during the turnaround. This strategy allows the towing vehicle to charge whilst on the aircraft stand and reduces the number of processes required per movement. Every towing vehicle will have to be connected and disconnected only once per taxi-in and taxi-out pair. This strategy will require the same or more towing vehicles to achieve the same fuel reduction potential as the shared towing vehicle used in this thesis.
- Improve the models used in the methodology:
  - The dynamic model can be improved by expanding the forces acting on the system, e.g. aerodynamic drag, dynamic forces, rotational forces, longitudinal and lateral forces.
  - The ground movement models can be improved for the conventional taxiing movements. Instead of assuming a constant acceleration of 0.7 $m/^2$, the thrust can be determined from the thrust setting and engine thrust rating. Also, the kinematics can be simulated over multiple links at a time if the links are oriented in the same direction, instead of simulating every link separately. The simulations of sharp turns can be improved by assuming the turn to consist of two straight links. The first of the links will be used to simulate the deceleration phase of the turn and the second link will be used to simulate the acceleration phase of the turn.
  - The vehicle routing problems can be improved by keeping track of the battery life during operations. If the problem is split in multiple parts, the results of one part should be integrated into the next part. Include the effects of traffic and delays in the model.

The following recommendations are additional ideas which can be used to improve the concept for a fully electric towing system:

- The aircraft engines will have to run at idle, during part of a fully electric tow, to warm up or cool down the engines, which consumes fuel. It is recommended that research will be performed on alternative methods of warming up and cooling down the aircraft engines during operational towing, where the engines can be shut off to save extra fuel.
- One of the disadvantages of operational towing are the additional stresses on the noselanding gear, which increases the rate of fatigue in the noselanding gear. A possible solution that can be investigated to overcome this problem, is the placement of a fully electric towing vehicle on every landing gear that are coordinated with each other. The force on the noselanding gear will be distributed over all landing gears, thus decreasing the rate of fatigue in the noselanding gear.
- Another suggestion is to investigate the automatic coupling and decoupling of the power and the PCA between the aircraft and the fully electric towing vehicle, as this process is labour intensive and currently requires human intervention. A spring system is a possible solution for automatic decoupling. Automatic coupling is a bigger challenge as the process requires precision and gravity works as a disadvantage in this case.

Bibliography

[1] Table 12 . 6 Carbon Dioxide Emissions From Energy Consumption : Electric Power Sector NA NA. Technical report, U.S. Energy Information Administration, Washington D.C., 2017.

[2] R. Algra, R. Snijder, R. Spaans, and J. Nieuwenhuizen. Analyse meldingen rondom Rotterdam The Hague Airport. Technical report, DCMR Milieudienst Rijnmond, Schiedam, 2017.

[3] J. Ban, J. León Arellano, A. Alawami, R. F. Aguilera, and M. Tallett. World oil outlook. Technical report, OPEC, 2016.

[4] M. Bay and S. Limbourg. TSP model for electric vehicle deliveries, considering speed, loading and road grades. *Sixth international workshop on Freight . . .*, 2015.

[5] L. Chen, S. Wang, G. Li, C. H. Lin, and T. Zhang. CFD modeling of moisture accumulation in the insulation layers of an aircraft. *Applied Thermal Engineering*, 102:1141–1156, 2016.

[6] C. Evertse. A Low Emissions Taxi Movement Planning Tool. Technical report, 2014.

[7] FlightGlobal. FlightStats, 2017.

[8] N. Guillaume. *Finding the viability of using an automated guided vehicle taxiing system for aircraft.* Master thesis, Delft University of Technology, 2018.

[9] J. Hospodka. Cost-benefit analysis of electric taxi systems for aircraft. *Journal of Air Transport Management*, 39:81–88, 2014.

[10] IBM. CPLEX Optimizer | IBM, 2019.

[11] ICAO. ICAO Aircraft Engine Emissions Databank, 2017.

[12] M. Ithnan, T. Selderbeek, and G. Beelaerts van Blokland, WWA Lodewijks. Aircraft Taxiing Strategy Optimization. 2013.

[13] U. Kesgin. Aircraft emissions at Turkish airports. *Energy*, 31(2-3):372–384, 2006.

[14] G. Macrina, G. Laporte, F. Guerriero, and L. Di Puglia Pugliese. An energy-efficient green-vehicle routing problem with mixed vehicle fleet, partial battery recharging and time windows. *European Journal of Operational Research*, 276(3):971–982, 2019.

[15] M. Rensen. The Value of Implementing Multiple Aircraft Receiving Stands (MARS). Technical report, Delft University of Technology, Delft, 2013.

[16] P. Roling. Airport Surface Traffic Planning Optimization: A Case Study of Amsterdam Airport Schiphol. *9th AIAA Aviation Technology, Integration, and Operations Conference (ATIO)*, (September):1–7, 2009.

[17] Rotterdam Airport B.V. Rotterdam-The Hague Airport, 2017.

[18] Schiphol. Schiphol Developer Center.

[19] S. Steenhart. Kwartaalrapportage Vliegtuigmeldingen rondom Rotterdam The Hague Airport 3 e kwartaal 2017. Technical Report 3rd Quarter, DCMR Milieudienst Rijnmond, Schiedam, 2017.

[20] S. Steenhart. Kwartaalrapportage Vliegtuigmeldingen rondom Rotterdam The Hague Airport 1 e kwartaal 2018. Technical report, DCMR Milieudienst Rijnmond, Schiedam, 2018.

[21] S. Steenhart. Kwartaalrapportage Vliegtuigmeldingen rondom Rotterdam The Hague Airport 3 e kwartaal gebruiksjaar 2018. Technical Report 3rd Quarter, DCMR Milieudienst Rijnmond, Schiedam, 2018.

A

Airport data

A.1. Rotterdam-The Hague Airport

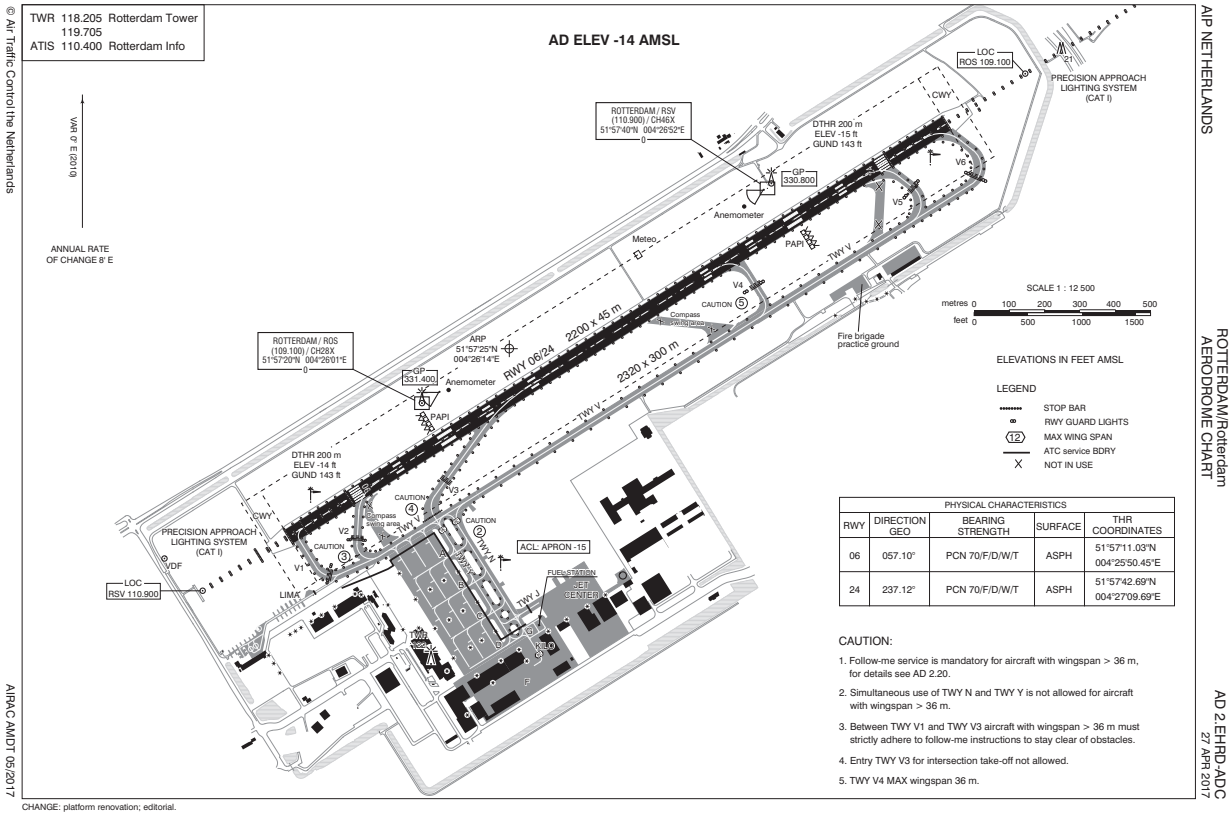

Figure A.1: The aerodrome chart of Rotterdam-The Hague Airport.

Table A.1: The flight schedule data of Rotterdam-the Hague Airport on 25^{th} July, 2017.

Index	Local date	Local time	Flight	Registration	Type	Platform	Direction
1	25/07/17	7:02	HV6035	PH-XRD	B737	C	D
2	25/07/17	7:04	HV6061	PH-HXJ	B738	C	D
3	25/07/17	7:08	BA4450	G-LCYN	E190	C	D
4	25/07/17	7:10	HV5053	PH-HZD	B738	B	D
5	25/07/17	7:26	HV5705	PH-XRB	B737	A	D
6	25/07/17	7:43	HV5021	PH-HXK	B738	B	D
7	25/07/17	8:05	HV5997	PH-XRY	B737	B	D
8	25/07/17	9:23	BA4451	G-LCYN	E190	C	A
9	25/07/17	10:04	BA4452	G-LCYN	E190	C	D
10	25/07/17	10:09	JP972	S5-AAY	CR7	A	D
11	25/07/17	10:17	HV5706	PH-XRB	B737	C	A
12	25/07/17	11:21	HV6285	PH-XRB	B737	C	D
13	25/07/17	11:51	HV6062	PH-HXJ	B738	C	A
14	25/07/17	11:55	HV5054	PH-HXE	B738	C	A
15	25/07/17	12:18	HV6036	PH-XRD	B737	B	A
16	25/07/17	12:20	HV5998	PH-XRY	B737	C	A
17	25/07/17	12:56	HV5689	PH-HXE	B738	C	D
18	25/07/17	13:09	HV6259	PH-XRD	B737	B	D
19	25/07/17	13:18	HV6301	PH-HXJ	B738	C	D
20	25/07/17	13:33	HV6081	PH-XRY	B737	C	D
21	25/07/17	15:30	HV6286	PH-XRB	B737	C	A
22	25/07/17	16:19	HV6093	PH-XRB	B737	C	D
23	25/07/17	17:01	HV6082	PH-XRY	B737	B	A
24	25/07/17	17:38	HV6260	PH-XRD	B737	C	A
25	25/07/17	18:05	HV6493	PH-XRY	B737	B	D
26	25/07/17	18:08	HV5690	PH-HXE	B738	B	A
27	25/07/17	18:22	HV6773	PH-XRD	B737	C	D
28	25/07/17	18:24	HV4457	G-LCYL	E190	C	A
29	25/07/17	18:43	HV6192	PH-HSC	B738	C	A
30	25/07/17	18:51	HV5067	PH-HXE	B738	B	D
31	25/07/17	19:35	HV6191	PH-HSC	B738	C	D
32	25/07/17	20:56	BA4458	G-LCYL	E190	C	D
33	25/07/17	22:06	HV6494	PH-XRY	B737	C	A
34	25/07/17	22:42	HV6094	PH-XRB	B737	C	A
35	25/07/17	22:42	HV6774	PH-XRD	B737	B	A
36	25/07/17	22:45	BA4459	G-LCYL	E190	A	A
37	25/07/17	22:47	HV6302	PH-HXJ	B738	B	A
38	25/07/17	22:51	HV5022	PH-HXI	B738	B	A
39	25/07/17	23:03	HV5068	PH-HXE	B738	C	A

A.2. Amsterdam Airport Schiphol

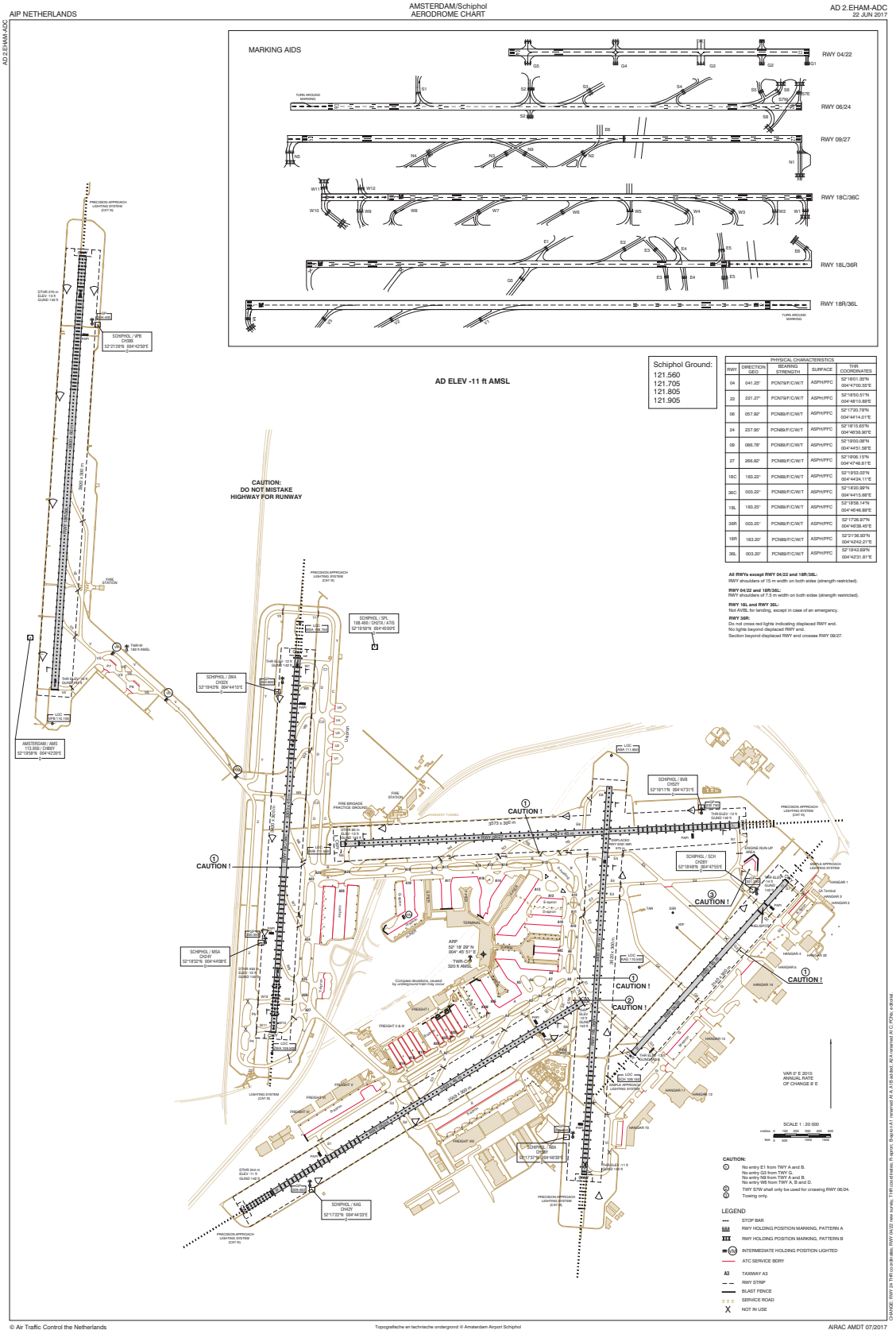

Figure A.2: The aerodrome chart of Amsterdam Airport Schiphol.

B

Ground movement simulations

B.1. Airport model data: Rotterdam-The Hague Airport

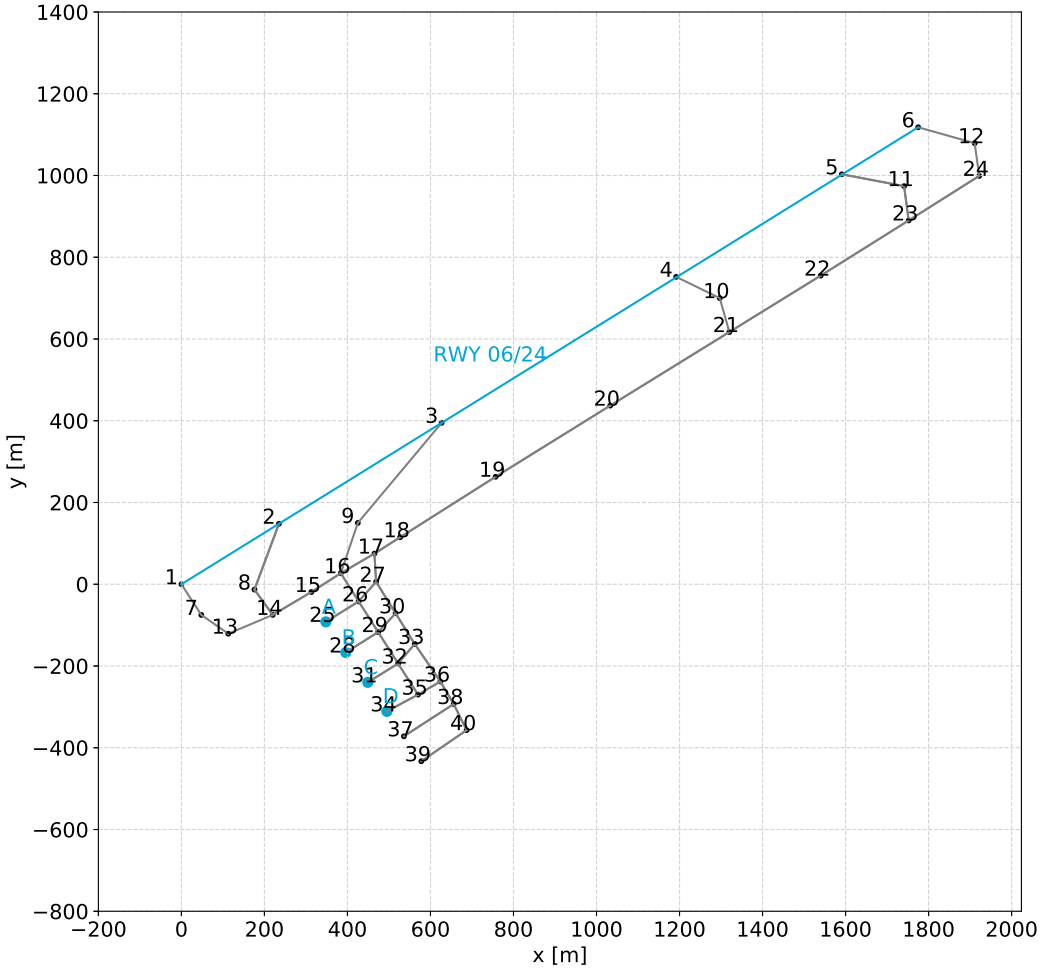

Figure B.1: The node and link diagram of Rotterdam-the Hague Airport

Table B.1: Node and link system data: Rotterdam-the Hague Airport

Node ID	Conn't Node1	Conn't Node2	Conn't Node3	Conn't Node4	Dist Node1	Dist Node2	Dist Node3	Dist Node4	Speed Node1	Speed Node2	Speed Node3	Speed Node4
1	0	0	0	0	0	0	0	0	0	0	0	0
2	8	0	0	0	172	0	0	0	10	10	10	10
3	9	0	0	0	318	0	0	0	10	10	10	10
4	10	0	0	0	117	0	0	0	10	10	10	10
5	11	0	0	0	153	0	0	0	10	10	10	10
6	0	0	0	0	0	0	0	0	10	10	10	10
7	1	0	0	0	89	0	0	0	10	10	10	10
8	2	14	0	0	172	76	0	0	10	10	10	10
9	16	0	0	0	130	0	0	0	10	10	10	10
10	21	0	0	0	86	0	0	0	10	10	10	10
11	5	23	0	0	153	85	0	0	10	10	10	10
12	6	0	0	0	141	0	0	0	10	10	10	10
13	7	0	0	0	80	0	0	0	10	10	10	10
14	8	13	15	0	76	117	108	0	10	10	10	10
15	14	16	0	0	108	85	0	0	10	10	10	10
16	15	17	26	0	85	94	81	0	10	8	4	10
17	16	18	27	0	94	74	69	0	8	10	4	10
18	17	19	0	0	74	274	0	0	10	12	10	10
19	18	20	0	0	274	326	0	0	12	14	12	12
20	19	21	0	0	326	339	0	0	14	14	14	14
21	20	22	0	0	339	260	0	0	14	14	14	14
22	21	23	0	0	260	251	0	0	14	14	14	14
23	11	22	24	0	85	251	202	0	14	14	14	14
24	12	23	0	0	81	202	0	0	10	10	10	10
25	26	28	0	0	93	90	0	0	4	4	4	4
26	16	25	27	29	81	93	64	88	4	4	4	4
27	17	26	30	0	69	64	90	0	4	4	4	4
28	29	31	25	0	93	88	90	0	4	4	4	4
29	26	28	30	32	88	93	62	91	4	4	4	4
30	27	29	33	0	90	62	88	0	4	4	4	4
31	32	34	28	0	86	111	88	0	4	4	4	4
32	29	31	33	35	91	86	62	90	4	4	4	4
33	30	32	36	0	88	62	111	0	4	4	4	4
34	35	37	31	0	85	64	111	0	4	4	4	4
35	32	34	36	0	90	85	63	0	4	4	4	4
36	33	35	38	0	111	63	64	0	4	4	4	4
37	38	0	34	0	144	0	64	0	4	4	4	4
38	36	37	40	0	64	144	71	0	4	4	4	4
39	40	0	0	0	133	0	0	0	4	4	4	4
40	38	39	0	0	71	133	0	0	4	4	4	4

B.2. Taxi Routes: Rotterdam-the Hague Airport

Table B.2: Taxi routes Rotterdam-the Hague Airport

From	To	Turns	Node sequence
32	128	1	32-63-62-70-47-128
32	130	1	32-63-62-61-69-130
32	131	1	32-63-62-61-60-59-67-131
51	128	2	51-56-64-65-66-67-68-69-70-47-128
51	130	2	51-56-64-65-66-67-68-130
51	131	2	51-56-64-65-66-67-131
79	128	2	79-90-89-88-87-86-85-96-64-65-66-67-68-69-70-47-128
79	130	3	79-90-89-88-87-86-85-96-64-65-66-67-68-130
128	71	3	128-47-46-45-44-26-25-24-23-22-21-20-19-92-81-71
128	80	3	128-47-43-63-62-61-60-59-58-57-56-97-98-99-100-91-80
128	109	3	128-47-43-63-62-61-60-59-58-57-56-97-98-87-76-107-136-121-120-119-117-109
130	71	2	130-68-60-59-58-57-56-97-86-85-84-83-82-81-71
130	109	3	130-68-60-59-58-57-56-97-98-87-76-107-136-121-120-119-117-109
131	71	2	131-67-59-58-57-56-97-86-85-84-83-82-81-71
131	80	3	131-67-59-58-57-56-97-98-99-100-91-80
131	109	3	131-67-59-58-57-56-97-98-87-76-107-136-121-120-119-117-109

B.3. Airport model data: Amsterdam Airport Schiphol

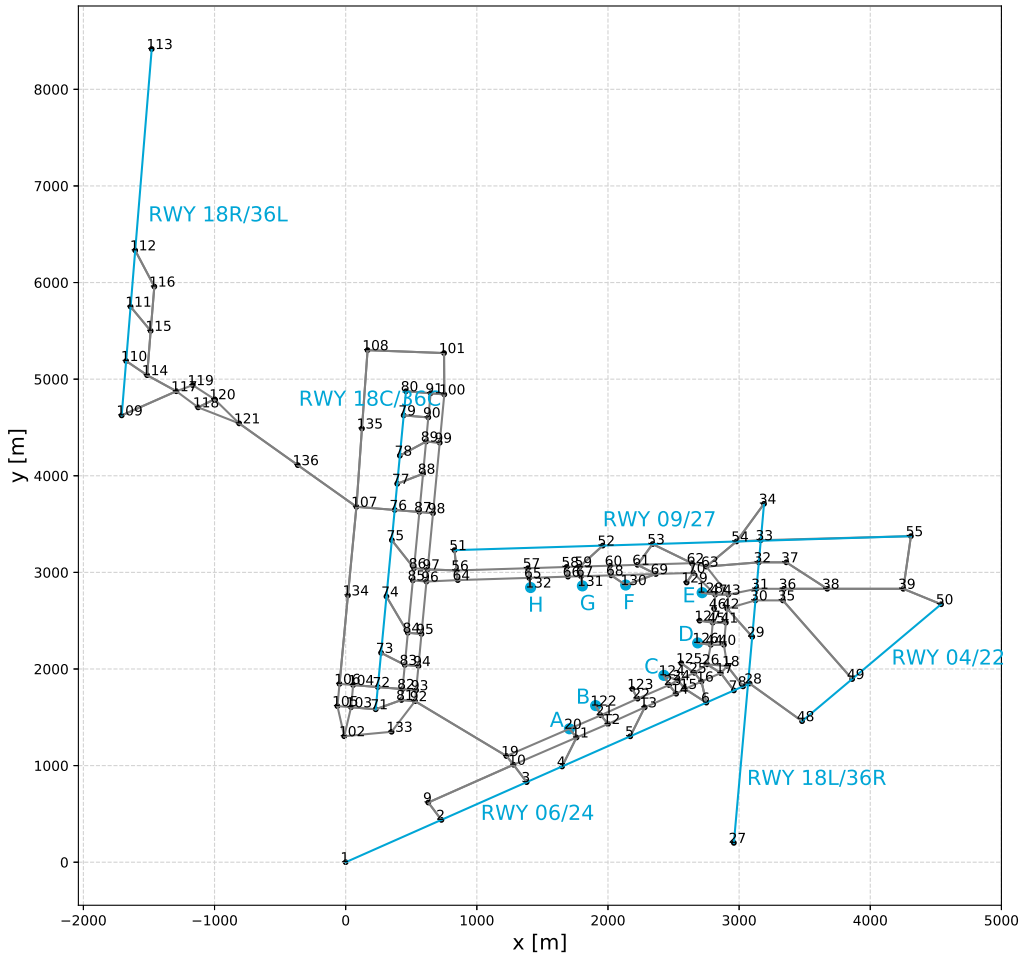

Figure B.2: The node and link diagram of Amsterdam Airport Schiphol

Table B.3: Node and link system data: Amsterdam Airport Schiphol - part 1 of 3

Node ID	Conn't Node1	Conn't Node2	Conn't Node3	Conn't Node4	Dist Node1	Dist Node2	Dist Node3	Dist Node4	Speed Node1	Speed Node2	Speed Node3	Speed Node4
0	0	0	0	0	0	0	0	0	0	0	0	0
1	0	0	0	0	0	0	0	0	10	10	10	10
2	0	9	0	0	0	206	0	0	10	10	10	10
3	0	10	0	0	0	206	0	0	10	10	10	10
4	0	11	0	0	0	320	0	0	10	10	10	10
5	0	13	0	0	0	320	0	0	10	10	10	10
6	0	15	16	0	0	216	221	0	10	10	10	10
7	0	17	0	0	0	206	0	0	7	7	7	7
8	0	18	28	0	0	242	58	0	7	7	7	7
9	2	10	0	0	206	758	0	0	10	10	10	10
10	9	19	11	3	758	105	557	206	10	10	10	10
11	0	20	12	4	0	105	278	320	10	10	10	10
12	0	21	13	0	0	105	329	0	10	10	10	10
13	0	14	5	0	0	278	320	0	10	10	10	10
14	0	23	15	0	0	105	84	0	7	7	7	7
15	0	24	16	6	0	105	147	216	7	7	7	7
16	0	25	17	6	0	105	171	221	7	7	7	7
17	0	26	18	7	0	138	88	206	7	7	7	7
18	0	26	40	8	0	155	221	242	7	7	7	7
19	10	92	0	0	105	899	0	0	10	10	10	10
20	19	11	0	0	557	105	0	0	10	10	10	10
21	20	12	0	122	278	105	0	108	10	10	10	10
22	21	0	0	123	329	0	0	108	10	10	10	10
23	22	14	0	124	278	105	0	108	10	10	10	10
24	23	15	0	124	84	105	0	118	10	10	10	10
25	24	16	0	125	147	105	0	141	7	7	7	7
26	25	17	0	0	131	138	0	0	7	7	7	7
27	0	0	0	0	0	0	0	0	7	7	7	7
28	8	0	48	0	58	0	559	0	7	7	7	7
29	0	42	0	0	0	349	0	0	7	7	7	7
30	0	0	0	35	0	0	0	210	7	7	7	7
31	0	43	0	0	0	222	0	0	7	7	7	7
32	0	63	0	37	0	403	0	210	9	9	9	9
33	0	54	0	55	0	186	0	1145	9	9	9	9
34	54	0	0	0	443	0	0	0	9	9	9	9
35	0	49	36	0	0	970	120	0	0	0	0	0
36	31	35	38	0	210	120	330	0	0	0	0	0
37	32	38	0	0	210	415	0	0	0	0	0	0
38	36	37	39	0	330	415	580	0	0	0	0	0
39	38	50	55	0	580	329	548	0	0	0	0	0
40	0	44	41	0	0	100	230	0	7	7	7	7
41	0	45	42	0	0	100	145	0	7	7	7	7
42	29	0	43	30	349	0	145	232	7	7	7	7
43	47	0	63	0	100	0	335	0	7	7	7	7
44	26	40	0	126	204	100	0	102	7	7	7	7
45	44	41	0	127	230	100	0	102	7	7	7	7
46	45	0	0	0	145	0	0	0	7	7	7	7
47	46	43	0	128	145	100	0	102	7	7	7	7
48	28	0	0	0	559	0	0	0	0	0	0	0
49	0	35	0	0	0	970	0	0	0	0	0	0
50	0	39	0	0	0	329	0	0	0	0	0	0
51	56	0	0	0	211	0	0	0	10	10	10	10
52	0	59	0	0	0	279	0	0	10	10	10	10
53	0	61	62	0	0	244	360	0	10	10	10	10
54	0	63	0	34	0	347	0	443	9	9	9	9
55	0	39	0	pa	0	548	0	0	9	9	9	9

Table B.4: Node and link system data: Amsterdam Airport Schiphol - part 2 of 3

Node ID	Conn't Node1	Conn't Node2	Conn't Node3	Conn't Node4	Dist Node1	Dist Node2	Dist Node3	Dist Node4	Speed Node1	Speed Node2	Speed Node3	Speed Node4
56	97	51	0	64	220	211	0	100	10	10	10	10
57	56	65	0	0	545	100	0	0	10	10	10	10
58	57	66	0	0	295	100	0	0	10	10	10	10
59	58	67	0	52	100	100	0	279	10	10	10	10
60	59	68	0	0	230	100	0	0	10	10	10	10
61	60	69	0	53	210	169	0	244	10	10	10	10
62	61	70	0	53	415	100	0	360	10	10	10	10
63	62	0	54	32	115	0	347	403	9	9	9	9
64	0	56	65	0	0	100	545	0	10	10	10	10
65	0	57	66	132	0	100	295	100	10	10	10	10
66	0	58	67	0	0	100	100	0	10	10	10	10
67	0	59	68	131	0	100	230	100	10	10	10	10
68	0	60	69	130	0	100	340	149	10	10	10	10
69	0	61	70	130	0	169	285	256	10	10	10	10
70	0	62	47	129	0	100	281	112	9	9	9	9
71	103	0	81	0	189	0	218	0	10	10	10	10
72	0	104	0	82	0	189	0	189	10	10	10	10
73	0	83	0	0	0	220	0	0	11	11	11	11
74	0	0	84	0	0	0	409	0	11	11	11	11
75	0	0	86	0	0	0	336	0	11	11	11	11
76	0	0	107	87	0	0	294	189	10	10	10	10
77	0	0	88	0	0	0	223	0	10	10	10	10
78	0	0	89	0	0	0	247	0	10	10	10	10
79	0	0	90	0	0	0	189	0	10	10	10	10
80	0	91	0	0	0	189	0	0	10	10	10	10
81	71	0	92	0	218	0	105	0	10	10	10	10
82	81	72	0	93	113	189	0	105	10	10	10	10
83	82	73	0	94	251	220	0	105	11	11	11	11
84	83	74	95	0	334	409	105	0	11	11	11	11
85	84	0	96	0	543	0	105	0	11	11	11	11
86	85	0	75	0	126	0	336	0	11	11	11	11
87	86	0	76	98	583	0	189	105	7	7	7	7
88	77	87	0	0	223	397	0	0	11	11	11	11
89	88	0	78	99	334	0	247	105	11	11	11	11
90	89	0	79	0	251	0	189	0	11	11	11	11
91	90	80	100	0	251	189	105	0	11	11	11	11
92	81	0	93	19	105	0	113	899	10	10	10	10
93	0	94	82	0	0	251	105	0	10	10	10	10
94	0	95	83	0	0	334	105	0	11	11	11	11
95	0	96	84	0	0	543	105	0	11	11	11	11
96	0	97	0	64	0	126	0	239	11	11	11	11
97	0	98	86	56	0	583	105	220	11	11	11	11
98	0	99	87	0	0	731	105	0	7	7	7	7
99	0	100	89	0	0	501	105	0	10	10	10	10
100	0	101	91	0	0	428	105	0	10	10	10	10
101	100	108	0	0	428	584	0	0	10	10	10	10
102	133	103	0	0	364	304	0	0	10	10	10	10
103	0	0	71	104	0	0	189	231	10	10	10	10
104	0	106	72	0	0	105	189	0	10	10	10	10
105	102	103	0	0	316	105	0	0	10	10	10	10
106	105	0	134	0	231	0	919	0	10	10	10	10
107	134	76	136	135	919	294	621	812	11	11	11	11
108	135	101	0	0	812	584	0	0	11	11	11	11
109	0	117	0	0	0	486	0	0	10	10	10	10
110	0	0	114	0	0	0	217	0	10	10	10	10

Table B.5: Node and link system data: Amsterdam Airport Schiphol - part 3 of 3

Node ID	Conn't Node1	Conn't Node2	Conn't Node3	Conn't Node4	Dist Node1	Dist Node2	Dist Node3	Dist Node4	Speed Node1	Speed Node2	Speed Node3	Speed Node4
111	0	115	0	0	0	293	0	0	10	10	10	10
112	0	116	0	0	0	402	0	0	10	10	10	10
113	0	0	0	0	0	0	0	0	0	0	0	0
114	110	117	115	0	217	278	460	0	10	10	10	10
115	114	111	116	0	460	293	459	0	10	10	10	10
116	115	112	0	0	459	402	0	0	10	10	10	10
117	109	114	0	118	486	278	0	235	10	10	10	10
118	0	120	121	0	0	151	354	0	10	10	10	10
119	117	0	0	0	140	0	0	0	10	10	10	10
120	119	118	0	0	221	151	0	0	10	10	10	10
121	120	0	136	0	313	0	621	0	12	12	12	12
122	21	0	0	0	108	0	0	0	4	0	0	0
123	22	0	0	0	108	0	0	0	4	0	0	0
124	23	24	0	0	108	118	0	0	4	0	0	0
125	25	0	0	0	141	0	0	0	4	0	0	0
126	44	0	0	0	102	0	0	0	4	0	0	0
127	45	0	0	0	102	0	0	0	4	0	0	0
128	47	0	0	0	102	0	0	0	4	0	0	0
129	70	0	0	0	112	0	0	0	4	0	0	0
130	68	69	0	0	149	256	0	0	4	0	0	0
131	67	0	0	0	100	0	0	0	4	0	0	0
132	65	0	0	0	100	0	0	0	4	0	0	0
133	92	0	0	0	364	0	0	0	0	0	0	0
134	106	107	0	0	919	919	0	0	14	14	14	14
135	107	108	0	0	812	812	0	0	14	14	14	14
136	107	121	0	0	621	621	0	0	12	12	12	12

B.4. Taxi routes: Amsterdam Airport Schiphol

Table B.6: Taxi routes Amsterdam Airport Schiphol - medium category aircraft

From	To	Turns	Node sequence
20	109	3	20-19-92-93-94-95-96-97-98-87-76-107-136-121-120-119-117-109
28	20	1	28-8-18-26-25-24-23-22-21-20
28	122	2	28-8-18-26-25-24-23-22-21-122
28	124	2	28-8-18-26-25-24-124
28	126	1	28-8-18-40-44-126
28	128	1	28-8-18-40-41-42-43-47-128
28	131	1	28-8-18-40-41-42-43-63-62-61-60-59-67-131
28	132	1	28-8-18-40-41-42-43-63-62-61-60-59-58-57-65-132
53	20	1	53-62-70-47-46-45-44-26-25-24-23-22-21-20
53	122	2	53-62-70-47-46-45-44-26-25-24-23-22-21-122
53	124	2	53-62-70-47-46-45-44-26-25-24-124
53	126	2	53-62-70-47-46-45-44-126
53	128	2	53-62-70-47-128
53	131	1	53-61-60-59-67-131
53	132	1	53-61-60-59-58-57-65-132
77	20	4	77-88-87-86-85-84-83-82-81-92-19-10-11-20
77	122	4	77-88-87-86-85-84-83-82-81-92-19-10-11-12-21-122
77	124	3	77-88-87-86-85-96-64-65-66-67-68-69-70-47-46-45-44-26-25-24-124
77	126	3	77-88-87-86-85-96-64-65-66-67-68-69-70-47-46-45-44-126
77	128	3	77-88-87-86-85-96-64-65-66-67-68-69-70-47-128
77	131	3	77-88-87-86-85-96-64-65-66-67-131
77	132	3	77-88-87-86-85-96-64-65-132
112	20	4	112-116-115-114-117-118-121-136-107-76-87-86-85-84-83-82-81-92-19-10-11-20
112	122	4	112-116-115-114-117-118-121-136-107-76-87-86-85-84-83-82-81-92-19-10-11-12-21-122
112	124	3	112-116-115-114-117-118-121-136-107-76-87-86-85-96-64-65-66-67-68-69-70-47-46-45-44-26-25-24-124
112	126	3	112-116-115-114-117-118-121-136-107-76-87-86-85-96-64-65-66-67-68-69-70-47-46-45-44-126
112	128	3	112-116-115-114-117-118-121-136-107-76-87-86-85-96-64-65-66-67-68-69-70-47-128
112	131	3	112-116-115-114-117-118-121-136-107-76-87-86-85-96-64-65-66-67-131
112	132	3	112-116-115-114-117-118-121-136-107-76-87-86-85-96-64-65-132
122	71	3	122-21-20-19-92-81-71
122	80	4	122-21-20-19-92-93-94-95-96-97-98-99-100-91-80
122	109	3	122-21-20-19-92-93-94-95-96-97-98-87-76-107-136-121-120-119-117-109
124	71	3	124-23-22-21-20-19-92-81-71
124	80	3	124-23-14-15-16-17-18-40-41-42-43-63-62-61-60-59-58-57-56-97-98-99-100-91-80
124	109	3	124-23-14-15-16-17-18-40-41-42-43-63-62-61-60-59-58-57-56-97-98-87-76-107-136-121-120-119-117-109
126	7	1	126-44-26-17-7
126	71	3	126-44-26-25-24-23-22-21-20-19-92-81-71
126	80	3	126-44-40-41-42-43-63-62-61-60-59-58-57-56-97-98-99-100-91-80
126	109	3	126-44-40-41-42-43-63-62-61-60-59-58-57-56-97-98-87-76-107-136-121-120-119-117-109
128	71	3	128-47-46-45-44-26-25-24-23-22-21-20-19-92-81-71
128	80	3	128-47-43-63-62-61-60-59-58-57-56-97-98-99-100-91-80
128	109	3	128-47-43-63-62-61-60-59-58-57-56-97-98-87-76-107-136-121-120-119-117-109
131	7	1	131-67-68-69-70-47-46-45-44-26-17-7
131	71	2	131-67-59-58-57-56-97-86-85-84-83-82-81-71
131	80	3	131-67-59-58-57-56-97-98-99-100-91-80
131	109	3	131-67-59-58-57-56-97-98-87-76-107-136-121-120-119-117-109
132	71	2	132-65-57-56-97-86-85-84-83-82-81-71
132	80	3	132-65-57-56-97-98-99-100-91-80
132	109	3	132-65-57-56-97-98-87-76-107-136-121-120-119-117-109

Table B.7: Taxi routes Amsterdam Airport Schiphol - heavy category aircraft

From	To	Turns	Node sequence
29	20	2	29-42-43-47-46-45-44-26-25-24-23-22-21-20
29	126	3	29-42-43-47-46-45-44-126
29	128	1	29-42-43-47-128
29	130	1	29-42-43-63-62-61-69-130
29	131	1	29-42-43-63-62-61-60-59-67-131
52	20	1	52-59-67-68-69-70-47-46-45-44-26-25-24-23-22-21-20
52	126	2	52-59-67-68-69-70-47-46-45-44-126
52	128	2	52-59-67-68-69-70-47-128
52	130	2	52-59-67-68-130
52	131	0	52-59-67-131
52	132	1	52-59-58-57-65-132
78	20	4	78-89-88-87-86-85-84-83-82-81-92-19-10-11-20
78	126	3	78-89-88-87-86-85-96-64-65-66-67-68-69-70-47-46-45-44-126
78	128	3	78-89-88-87-86-85-96-64-65-66-67-68-69-70-47-128
78	130	3	78-89-88-87-86-85-96-64-65-66-67-68-130
78	131	3	78-89-88-87-86-85-96-64-65-66-67-131
111	132	3	111-115-114-117-118-121-136-107-76-87-86-85-96-64-65-132
122	109	3	122-21-20-19-92-93-94-95-96-97-98-87-76-107-136-121-120-119-117-109
124	109	3	124-23-14-15-16-17-18-40-41-42-43-63-62-61-60-59-58-57-56-97-98-87-76-107-136-121-120-119-117-109
126	71	3	126-44-26-25-24-23-22-21-20-19-92-81-71
126	109	3	126-44-40-41-42-43-63-62-61-60-59-58-57-56-97-98-87-76-107-136-121-120-119-117-109
128	71	3	128-47-46-45-44-26-25-24-23-22-21-20-19-92-81-71
128	80	3	128-47-43-63-62-61-60-59-58-57-56-97-98-99-100-91-80
128	109	3	128-47-43-63-62-61-60-59-58-57-56-97-98-87-76-107-136-121-120-119-117-109
130	71	2	130-68-60-59-58-57-56-97-86-85-84-83-82-81-71
130	80	3	130-68-60-59-58-57-56-97-98-99-100-91-80
130	109	3	130-68-60-59-58-57-56-97-98-87-76-107-136-121-120-119-117-109
131	71	2	131-67-59-58-57-56-97-86-85-84-83-82-81-71
131	109	3	131-67-59-58-57-56-97-98-87-76-107-136-121-120-119-117-109

Table B.8: Taxi routes Amsterdam Airport Schiphol - super heavy category aircraft

From	To	Turns	Node sequence
32	128	1	32-63-62-70-47-128
32	130	1	32-63-62-61-69-130
32	131	1	32-63-62-61-60-59-67-131
51	128	2	51-56-64-65-66-67-68-69-70-47-128
51	130	2	51-56-64-65-66-67-68-130
51	131	2	51-56-64-65-66-67-131
79	128	2	79-90-89-88-87-86-85-96-64-65-66-67-68-69-70-47-128
79	130	3	79-90-89-88-87-86-85-96-64-65-66-67-68-130
128	71	3	128-47-46-45-44-26-25-24-23-22-21-20-19-92-81-71
128	80	3	128-47-43-63-62-61-60-59-58-57-56-97-98-99-100-91-80
128	109	3	128-47-43-63-62-61-60-59-58-57-56-97-98-87-76-107-136-121-120-119-117-109
130	71	2	130-68-60-59-58-57-56-97-86-85-84-83-82-81-71
130	109	3	130-68-60-59-58-57-56-97-98-87-76-107-136-121-120-119-117-109
131	71	2	131-67-59-58-57-56-97-86-85-84-83-82-81-71
131	80	3	131-67-59-58-57-56-97-98-99-100-91-80
131	109	3	131-67-59-58-57-56-97-98-87-76-107-136-121-120-119-117-109

C

Vehicle routing problem emissions

The emissions production can be deduced from the solutions to the vehicle routing problems in Section 6.3. The emissions are calculated using the emission indices of aircraft engines at idle conditions using the ICAO aircraft emissions databank [11]. The types of emissions calculated are carbon dioxide, carbon monoxide, hydrocarbons, and nitrogen oxides. First the emission production at Rotterdam-the Hague Airport are displayed, followed by the emission production at Amsterdam Airport Schiphol.

C.1. Rotterdam-The Hague Airport

The emissions for Rotterdam-the Hague Airport are calculated for a scenario where runway 06 is active the entire day, and for a scenario where runway 24 is active the entire day. Both scenarios are represented in Figures C.1-C.4.

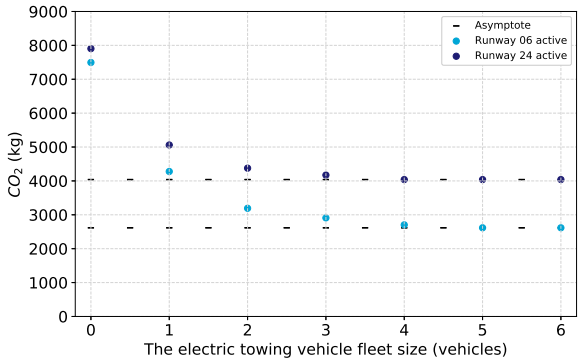

Figure C.1: The total carbon dioxide emissions by aircraft at Rotterdam-the Hague Airport with a varying number of medium category towing vehicles deployed.

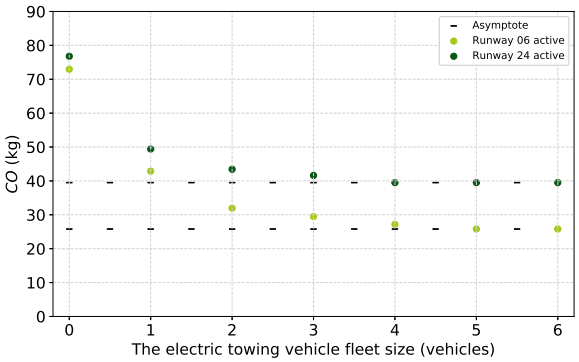

Figure C.2: The total carbon monoxide emissions by aircraft at Rotterdam-the Hague Airport with a varying number of medium category towing vehicles deployed.

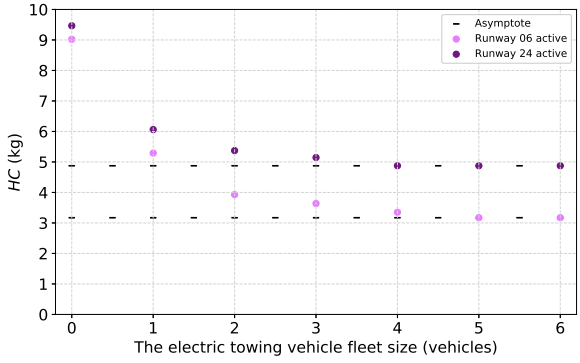

Figure C.3: The total hydrocarbon emissions by aircraft at Rotterdam-the Hague Airport with a varying number of medium category towing vehicles deployed.

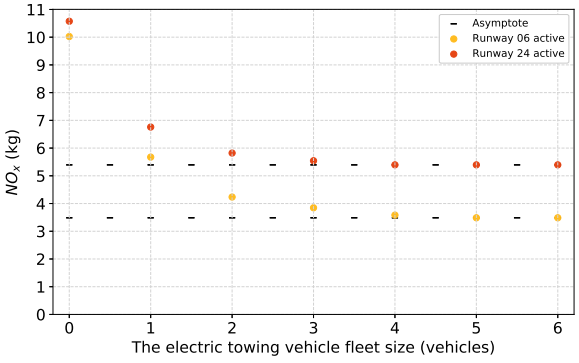

Figure C.4: The total nitrogen oxides emissions by aircraft at Rotterdam-the Hague Airport with a varying number of medium category towing vehicles deployed.

C.2. Amsterdam Airport Schiphol

The emissions for Amsterdam Airport Schiphol are calculated per aircraft category. The medium category emissions are represented in C.5-C.8, the heavy category emissions are represented in C.9-C.12, and the super heavy category emissions are represented in C.13-C.16.

C.2.1. Medium category

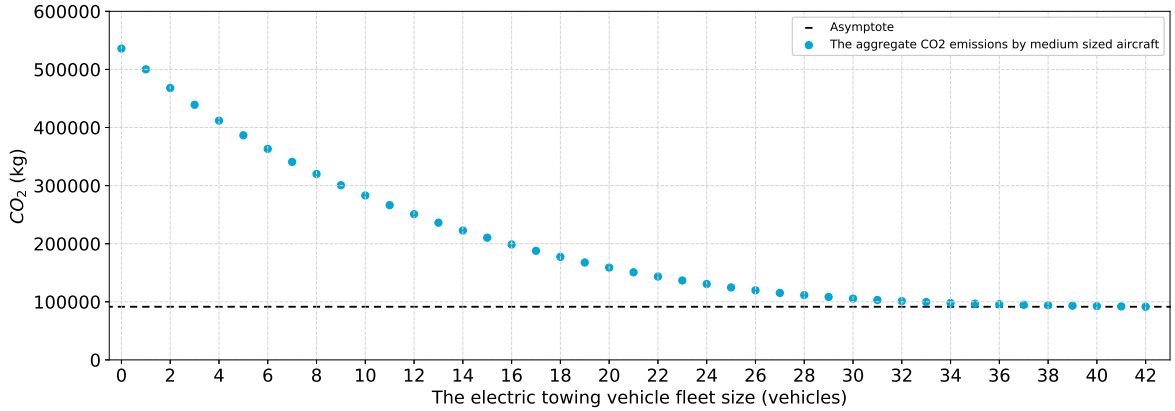

Figure C.5: The total carbon dioxide emissions by aircraft at Amsterdam Airport Schiphol with a varying number of medium category towing vehicles deployed.

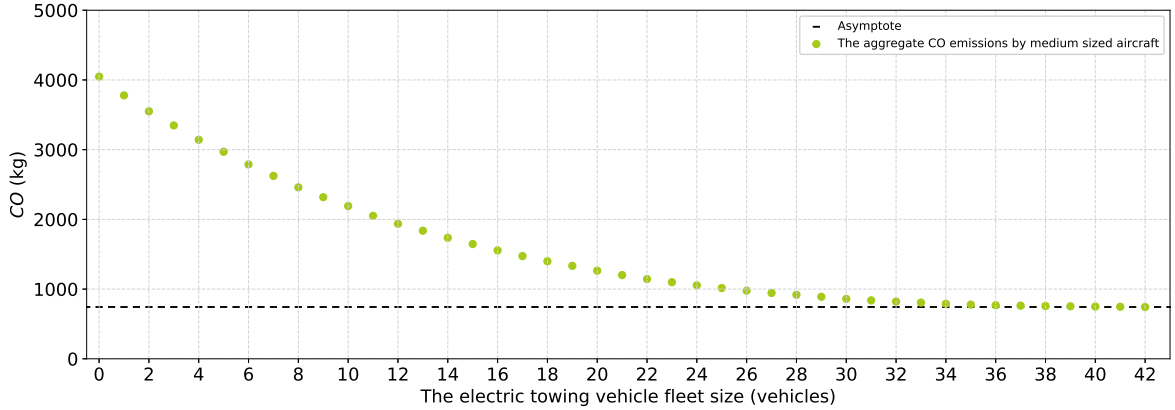

Figure C.6: The total carbon monoxide emissions by aircraft at Amsterdam Airport Schiphol with a varying number of medium category towing vehicles deployed.

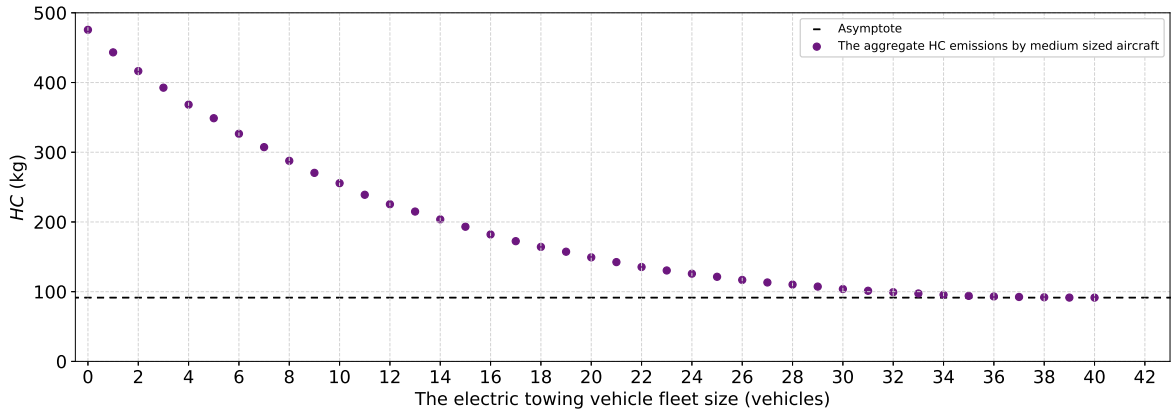

Figure C.7: The total hydrocarbon emissions by aircraft at Amsterdam Airport Schiphol with a varying number of medium category towing vehicles deployed.

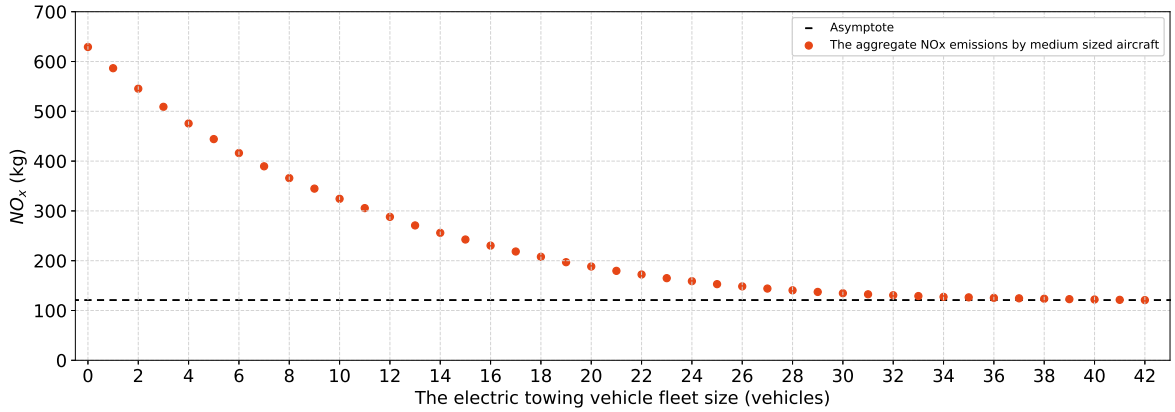

Figure C.8: The total nitrogen oxide emissions by aircraft at Amsterdam Airport Schiphol with a varying number of medium category towing vehicles deployed.

C.2.2. Heavy category

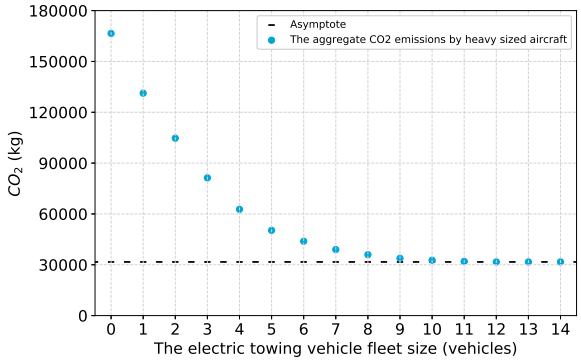

Figure C.9: The total carbon dioxide emissions by aircraft at Amsterdam Airport Schiphol with a varying number of heavy category towing vehicles deployed.

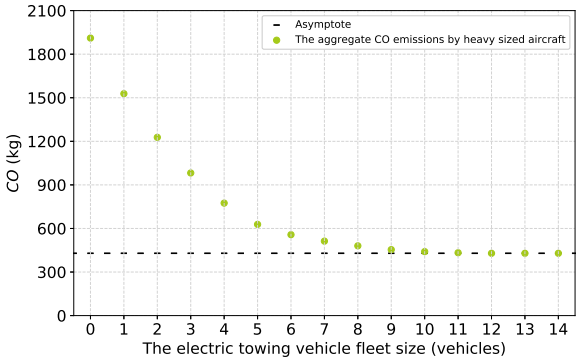

Figure C.10: The total carbon monoxide emissions by aircraft at Amsterdam Airport Schiphol with a varying number of heavy category towing vehicles deployed.

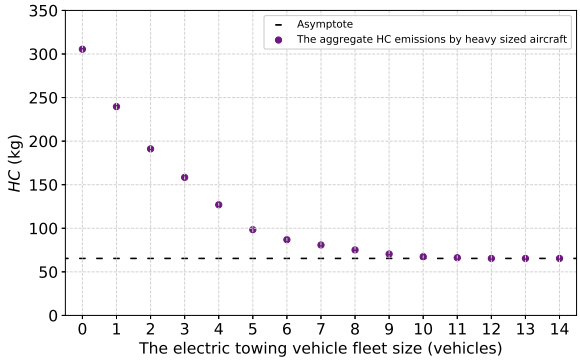

Figure C.11: The total hydrocarbon emissions by aircraft at Amsterdam Airport Schiphol with a varying number of heavy category towing vehicles deployed.

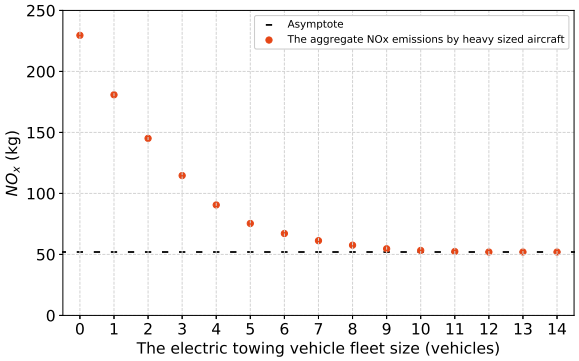

Figure C.12: The total nitrogen oxide emissions by aircraft at Amsterdam Airport Schiphol with a varying number of heavy category towing vehicles deployed.

C.2.3. Super heavy category

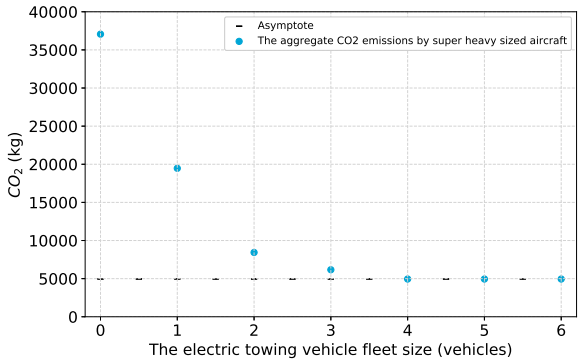

Figure C.13: The total carbon dioxide emissions by aircraft at Amsterdam Airport Schiphol with a varying number of super heavy category towing vehicles deployed.

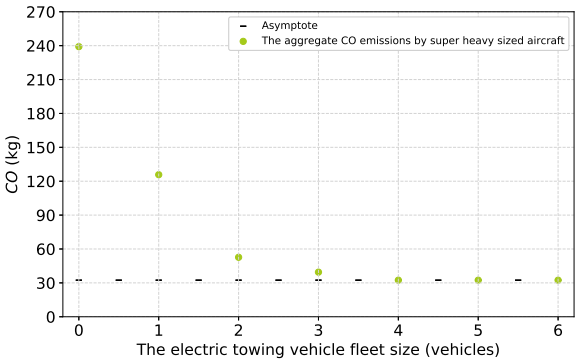

Figure C.14: The total carbon monoxide emissions by aircraft at Amsterdam Airport Schiphol with a varying number of super heavy category towing vehicles deployed.

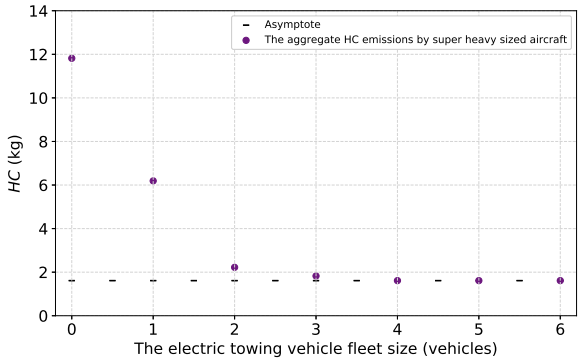

Figure C.15: The total hydrocarbon emissions by aircraft at Amsterdam Airport Schiphol with a varying number of super heavy category towing vehicles deployed.

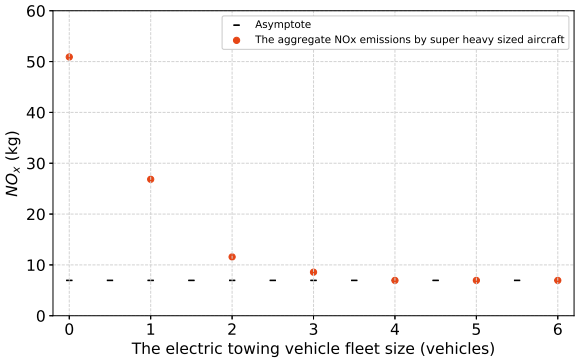

Figure C.16: The total nitrogen oxide emissions by aircraft at Amsterdam Airport Schiphol with a varying number of super heavy category towing vehicles deployed.